NAVAL POSTGRADUATE SCHOOL
Monterey, California

THESIS

MESOSCALE VERTICAL STRUCTURE OF AN EXPLOSIVE OCEANIC CYCLONE

by

Elizabeth B. Gardner

June 1991

Thesis Advisor Wendell A. Nuss

Approved for public release; distribution is unlimited.

T256209

nclassified

curity classification of this page

REPORT DOCUMENTATION PAGE

a Report Security Classification Unclassified		1b Restrictive Markings	
a Security Classification Authority		3 Distribution Availability of Report	
b Declassification Downgrading Schedule		Approved for public release; distribution is unlimited.	
Performing Organization Report Number(s)		5 Monitoring Organization Report Number(s)	
a Name of Performing Organization Naval Postgraduate School	6b Office Symbol *(if applicable)* 35	7a Name of Monitoring Organization Naval Postgraduate School	
c Address *(city, state, and ZIP code)* Monterey, CA 93943-5000		7b Address *(city, state, and ZIP code)* Monterey, CA 93943-5000	
a Name of Funding Sponsoring Organization	8b Office Symbol *(if applicable)*	9 Procurement Instrument Identification Number	
c Address *(city, state, and ZIP code)*		10 Source of Funding Numbers	
		Program Element No / Project No / Task No / Work Unit Accession No	

1 Title *(Include security classification)* MESOSCALE VERTICAL STRUCTURE OF AN EXPLOSIVE OCEANIC CYCLONE

2 Personal Author(s) Elizabeth B. Gardner

3a Type of Report	13b Time Covered	14 Date of Report *(year, month, day)*	15 Page Count
Master's Thesis	From To	June 1991	88

6 Supplementary Notation The views expressed in this thesis are those of the author and do not reflect the official policy or position of the Department of Defense or the U.S. Government.

7 Cosati Codes			18 Subject Terms *(continue on reverse if necessary and identify by block number)*
Field	Group	Subgroup	rapid cyclogenesis,upper-level front/jet,PVA,tropopause fold

9 Abstract *(continue on reverse if necessary and identify by block number)*

The mesoscale vertical structure of an explosively deepening oceanic cyclone on 19-20 January 1989 during the Experiment on Rapidly Intensifying Cyclones over the Atlantic (ERICA) was studied. Hand analyses of height, temperature, and dewpoint, and cross-sections of θ and θ_e were prepared using aircraft and sounding data through the warm-frontal region in order to document the vertical structure. The results showed that the initial disturbance formed under a region of strong upper-level confluence between a southern jet streak and an approaching upper-level short-wave from the northwest. Upper-level frontogenesis associated with the confluent flow was strong enough to produce tropopause folding and stratospheric extrusion as low as 700 mb about 750 km upstream from the surface low prior to rapid deepening.

The mesoscale analyses during the initial occlusion phase showed the upper-level temperature and moisture patterns spiraling around the low center with strong warm air advection occuring under a pocket of cold air aloft, producing significant convective instabilty. The cross-sections of θ_e throughout the rapid deepening period showed unstable conditions, which suggests that moist potential instability in the warm frontal region was a factor in the rapid development of this storm.

0 Distribution Availability of Abstract	21 Abstract Security Classification	
☒ unclassified unlimited ☐ same as report ☐ DTIC users	Unclassified	
2a Name of Responsible Individual Vendell A. Nuss	22b Telephone *(include Area code)* (408) 646-2308	22c Office Symbol Mr(Nu)

D FORM 1473,84 MAR 83 APR edition may be used until exhausted
All other editions are obsolete

security classification of this page

Unclassified

Approved for public release; distribution is unlimited.

Mesoscale Vertical Structure of an
Explosive Oceanic Cyclone

by

Elizabeth B. Gardner
Captain, United States Air Force
B.S., Florida State University, Tallahassee, 1985

Submitted in partial fulfillment of the
requirements for the degree of

MASTER OF SCIENCE IN METEOROLOGY

from the

NAVAL POSTGRADUATE SCHOOL
June 1991

Robert L. Haney, Chairman,
Department of Meteorology

ABSTRACT

The mesoscale vertical structure of an explosively deepening oceanic cyclone on 19-20 January 1989 during the Experiment on Rapidly Intensifying Cyclones over the Atlantic (ERICA) was studied. Hand analyses of height, temperature, and dewpoint, and cross-sections of θ and θ_e were prepared using aircraft and sounding data through the warm-frontal region in order to document the vertical structure. The results showed that the initial disturbance formed under a region of strong upper-level confluence between a southern jet streak and an approaching upper-level short-wave from the northwest. Upper-level frontogenesis associated with the confluent flow was strong enough to produce tropopause folding and stratospheric extrusion as low as 700 mb about 750 km upstream from the surface low prior to rapid deepening.

The mesoscale analyses during the initial occlusion phase showed the upper-level temperature and moisture patterns spiraling around the low center with strong warm air advection occuring under a pocket of cold air aloft, producing significant convective instabilty. The cross-sections of θ_e throughout the rapid deepening period showed unstable conditions, which suggests that moist potential instability in the warm frontal region was a factor in the rapid development of this storm.

G1854
c.1

TABLE OF CONTENTS

I. INTRODUCTION 1

II. BACKGROUND 3

III. DATA COLLECTION AND ANALYSIS METHODOLOGY 8
A. DATA COLLECTION AND PROCESSING 8
B. TRANSLATION OF DATA 8
C. HAND ANALYSIS 9
1. Discrepancies in Aircraft Observations 10
2. Time Evolution of Structure 13

IV. SYNOPTIC DISCUSSION OF IOP-5 16
A. 0000 UTC 19 JANUARY 1989 16
B. 0600 UTC 19 JANUARY 1989 18
C. 1200 UTC 19 JANUARY 1989 25
D. 1800 UTC 19 JANUARY 1989 32
E. 0000 UTC 20 JANUARY 1989 37
F. MESOSCALE ANALYSIS AT 0000 UTC 20 JANUARY 1989 41
G. 1200 UTC 20 JANUARY 1989 50

V. DISCUSSION 51

VI. CONCLUSIONS AND RECOMMENDATIONS 54

APPENDIX HAND ANALYSES 56

LIST OF REFERENCES 74

INITIAL DISTRIBUTION LIST 78

LIST OF TABLES

Table 1. SUMMARY OF SOUNDING ERRORS 12
Table 2. AIRCRAFT PASSES 14

LIST OF FIGURES

Fig. 1. Aircraft Errors 11
Fig. 2. 300 mb NMC Final Analysis at 19/0000 UTC Jan 89 17
Fig. 3. GOES enhanced infrared imagery for 19/0601 UTC Jan 89. 18
Fig. 4. 850 mb analysis at 19/0600 UTC Jan 89 19
Fig. 5. 500 mb analysis at 19/0600 UTC Jan 89 20
Fig. 6. 400 mb analysis at 19/0600 UTC Jan 89 22
Fig. 7. 400 mb dewpoint analysis at 19/0600 UTC Jan 89 23
Fig. 8. 19/0600 UTC 19 January 1989 Cross-sections 24
Fig. 9. Hatteras, NC Sounding 26
Fig. 10. GOES enhanced infrared imagery for 19/1201 UTC Jan 89. 27
Fig. 11. 850 mb analysis at 19/1200 UTC Jan 89 28
Fig. 12. 500 mb analysis at 19/1200 UTC Jan 89 29
Fig. 13. 400 mb analysis at 19/1200 UTC Jan 89 30
Fig. 14. 400 mb dewpoint analysis at 19/1200 UTC Jan 89 31
Fig. 15. 19/1200 UTC Jan 89 Coastal Cross-section 32
Fig. 16. GOES enhanced infrared imagery for 19/1801 UTC Jan 89. 34
Fig. 17. 850 mb analysis at 19/1800 UTC Jan 89 35
Fig. 18. 700 mb analysis at 19/1800 UTC Jan 89 36
Fig. 19. 500 mb analysis at 19/1800 UTC Jan 89 37
Fig. 20. GOES enhanced infrared imagery for 20/0001 UTC Jan 1989 38
Fig. 21. 850 mb analysis at 20/0000 UTC Jan 89 39
Fig. 22. 500 mb analysis at 20/0000 UTC Jan 89 40
Fig. 23. 400 mb analysis at 20/0000 UTC Jan 89 41
Fig. 24. 850 mb mesoscale analysis at 20/0000 UTC Jan 89 42
Fig. 25. Aircraft LeSondes 44
Fig. 26. 20/0000 UTC Jan 89 Cross-sections 45
Fig. 27. 700 mb mesoscale analysis at 20/0000 UTC Jan 89 47
Fig. 28. 500 mb mesoscale analysis at 20/0000 UTC Jan 89 48
Fig. 29. 400 mb mesoscale analysis at 20/0000 UTC Jan 89 49
Fig. 30. 400 mb mesoscale dewpoint analysis at 20/0000 UTC Jan 89 50
Fig. 31. 700 mb analysis at 19/0600 UTC Jan 89 56

Fig. 32. 700 mb analysis at 19/1200 UTC Jan 89 57
Fig. 33. 700 mb analysis at 20/0000 UTC Jan 89 58
Fig. 34. 400 mb analysis at 19/1800 UTC Jan 89 59
Fig. 35. 850 mb dewpoint analysis at 19/0600 UTC Jan 89 60
Fig. 36. 850 mb dewpoint analysis at 19/1200 UTC Jan 89 61
Fig. 37. 850 mb dewpoint analysis at 19/1800 UTC Jan 89 62
Fig. 38. 850 mb dewpoint analysis at 20/0000 UTC Jan 89 63
Fig. 39. 700 mb dewpoint analysis at 19/0600 UTC Jan 89 64
Fig. 40. 700 mb dewpoint analysis at 19/1200 UTC Jan 89 65
Fig. 41. 700 mb dewpoint analysis at 19/1800 UTC Jan 89 66
Fig. 42. 700 mb dewpoint analysis at 20/0000 UTC Jan 89 67
Fig. 43. 500 mb dewpoint analysis at 19/0600 UTC Jan 89 68
Fig. 44. 500 mb dewpoint analysis at 19/1200 UTC Jan 89 69
Fig. 45. 500 mb dewpoint analysis at 19/1800 UTC Jan 89 70
Fig. 46. 500 mb dewpoint analysis at 20/0000 UTC Jan 89 71
Fig. 47. 400 mb dewpoint analysis at 19/1800 UTC Jan 89 72
Fig. 48. 400 mb dewpoint analysis at 20/0000 UTC Jan 89 73

I. INTRODUCTION

Rapid cyclogenesis over the ocean has been given considerable attention since the early 1980's when Sanders and Gyakum (1980) presented the first climatological study of the "bomb". They defined rapid cyclogenesis as an extratropical cyclone whose central pressure falls an average of 1 mb h^{-1} for 24 h. Studies since then have not only addressed the climatology but also the processes involved in rapid cyclogenesis. Researchers have identified upper-level processes such as jet streaks, upper-level short-wave troughs, and tropopause folds/stratospheric extrusions as critical to rapid deepening (Uccellini et al. 1985, Keyser and Shapiro 1986, Elsberry and Kirchoffer 1988). Low-level process include surface sensible and latent heat fluxes as well as strong low-level baroclinicity (Neiman et al. 1990, Kuo et al. 1991). Although advances have been made in identifying these processes and numerically modeling rapid cyclogenesis (Sanders 1987), there are still problems with accurately forecasting these events. The relative importance of the different processes and the interactions between them during the evolution of an explosive cyclone makes forecasting a much more complicated issue. The lack of sufficient data over the ocean combined with inadequate physical parameterizations in numerical weather prediction models tends to obscure some of the important mesoscale physical and dynamical processes critical to rapid development. So, the key to progress in solving some of the finer details that occur during the evolution of rapidly developing cyclones depends on adequate and detailed mesoscale analyses over the ocean which are not based on models that are inherently biased. This will allow researchers to actually observe and analyze important physical and dynamical processes that occur during rapid cyclogenesis. These processes can then be incorporated into models to help further the research effort in this area.

The Experiment on Rapidly Intensifying Cyclones over the Atlantic (ERICA) provides such datasets with which to make independent analyses and determine the true physical processes occurring in nature. The Office of Naval Research (ONR) initiated and funded Heavy Weather at Sea of which ERICA was a part. The focus of the ERICA field study was to determine the fundamental physical processes occuring during rapid intensification of oceanic cyclones, parameterize the processes needed in numerical prediction models, and identify measurable precursors that must be included in the initial analysis to accurately forecast explosive cyclogenesis (Hadlock and Kreitzberg, 1988).

Heavy emphasis during ERICA was placed on field measurements with data collected from a wide variety of observing systems including Navy, National Center for Atmospheric Research (NCAR), National Oceanic and Atmospheric Administration (NOAA), and Air Force aircraft, a drifting buoy network, ships of opportunity, increased frequency of rawinsonde observations (RAOBS), Geostationary Operational Environmental Satellite (GOES) imagery, wind profilers, and conventional and Doppler radar both on-ground and airborne.

The primary objective of this thesis is to analyze the detailed structure of the Intensive Observing Period (IOP) 5 cyclone in order to describe the relationship between the evolution of important mesoscale features that contributed to rapid cyclogenesis. This was accomplished through hand analysis of six-hourly upper-level charts at 850 mb, 700 mb, 500 mb, and 400 mb. Aircraft flight level observations above 400 mb were sparse which precluded upper-level jet analyses at 300 mb. Cross-sections through the cyclone at various stages of development were also hand-analyzed using extensive aircraft soundings and observations. Specific objectives of this study are:

1. To describe the mesoscale structure of the IOP-5 cyclone from 850 mb to 400 mb during the period of most rapid development.
2. To document the interactions of upper-level features with the surface cyclone.
3. To describe the stability structure of an explosively deepening cyclone as it evolves from an initial disturbance to an occluded cyclone.

A background on explosive cyclogenesis and upper-level forcing is presented in Chapter II. Chapter III describes the available dataset and the methods used for hand-analysis. The evolution of IOP-5 is fully explored in Chapter IV, including both synoptic and mesoscale forcing in the upper levels. A discussion of characteristics of the forcing in IOP-5 is given in Chapter V followed by conclusions and recommendations in Chapter VI.

II. BACKGROUND

Understanding the role of upper-level forcing in relationship to explosive cyclogenesis continues to be an important area of research. Many upper-level processes that contribute to rapid cyclogenesis have been identified, but the exact role they play relative to surface and boundary layer processes is still not resolved (Uccellini 1990). This chapter describes background on explosive cyclogenesis and highlights current issues surrounding the role and extent of upper-level forcing in these rapidly deepening storms.

Since the first statistical and climatological studies of explosively deepening cyclones by Sanders and Gyakum (1980) and Roebber (1984), upper-level as well as low-level processes have been identified as possible contributors to rapid development. Sanders and Gyakum found that the initial cyclone development occurred in regions of upper-level diffluence 500 km downstream from a mobile 500 mb trough and formed near the warm ocean currents mainly in the winter season. An early study by Roebber (1984) found that the development rates using baroclinic instability theory were less than observed during explosive cyclogenesis and that the physical processes governing these storms may be fundamentally different than baroclinically developed storms. These early studies indicate that both strong upper-level forcing and surface fluxes over the warm ocean currents potentially influence the rate of cyclogenesis.

Current research continues to explore the role of both upper- and lower-level processes and the way in which they interact to produce explosively deepening cyclones. Current work by Uccellini (1990) suggests that there are no fundamentally different processes, just the traditional upper and lower processes interacting in a more efficient manner. The exact degree of interaction between the upper and lower processes is presently not clear although many studies have been done to define common features of explosive cyclogenesis (e.g. Lange 1986; Reed and Albright 1986; Sanders 1986; Gyakum and Barker 1988). These studies tend to put the emphasis back onto the traditional baroclinic instability theory as presented by Holton (1979). He recognized that the main cause of cyclone development was baroclinic instability, which depends primarily on the vertical shear of the jet stream.

A number of studies have characterized the nature of the upper-level forcing as primarily due to jet streak dynamics and strong positive vorticity advection (PVA).

Uccellini (1984) and Wash et al. (1988) showed that significant divergence aloft from jet streaks was associated with rapid development below. Elsberry and Kirchoffer (1988) found that the presence of a jet maximum over the storm was a major factor in storm development, with larger pressure falls directly related to higher 300 mb winds. They also noted that the surface cyclone was in the left-front quadrant of the jet at some time during development in 20 out of the 23 cases they analyzed. Studies by Kocin and Uccellini (1990), Kocin et al. (1985), and Uccellini et al. (1987) all note that the left-front exit region appears to be an important feature in rapid cyclogenesis. Smith (1986) also found that the largest difference between explosive and non-explosive cases is found in the magnitude of upper-level divergence and positive vorticity advection (PVA).

Although these previous studies have identified the left-front exit region as important in explosive cyclogenesis; the geometry,timing, and the extent of interactions between the left-exit region and the surface is not completely clear. The effects of curvature on the jet streak dynamics as described by Keyser and Shapiro (1986) are not well documented for explosive cyclogenesis. Kocin et al. (1985) found that cyclogenesis occurred on the cyclonic side of a cyclonically curved polar jet streak while Uccellini et al. (1987) found that the left-front exit region of an anticyclonically curved subtropical jet streak was favorable for cyclogenesis. Elsberry and Kirchoffer (1988) studied some complex cases of cyclogenesis with both polar and subtropical jet streaks but did not study the effects of curvature on the cyclone development. In a case of a low moving from one side of the jet to the other, they found that larger pressure falls occurred on the cyclonic side of the jet. This still does not solve the problem of curvature and its effect on initial development. The net result of increasing the divergence by the indirect transverse circulation of the jet exit region is similar in all these cases but the effect of jet curvature on the magnitude and intensity of the transverse circulation and on the surface cyclogenesis has not been addressed in these studies.

Strong subsidence associated with tropopause folding and strong upper-level frontogenesis has been shown to be associated with some explosive cyclones. Newton (1954) recognized the importance of subsidence in the upper and middle troposphere to upper-level frontogenesis, while Danielsen (1968) related the upper-level front and jet axis with its associated transverse circulations to tropopause folding and the subsequent displacement of stratospheric air down towards the 500 mb to 700 mb layer. Uccellini et al. (1985), in a study of the President's Day Cyclone of February 1979 found an increase in the subtropical jet (STJ) intensity and a deepening trough in the polar front jet (PFJ) were crucial to the rapid development of this storm. Bosart and Lin (1984) and

Uccellini et al. (1985) confirmed that rapid cyclogenesis was marked by the approach of a potential vorticity maximum in the middle and upper troposphere. Uccellini et al. (1985) associated the potential vorticity maximum with tropopause folding and a stratospheric extrusion down as low as 800 mb to the west of the President's Day cyclone, which enhanced rapid development as hypothesized by Newton and Danielsen in the early 1950's. Descent of stratospheric air and the extension of high potential vorticity were also found by Uccellini et al. to be just above the storm center as explosive deepening occurred. In a model-based diagnostic study of the President's Day storm, Whitaker et al. (1988) confirmed the strong subsidence that occurred prior to rapid deepening. They proposed that the indirect transverse circulation beneath the jet core concentrated the subsidence on the warm side of the upper-level front. This contributed to the intensification of the middle- and upper-tropospheric fronts and the descent of dry stratospheric air into the storm.

Most of the storms in these previous studies have been in the North Atlantic, but a study by Reed and Albright (1986) of an Eastern Pacific storm shows that the same upper-level features occur in other regions as well. The prestorm environment of this cyclone was characterized by strong baroclinicity and a jet stream aloft, a shallow surface frontal structure, and sensible and latent heat fluxes from the ocean that contributed to destabilization prior to deepening. The explosive deepening occurred when the disturbance passed beneath the jet stream axis and advanced to the forward side of the long-wave trough. They also found indirect evidence that strong subsidence occurred west of the storm immediately before explosive development. They noted that the subsidence strengthened the upper-tropospheric vorticity and that the strong upper-level winds allowed the subsided air to overtake the surface low and enhanced the rapid deepening.

Gyakum and Barker (1988) explored a rare case of explosive cyclogenesis over land to document similar processes for land cyclones. This storm developed over Eastern Georgia and moved across the mid-Atlantic on February 28-29, 1984. It is not quite a true explosive cyclone as defined earlier because it only lasted 18 hours, but it did deepen 12 mb in a 4 hour period and is a good case with which to explore the similarities between rapidly deepening oceanic and land cyclones. They found that the cyclone developed along an intensifying surface frontal zone that developed primarily due to surface geostrophic frontogenetical forcing prior to the formation of the surface low. This was aided by strong diabatic heating, reduced static stability, surface warming and moistening, and a strong upper-level jet streak and trough with associated PVA up-

stream from the surface cyclone. A potential vorticity analysis suggested that lower tropospheric heights occurred although their model runs were not sufficient to do a complete analysis of possible tropopause folding in this land-based case of explosive cyclogenesis. The authors suggest that several physical processes, occurring on different scales, combine synergistically to effect this case of explosive deepening over land.

All of these studies have found that the left-front quadrant of an upper-level jet exit region plays an important role in enhancing the divergence aloft and inducing a transverse ageostrophic circulation below, greatly increasing the vertical motion and ultimately the low-level convergence over the developing system. This process alone, however, can not explain the total deepening seen in rapid cyclogenesis. The surface heat and moisture fluxes, latent heat release, diabatic processes and convection are also critical processes that have been identified as contributing to explosive cyclogenesis. The low-level influences lower the static stability by sensible and latent heat fluxes and contribute to increasing the diabatic heating. Strong diabatic heating and convection have been associated with explosive cyclogenesis in numerous studies (Bosart and Lin 1984; Gyakum 1983; and others). These studies suggest that low static stability or moist symmetric neutrality as hypothesized by Emmanuel (1985, 1988) also characterize explosive cyclones.

Although the dynamics of individual upper-level processes that enhance explosive cyclogenesis are fairly well known, the problem is to determine the exact relationship between these upper-level processes and the low-level baroclinic and diabatic processes that occur in rapidly deepening cyclones. Uccellini (1990) notes that the growing opinion is that rapid cyclogenesis cannot be described as a product of discreet physical processes, but occurs as all of these processes act together in some sort of nonlinear synergistic manner. For instance, upper-level fronts, jet streaks, troughs, and PVA must act together with boundary layer sensible and latent fluxes, latent heat release and low-level baroclinic zones in order to produce rapid versus normal development of cyclones. These nonlinear interactions may occur on substantially smaller spatial scales and time scales than the dominant wavelength of the cyclone. The small space and time scales lead to instances of unbalanced conditions in the atmosphere that can't be properly modeled using the quasi-geostrophic and hydrostatic approximations (Uccellini 1990).

Shapiro and Keyser (1990) studied the low-level small-scale processes involved in explosive cyclogenesis. Their research was based on both numerical simulations and field studies of rapidly deepening storms. They found that the largest frontal baroclinicity at low-levels occurred within the bent-back warm front to the west of the

cyclone, and that a warm-core frontal seclusion formed in the occluded stage. The fact that these processes were not fully explained by the early Norwegian frontal-cyclone model led Shapiro and Keyser to propose a 4-phase evolution of explosively developing cyclones that differed from the earlier cyclone models. Their 4-phase model includes an incipient frontal cyclone stage, a frontal fracture stage, a frontal T-bone and bent-back warm front stage, and finally, a warm-core seclusion stage marking the end of cyclogenesis.

In order to advance our understanding of explosive cyclogenesis, the nonlinear interactions between these various processes needs to be explored more fully. In order to resolve the various processes, the processes need to be observed in nature first, then incorporated in numerical models to improve current forecast capabilities. Analysis of the IOP-5 cyclone using the high-resolution observations available during ERICA will help improve the understanding of how these processes interact and help determine the role and evolution of upper-level dynamical forcing on explosive cyclogenesis.

III. DATA COLLECTION AND ANALYSIS METHODOLOGY

A. DATA COLLECTION AND PROCESSING

The ERICA field study was designed to collect data in an area of the western North Atlantic extending from 40°N to 47°N between 59°W to 69°W. Data was collected over this area from aircraft, buoys, Doppler and conventional radars, land-based rawinsondes, satellite imagery, and ships. The data used in this research is primarily asynoptic data from aircraft flight-level observations, Omega and LeSonde dropsondes deployed from aircraft, and land-based rawinsonde soundings. The aircraft flight-level data was averaged over 30 second intervals and grouped into 3-hour blocks centered on synoptic times. Thus, the upper-level charts throughout this thesis incorporate data up to 1 1/2 hours on either side of the analysis time. The aircraft flight-level observations are denoted on the charts with the prefix P for NOAA WP-3D's or E for the NCAR Electra followed by three numbers that represent the number of 30 second intervals from takeoff. If the aircraft was ascending or descending with heading changes greater than 0.7 degrees/second or altitude changes greater than 8.0 meters/second the winds were considered non-representative and were not plotted.

The NOAA WP-3D aircraft also deployed a new NCAR-developed dropwindsonde called a LeSonde, and the USAF WC-130 aircraft deployed Omega dropsondes. The NOAA WP-3D dropsonde data is denoted on the analysis charts by the prefix N whereas the USAF WC-130 soundings are preceded by an A. The three digits following the prefix are the time of the sounding with the last digit dropped so that N234 represents the NOAA aircraft at 2340 UTC. There were some data sparse times during the explosive deepening phase of this storm due to problems with dropsonde deployments, bad readings, and no wind reports. The soundings were beneficial though in locating many of the upper-level features as the aircraft flew patterns across the storm center at various altitudes.

B. TRANSLATION OF DATA

Once the data were collected, the next step was translating the observations to standard 6-hourly upper-level charts. Height, temperature, and dewpoint temperature were analyzed at 850 mb, 700 mb, 500 mb, and 400 mb; the analyses not specifically mentioned in subsequent chapters are in the attached appendix in order to provide a complete set of upper-air analyses. Data were taken approximately 50 mb on either side

of the standard pressure levels, and then the height, temperature and dewpoint were adjusted to that pressure level. Taking a narrow layer limits the number of data points in the analysis but helps reduce the magnitude of the error in using a simple standard lapse rate to adjust the data. The winds were not adjusted to standard pressure levels and represent the actual flight-level winds.

The analysis was accomplished with aircraft data up to 1 1/2 hours on either side of the analysis time and soundings up to 2 1/2 hours prior and 2 1/2 hours after the analysis time in the earlier stages of the cyclone development. The relative position of the data compared to the storm was determined by translating the aircraft and sounding data according to the cyclone's speed and direction of movement. The Sanders (1989) analysis positions of the surface low center were taken as ground truth, and then the speed and direction were estimated over 6-hour intervals to translate the aircraft locations in time. The translation was needed to move the observations in time to conform to a standard analysis time, and no attempt was made to adjust the thermodynamic variables although the storm was changing dynamically with time also. This was evident in the analysis as some soundings and aircraft observations no longer fit the analyses after they were moved, but the overall quality of the analysis was better after the data were translated. An attempt to determine the time evolution of the storm using aircraft observations is discussed in the next section.

C. HAND ANALYSIS

Data analysis was a crucial step in determining the true vertical structure in IOP-5. The data for a complete synoptic-scale vertical analysis throughout the entire IOP was limited. The upper-air observations at each level were on the order of 50-70 data points, whereas the available surface data was on the order of several hundred data points. The aircraft data were basically confined to the low center and warm-frontal regions, and there were big gaps in data coverage south of the surface low along the cold front and in the warm sector between the cold and warm fronts.

The limited amount of data for the upper-air analyses made it imperative to attempt to utilize all available observations. In order to accurately analyze the data, an estimate of the errors and biases in the different observing systems was needed. Sanders (1990) looked at the errors involved in analyzing surface observations over the ocean in ERICA IOP-2 and found Root Mean Square (RMS) errors of 1.5 mb for the surface pressure analyses. He noted the necessity for examining the observations, noting problems with individual ship and buoy reports and utilizing satellite imagery and low-level aircraft

traverses to make a consistent, accurate analysis. The same advice holds true for the upper-air analyses with the following additional quality checks applied to the IOP-5 upper-air analyses:

1. Note error tendencies in individual aircraft and discrepancies between aircraft reports in the same location.
2. Recognize errors between aircraft and sounding reports.
3. Note errors between the Omega and LeSonde dropwindsonde systems.
4. Use aircraft passes over the same location to help pin down the evolution of upper-level features.
5. Utilize aircraft ascents/descents to help determine the vertical structure but be wary of wind reports if the ascent/descent is too fast.
6. Use land-based rawinsonde reports to help identify and verify features as they move offshore where data is less abundant and more uncertain.

The error estimates and descrepancies presented in the following sections are representative of the range of variability of the data in IOP-5. Part of the error is due to the translation of data, while another part is due to errors in the measuring equipment. An attempt to distinguish between the two separate errors is not feasible, but the important result from the error analysis is to find the range of variability of the data in order to have reasonably consistent final hand-analyses of the upper atmosphere.

1. Discrepancies in Aircraft Observations

There were several discrepancies in the measuring equipment discovered while doing the hand-analysis. It is evident that there is a problem with the calibration of aircraft instruments as can be seen in Fig. 1 . The NCAR Electra aircraft and one of the two NOAA WP-3D aircraft flying out of Brunswick, Maine show upwards of 20 meter differences in height at approximately 0500 UTC on January 19, 1989 when they were only 14 minutes apart. This was seen again at approximately 1120 UTC as the Electra flight was returning and another NOAA WP-3D plane was leaving Brunswick. These two aircraft reports were only 4 minutes apart and the height difference at 500 mb was 25 meters. Both of these examples showed slight discrepancies in the temperature and dewpoint observations also. There were no examples of two NOAA WP-3D aircraft passing each other in the same region at the same time so that the calibration error, if any, between two similar aircraft is unknown at this point.

Along with the aircraft differences, there is evidence of problems between the aircraft flight-level observations and the LeSondes. The NOAA WP-3D leaving Brunswick around 1800 UTC on January 19 dropped a LeSondé at 1850 UTC, and there

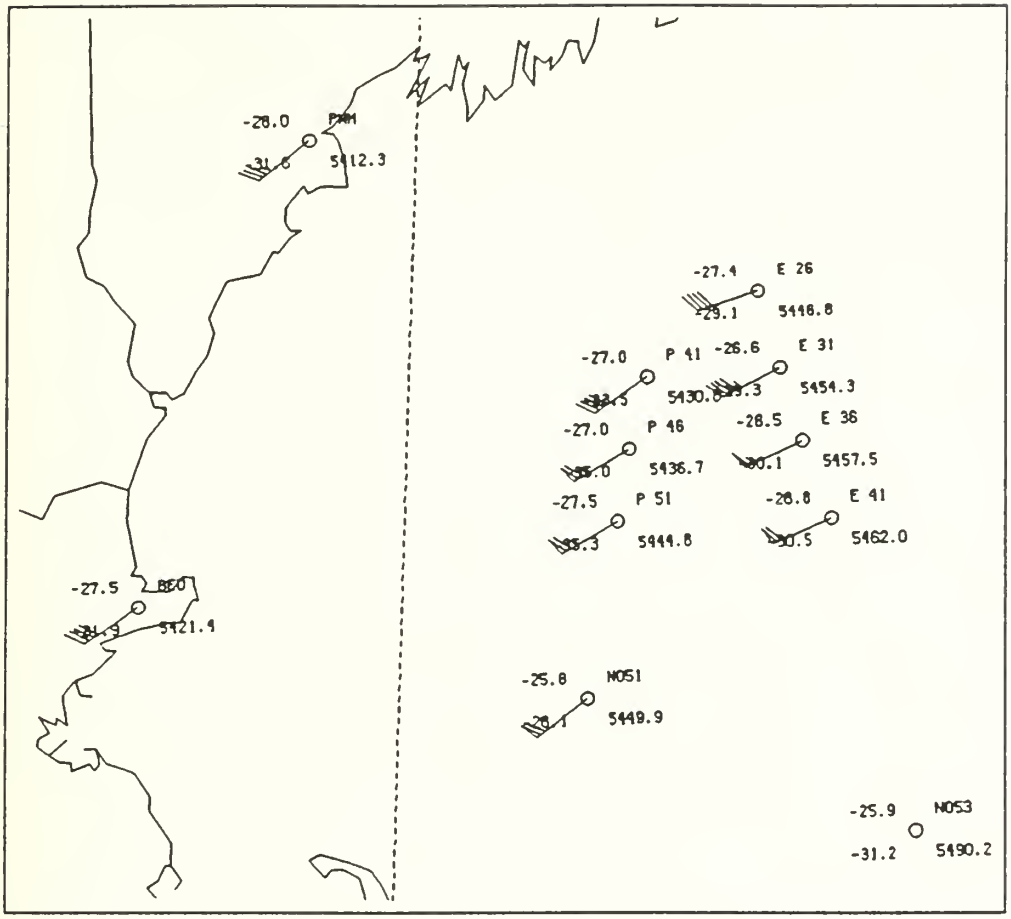

Fig. 1. Aircraft Errors: Aircraft observational discrepancies between a NCAR Electra and a NOAA WP-3D aircraft leaving Brunswick, Maine approximately 0500 UTC January 19, 1989.

was a 22 meter height difference, a 1.9° C temperature difference, and a 3° C dewpoint difference between the aircraft and the LeSonde at 500 mb at that time. All of the comparisons were well removed from the storm center so that the translation of data should not have been a major factor. What we are seeing therefore is representative of the aircraft and sounding biases.

A subjective measurement of the LeSonde and the Omega dropsondes errors was done by comparing the hand-analyzed height and temperature fields with the sounding observations and is presented in Table 1. The dashes with no numbers indicate no error in that particular field, while the minus sign in front of a number indicates negative errors and the plus sign indicates positive errors in either temperature or height.

The overall trend seems to be that the heights are consistently too high or too low throughout the vertical, whereas the temperatures errors are much more erratic for any given sounding. Sounding N055 shows that the temperature errors increase with altitude, from +0.5° C at 850 mb to +1.5° C at 500 mb. This is due to some extent by taking data 50 mb on either side of the standard pressure level at all levels. The 450-550 mb layer is much thicker than the 800-900 mb layer which allows for greater translation errors at the upper levels. This is true in the early period of storm development but by 20/0000 UTC, the lowest levels are more prone to error due to the rapid changes occurring at the surface. N223 was 5° C too cold at 850 mb but only 0.5° C too warm at 700 mb. The longer the time block in which data was collected, the more error-prone the data became. A093 for instance, was 2 2/3 hour prior to the 1200 UTC analysis and was taken near the low center at 0930 UTC. Thus, the heights are significantly lower than the 1200 UTC analysis and do not "fit" the analysis anymore. Sounding A103 has the same pattern although it was located in the ridge at 1030 UTC and is 65-80 m too high for the 1200 UTC analysis. These are important features to note. Although all the soundings may not conform exactly to the analyses, knowing how the errors change with height, time, and location of data relative to the storm allows for a much more accurate analysis than disregarding the data altogether.

Table 1. SUMMARY OF SOUNDING ERRORS

Time	Sounding	Pressure Level (mb)					
		850		700		500	
		Hght(m)	Temp(C)	Hght(m)	Temp(C)	Hght(m)	Temp(C)
19/0600	A042	+15.0	-	+20.0	-3.5	+5.0	-0.5
	N055	-	+0.5	-	+1.0	-	+1.5
19/1200	A093	-50.0	+2.5	-60.0	-	-40.0	-
	N105	+40.0	+0.5	+40.0	-	+30.0	+1.0
	N102	+50.0	-	+50.0	-	+45.0	-
	A103	+65.0	-	+75.0	+1.0	+80.0	-1.0
19/1800	N191	-25.0	-	-10.0	-0.5	-10.0	-
20/0000	N223	-	-5.0	-	+0.5	-	-
	N013	+65.0	+2.0	+25.0	-3.0	-	+2.0
	N015	-25.0	-	-30.0	-	-20.0	+4.0
	N220	-	-2.0	-	+2.0	-	-

Once again, part of this error is inherent in translating the observations without adjusting the thermodynamic variables over a 3-hour period and some part is due to the data measurement errors. The error due to translation alone is hard to account for. Lyne et al. (1982) performed a data assimilation experiment to see how aircraft data compared to the model analysis in the First GARP Global Experiment (FGGE). They found that the RMS height errors were generally greater than the operational analyses and the wind errors were less. The RMS wind errors for dropsondes ranged from 8 ms^{-1} at low-levels to 18 ms^{-1} at the upper levels. The aircraft data on the other hand had a steady 32 ms^{-1} RMS error in winds. The temperature RMS errors were 2-3 K and 6 K for the dropsonde and aircraft data respectively. The same RMS error statistics may not apply to this case during ERICA but it does give some indication of the value of aircraft observations. Awareness of these trends gave a little more confidence in the placement of the final hand-analysis.

2. Time Evolution of Structure

To further refine the analysis, the time evolution of the storm at various locations was examined. By noting the height, temperature, dewpoint, wind speed, and wind direction differences between these times, the analysis and structure of the storm as it evolved was better defined. The changes in the variables are at that particular location in space and give an indication of the local change with time. Table 2 shows the aircraft passes and the changes over time. The pressure levels varied over no more than 10 mb and the height, temperature, and dewpoint fields were adjusted using a standard lapse rate. The first two aircraft, EL and F1 at 969 mb, were approximately 50 km southwest of the 0900 UTC low and show significant height falls, temperature falls, and drying that occurred behind the cold front early in the development. At about the same time, the two measurements from the F1 aircraft at 939 mb show very slight height rises and temperature and dewpoint changes over the same amount of time. Only 1.8° C hr^{-1} warming occured 150 km northeast of the 0900 UTC surface low, ahead of the warm front. The F3 aircraft flying at 952 mb approximately 100 km northeast of the occluded front 12 hours later, documents much stronger changes. There is a rapid height fall as the system approaches with a 50 m hr^{-1} height fall. This significant height fall indicates the approach of a much more intense cyclone with an increased height gradient. The winds remain easterly but decrease slightly as the occlusion approaches. Another feature to be analyzed in more detail in the synoptic discussion is the dry-air intrusion into the storm from the northwest. At 1200 UTC, aircraft F1 reported a -50.8° C dewpoint temperature, indicative of very strong subsidence occuring offshore.

Table 2. AIRCRAFT PASSES

Aircraft	Level (mb)	Location	Date/Time (UTC JAN 89)	Height Change (m hr^{-1})	Temp Change (°Chr^{-1})	Dwpt Change (°Chr^{-1})	Wind (ddd/kt)
EL F1	969	38.5 N 66.8 W	19/0955 19/1034	-21.0	-5.4	-6.6	- 005/35
F1 F1	939	39.2 N 65.9 W	19/1013 19/1058	+3.0	+1.8	+3.0	120/24 080/23
F1 F2	500	42.1 N 67.4 W	19/1149 19/1236	+10.8	-3.0	+23.4	225/40 245/25
F2 F2	524	39.7 N 64.2 W	19/1229 19/1342	-12.6	-0.24	+1.2	220/48 205/34
F3 F3	952	41.1 N 57.4 W	19/2105 19/2133	-50.0	+1.8	+3.0	110/47 110/38
F3 F3	428	42.3 N 61.2 W	19/2245 20/0125	-2.4	-1.2	-3.0	205/09 260/28

The upper-level features are not changing as rapidly, although there is an 11 m hr^{-1} height fall documented by the F2 aircraft at 524 mb downstream from the trough axis. This gave some indication of the intensity and location of the upper-level trough. The upper-level changes at 428 mb were observed by the F3 aircraft approximately 325 km northwest of the surface low. There was very little change in the variables over 1 2/3 hours, but the wind speed increase and directional shift to the west helped place the upper-level low and trough axis, as the low started to close off in the upper levels at 20/0000 UTC.

After the data were translated, there were several aircraft observations that were found to have been translated to the same location. These were primarily two different aircraft observations or an aircraft observation and a sounding. The value of such information is obscured by the errors noted previously between the different observation types. There was one interesting case though when two soundings were translated to the same location, approximately 150 nm west of the 0000 UTC surface low center. The soundings were taken 80 minutes apart at 19/2310 UTC and 20/0130 UTC and the height rose 60 meters at 850 mb, 30 meters at 700 mb, and fell 17 meters at 500 mb. The temperature fell 3.4° C, 4.6° C, and 4.9°, and the dewpoint fell 7° C, 6.4° C, and 13.4° at 850 mb, 700 mb, and 500 mb respectively. This gives an indication of how fast the

thermodynamic structure was changing between those two soundings as the cyclone deepened as well as some of the differences in errors between the two soundings.

Ultimately , the final hand-analyzed upper-air analyses were accomplished using a combination of the asynoptic aircraft and sounding data, the National Meteorolical Center (NMC) Global Spectral Model (GSM) gridded initial analyses, U.S. and Canadian rawinsondes, and GOES satellite imagery. This combination of data sources made it possible to construct an accurate picture of the evolution of the explosive cyclogenesis period in IOP-5 that is dynamically consistent.

IV. SYNOPTIC DISCUSSION OF IOP-5

The explosive cyclogenesis of IOP-5 is characterized by an initial low-level disturbance that formed along the axis of the Gulf Stream interacting with a southwesterly jet streak and an upper-level short-wave from the northwest. The maximum deepening occurred between 19/1200 UTC and 20/1200 UTC as the central pressure decreased from 1004 mb to 972 mb as determined by Greer (1991), which yielded a total decrease of 32 mb in the 24-hour period. The rapid development occurred primarily between the period from 1500 UTC to 2100 UTC when the pressure decreased 14 mb from 1002 to 988 mb. This period was preceded and followed by periods of modest deepening. By 20/0000 UTC, the storm was occluded and moving out of the ERICA observing region.

A. 0000 UTC 19 JANUARY 1989

Prior to 0600 UTC, the surface was characterized by a non-developing open wave trough that had only a small area of cloudiness off the coast of the Carolinas. This open-wave surface trough is located along the Gulf Stream and on the poleward side of a 300 mb jet streak moving across the Gulf Coast states, as seen in Fig. 2. The southwesterly jet curves anticyclonically from eastern Texas and central Arkansas to the east coast near Hatteras, North Carolina (HAT) and then across Bermuda, United Kingdom (XKF). Maximum winds along this jet of 115 kt at Greensboro, North Carolina (GSO) suggest that the left-front exit region is located near the coast where the surface wave is located. The missing 300 mb winds from the sounding at HAT at 0000 UTC (not shown) suggests that the jet may actually extend offshore at this time, which places the exit region off the coast. North of this anticyclonically curved jet is a trough centered over Ohio with a jet streak located in the northwesterly flow near St Cloud, Minnesota (STC). The orientation of these two jets leads to strong confluence in the region from eastern Kentucky through western North Carolina at 0000 UTC with diffluence over the ocean near 38° N, 71° W, which is the area of initial cyclone development 6-12 hours later. The region of confluence between the two jets is highly favorable for upper-level frontogenesis and jet intensification. Temperatures of -52° C characterize the northern jet streak while the southern jet streak has warmer temperatures of approximately -42° C associated with it. Confluent flow in the presence of a temperature gradient leads to frontogenesis. The frontogenesis acts to increase the horizontal temperature gradient perpendicular to the jet axis, which then requires an accel-

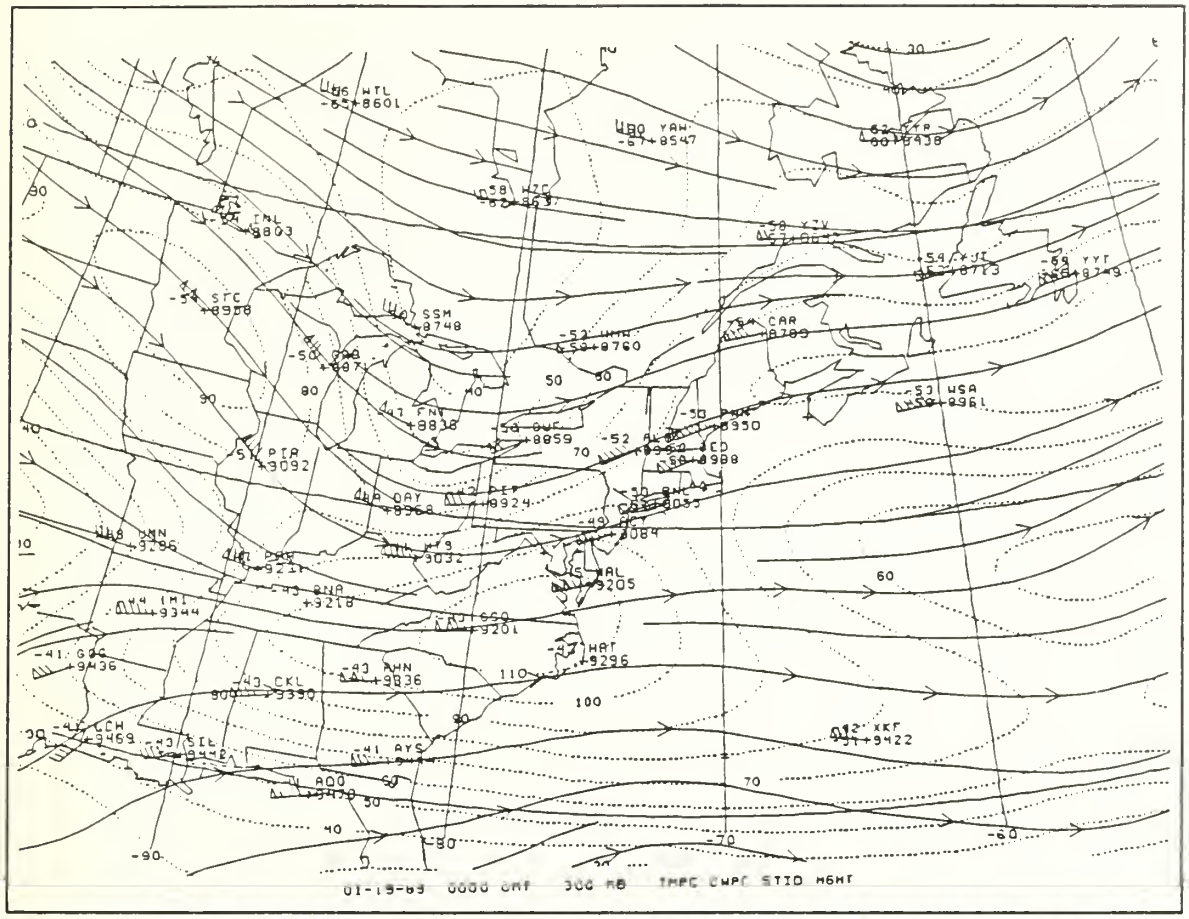

Fig. 2. 300 mb NMC Final Analysis at 19/0000 UTC Jan 89: Isotachs (dashed) every 10 kt and streamlines (solid).

eration of the zonal flow to maintain geostrophic balance. Evidence that jet intensification and frontogenesis are occurring in this case is reflected in the winds aloft over Norfolk, Virginia (ORF) at 0300 UTC, which had a wind increase from 100 kt to 140 kt in 3 hours. The winds aloft also increased at Greensboro, North Carolina (GSO) from 105 kt to 130 kt between 0000 UTC and 0600 UTC, which further indicates the upper-level frontogenesis.

With the jet maximum over ORF by 0300 UTC, the left-front quadrant of the southern anticyclonic jet streak is over the cyclogenesis region off the coast of North Carolina-Virginia. The secondary transverse circulation in the jet exit region contributes to increased divergence aloft and possibly enhances development of the surface disturbance. This structure is similar to that seen in studies by Kocin and Uccellini (1990),

Uccelini et al. (1987), Wash et al. (1988), and Elsberry and Kirchoffer (1988), which placed the incipient cyclone in the left-front quadrant of a upper-level jet streak.

B. 0600 UTC 19 JANUARY 1989

The best evidence for upper-level divergence in the left-front quadrant of the intensifying jet is provided by the satellite imagery. The satellite imagery at 0600 UTC (Fig. 3) shows deep cloudiness has developed off the coast of North Carolina/ Virginia, which is in the jet exit region. At the surface, an open-wave trough is indicated by the Sanders (1989) analyses with several possible circulation centers visible in the 0600 UTC GOES satellite image. The enhanced infrared satellite imagery shows a widespread area of cloudiness extending from 33° N to 42° N between 63° W and 73° W. The colder cloud tops to the north are associated with a low-level circulation center to the north,

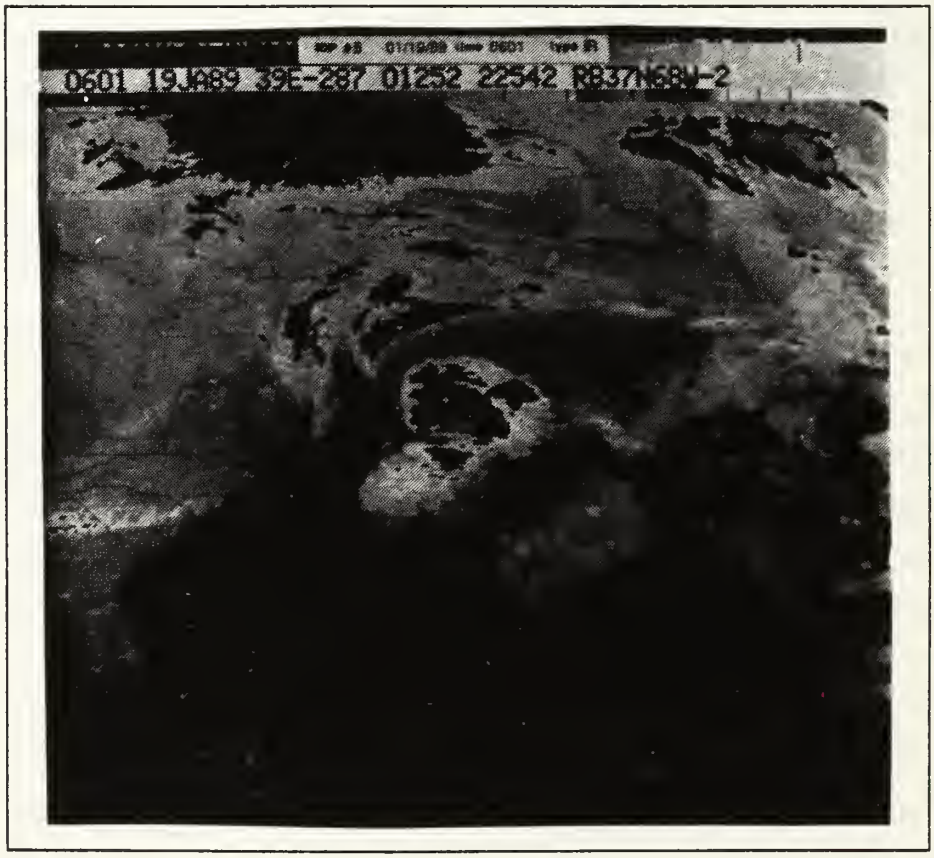

Fig. 3. GOES enhanced infrared imagery for 19/0601 UTC Jan 89.: U.S. East Coast sector

while the warmer cloud tops to the south are associated with the open- wave trough and developing vorticity center in the cyclogentic region.

The 850 mb analysis of height and temperature (Fig. 4) shows a broad baroclinic zone forming with slight cold air advection upstream from the trough axis and stronger warm air advection just downstream from the trough axis. The satellite imagery reflects this structure, as the enhanced upward motion in the warm frontal region of the open-wave trough coincides with the colder convective cell that is isolated in the southernmost cloud mass. Low-level wind convergence as documented by aircraft flight level winds and dropsonde winds across the base of the trough also contributes to surface pressure falls

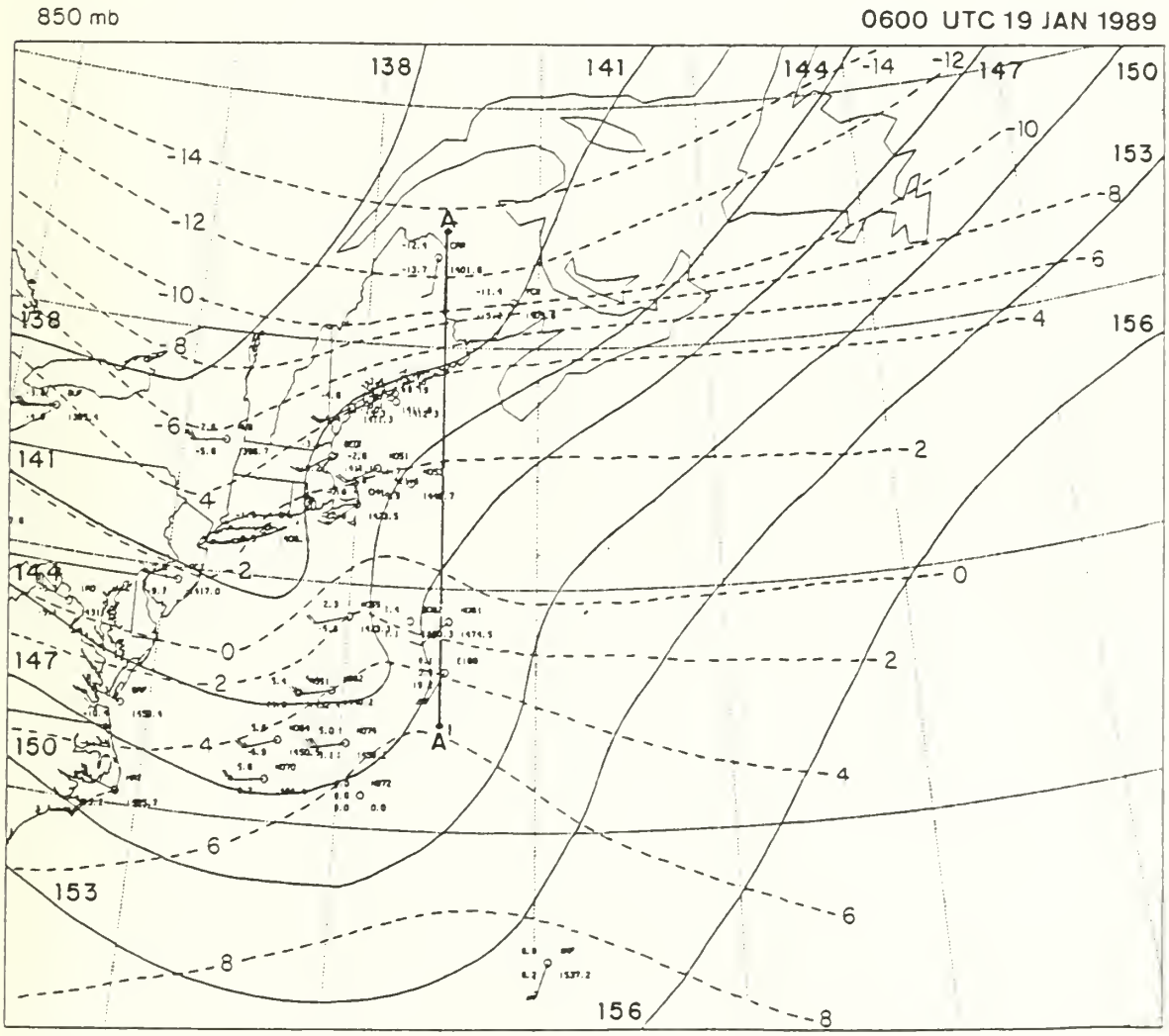

Fig. 4. 850 mb analysis at 19/0600 UTC Jan 89: Height (solid) every 30 m and temperature (dashed) every 2 °C.

in the base of the trough. The development of a low-level cyclone is supported the approach of a 500 mb short-wave trough (Fig. 5), which has just passed the coast. This position is consistent with the jet maximum aloft, and both indicate upper-level divergence and PVA over the surface and the 850 mb open wave. The trough has moved several hundred miles from the Ohio Valley to just off the East Coast in 6 hours. The NMC final analysis of 500 mb heights/vorticity (not shown) indicates a vorticity maximum in excess of $20 \times 10^{-5} s^{-1}$ over New Jersey providing strong (PVA) over the surface disturbance. The magnitude of the PVA may be stronger due to the underestimate of the jet intensity by the NMC final analyses.

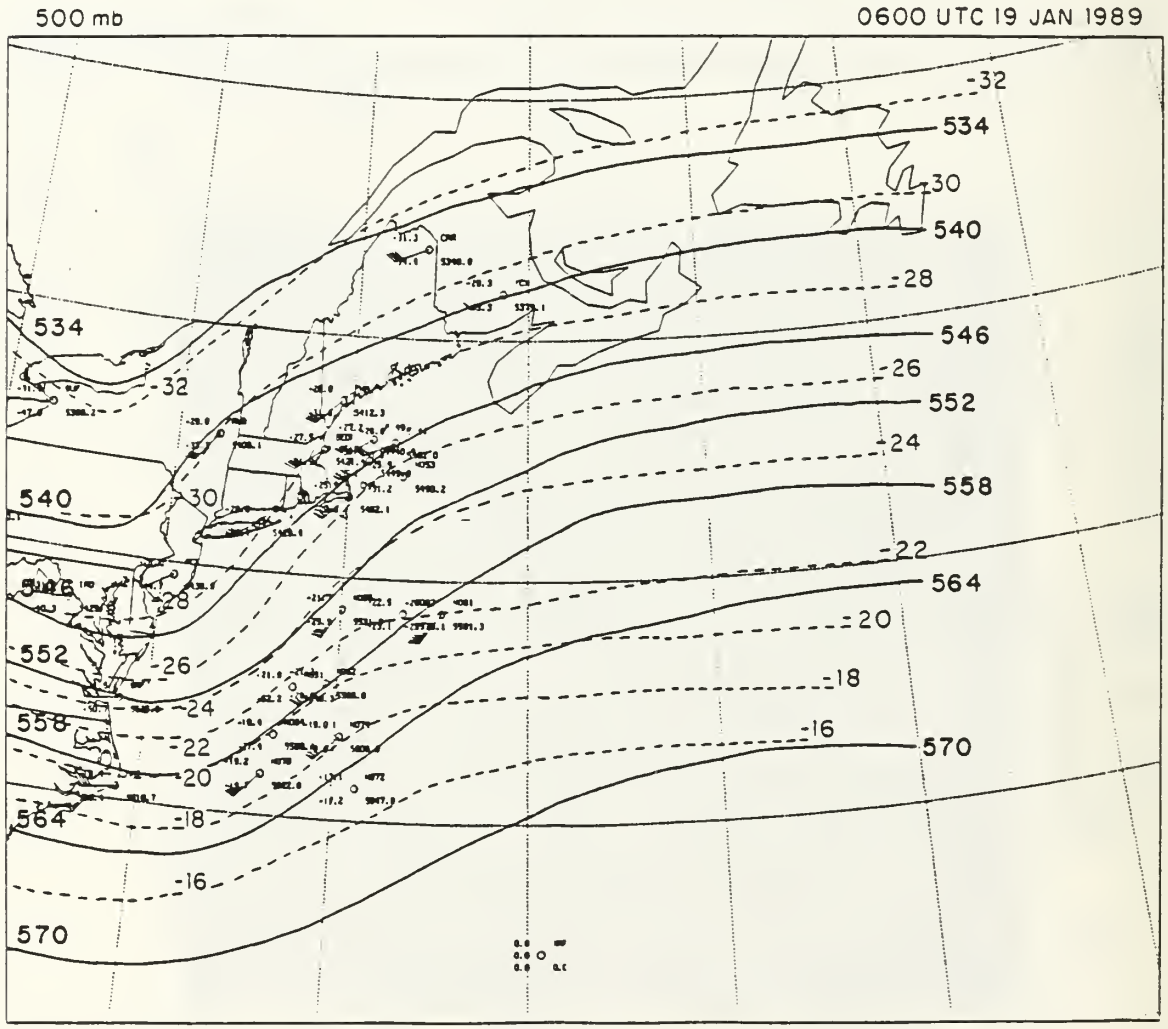

Fig. 5. **500 mb analysis at 19/0600 UTC Jan 89:** Height (solid) every 60 m and temperature (dashed) every 2 °C.

The strong confluence and upper-level frontogenesis in the Virginia North Carolina region is strengthening as the upper-level trough amplifies along the coast, as seen in the soundings from Huntington, Virginia (HTS) and Pittsburg, Pennsylvania (PIT). The 300 mb winds at HTS and PIT have shifted to the northwest with speeds increasing as much as 25 kt. To the south, westerly winds in the base of the trough at GSO have increased from 100 kt to 130 kt between 0300 and 0600 UTC, which is further evidence of the strong frontogenesis and confluence occurring over the region.

The 400 mb analysis (Fig. 6) shows a broad trough over the coast, which is consistent with the lower levels. The sounding and aircraft wind reports near the coast indicate the core of 90 kt or greater winds to be over HAT and extending out to about 37.5° N 70° W, which is near the area of cyclogenesis. Although the aircraft winds are not precisely at 400 mb, the aircraft at 70° W and 67.5° W are at similar pressure levels (approximately 420 mb). The wind decreases from 90 kt to 70 kt in this region, which indicates the exit region of the jet streak. Upstream from the coast, the Dayton, Ohio (DAY) and HTS soundings indicate 400 mb wind speeds in excess of 100 kt in the northwesterly flow. South of this jet core is a relative minimum of 60 kt near Nashville, Tennessee (BNA) and Atlanta, Georgia (AHN) and then stronger winds again further south. This indicates two separate jets still providing confluence in the base of the trough. The dewpoint analysis at 400 mb (Fig. 7) shows a dry tongue along the axis of the southernmost jet as well as an axis of dry air to the northwest across New York, which supports the dual jet structure. Aircraft observations as well as LeSondes dropped in the region verify the very low dewpoint temperatures of -50° C to -60° C and 30° C dewpoint depressions associated with the jet in the trough. About 250 km to the east, aircraft reports of -35° C with only 6-8° C dewpoint depressions indicate the tremendous moisture gradient from the very dry, clear air to the nearly saturated air in the deep clouds in the warm sector of the surface low seen in Fig. 3.

To examine the developing warm frontal structure to the east of the surface low, cross-sections of equivalent temperature (θ) and equivalent potential temperature (θ_e) across the warm front were constructed from sounding, dropsonde and flight-level aircraft data. The cross-section of θ (Fig. 8a) indicates a relatively broad, shallow warm front at this stage of development, with very little packing of isentropes at the warm front near N061. The cross-section shows a fairly stable planetary boundary layer (PBL) throughout the warm frontal region. The left-front jet exit region is about 100 km southeast of the cross-section as seen in Fig. 6 at 400 mb where the winds decrease from 90 kt to 65 kt near sounding N061. The lone aircraft report of 75 kt south of N061 at

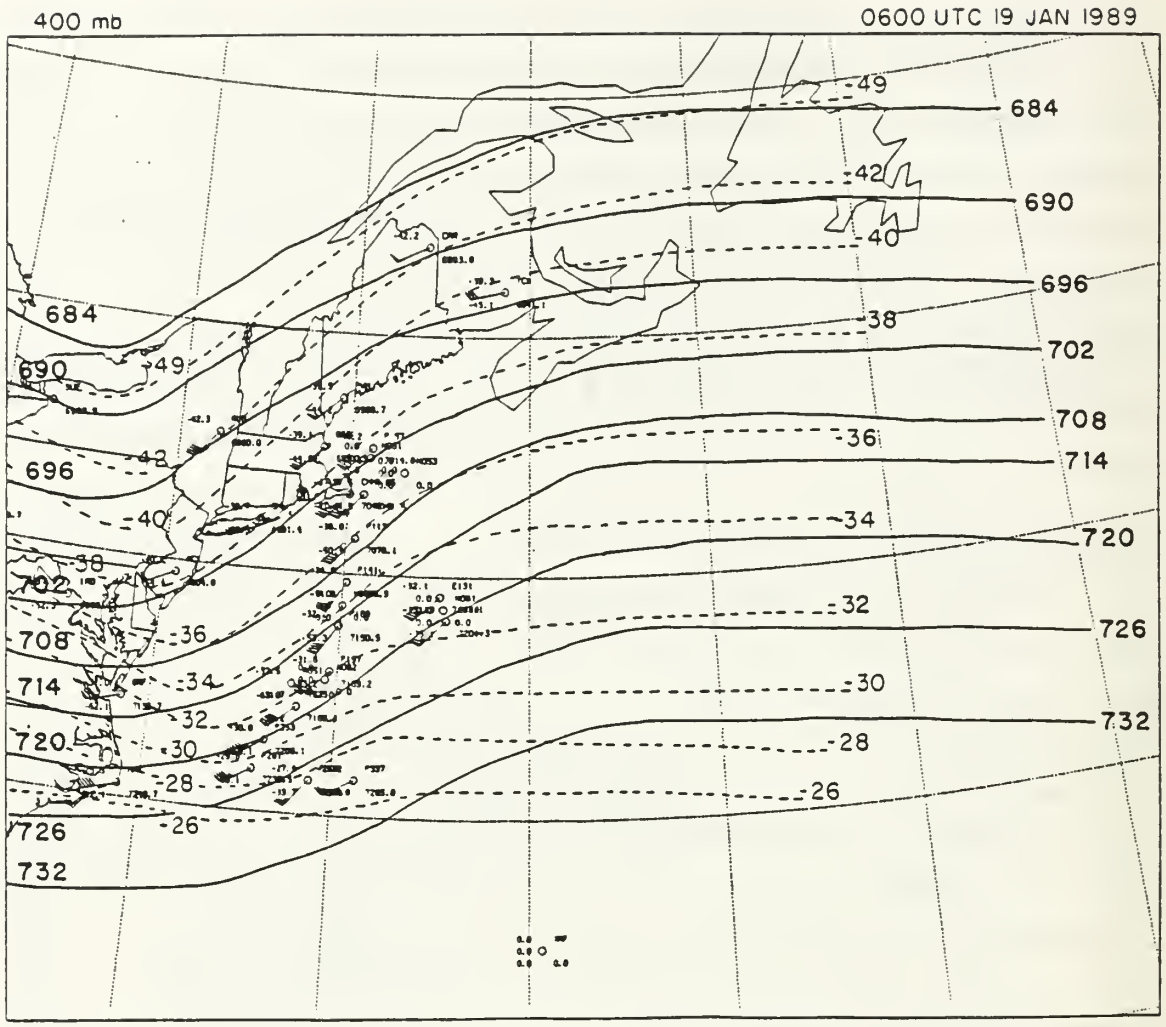

Fig. 6. 400 mb analysis at 19/0600 UTC Jan 89: Height (solid) and temperature (dashed) as described in Fig. 5.

420 mb and the tighter packing aloft also confirms the jet location to the southeast. The Caribou, Maine (CAR) and Gagetown, New Brunswick (YCX) soundings show the extent of the northern jet streak with winds in excess of 100 kt at 300 mb. The cross-section of θ_e (Fig. 8b) shows that the region north of the warm front is characterized by moist potential instability in the boundary layer. The warm frontal region indicated by the tightly packed θ_e contours exhibits moist potential instability through a deep layer in and south of the warm front in the convectively active region seen in the 0600 UTC satellite imagery.

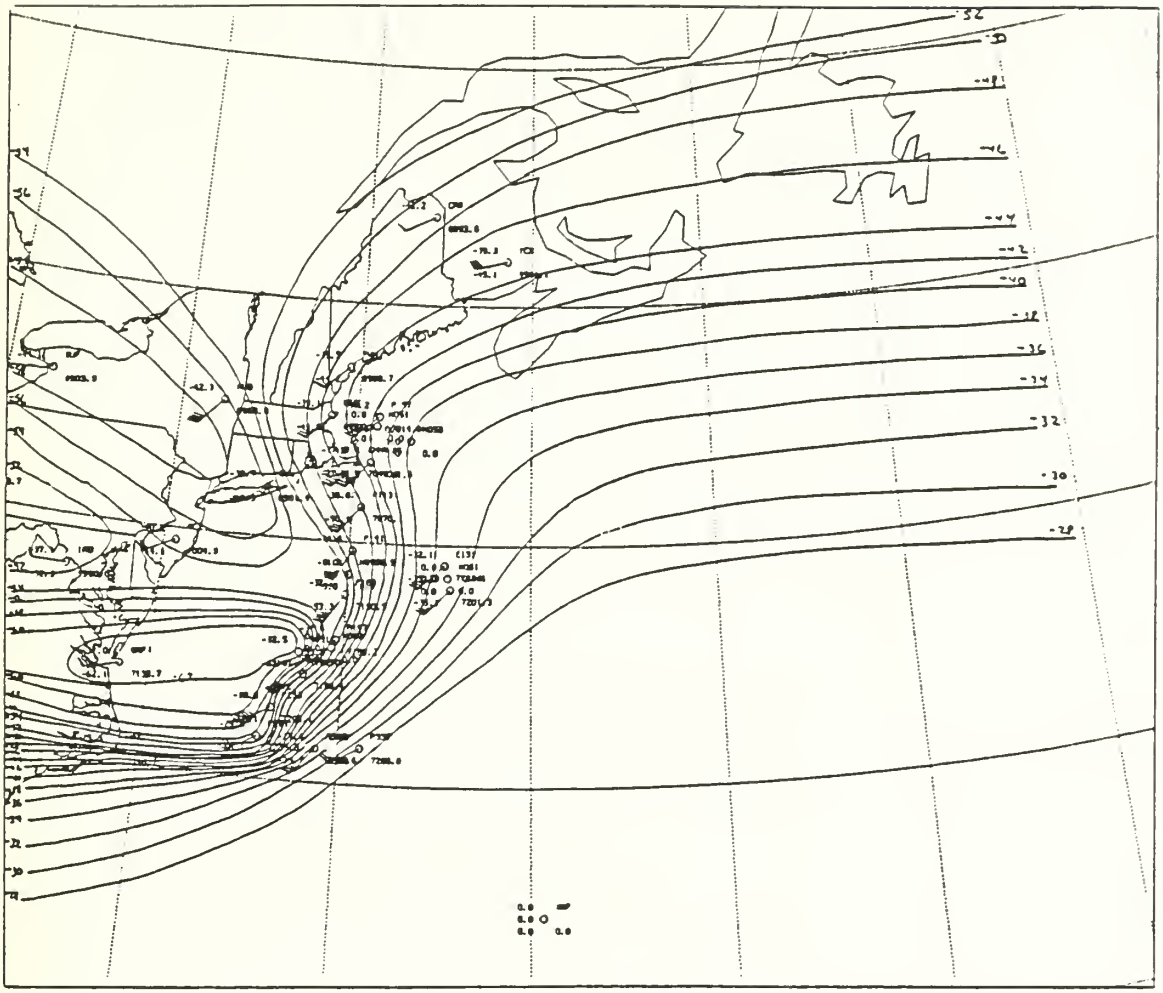

Fig. 7. 400 mb dewpoint analysis at 19/0600 UTC Jan 89: Dewpoint contours every 2 °C.

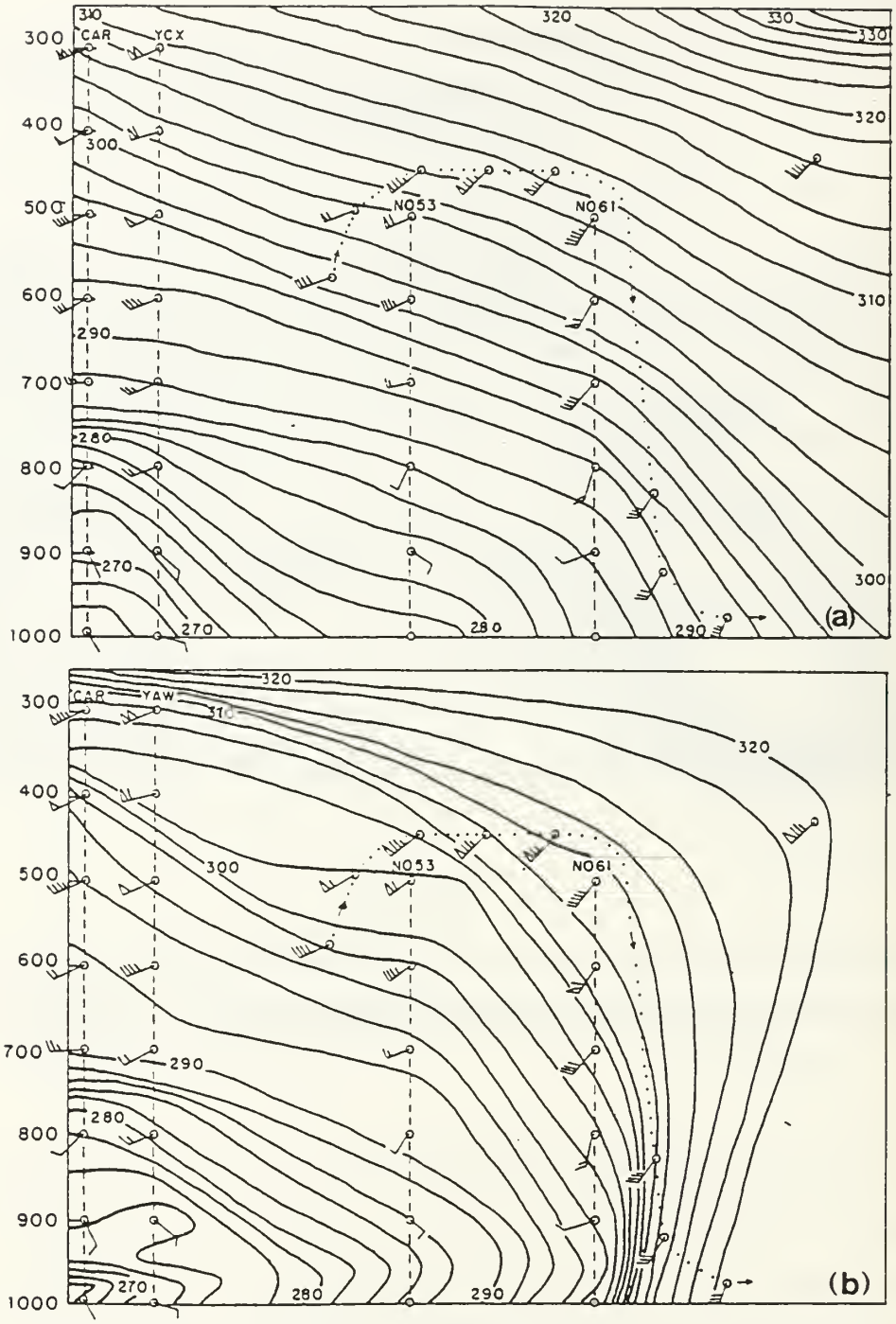

Fig. 8. 19/0600 UTC 19 January 1989 Cross-sections: (a) Cross-section of potential temperature and (b) equivalent potential temperature every 2 K along projection line AA′ shown in Fig. 4. Flight track (dotted line) between 0514 and 0643 UTC.

The upper-level front and jet stream intensifies tremendously in the period from 0600-0900 UTC. The soundings along the coast of North Carolina and Virginia show the level of maximum wind steadily rising between 0600 and 1200 UTC as well as increasing wind speeds. This is evident in the dramatic increase in wind on the coast of North Carolina at HAT. The 300 mb wind speed increased 75 kt between 0600 and 0900 UTC, from 80 kt out of the southwest to 155 kt out of the west. The 0900 UTC sounding (Fig. 9) indicates the upper-level front and tropopause fold is at approximately 350 mb. A 50 kt wind shear just below the jet maximum indicates that the region of confluence and strengthing of the upper-level front is concentrated in a very narrow layer in the vertical. By 1200 UTC, the winds have increased to 165 kt with the level of maximum winds rising to 250 mb. This gradual increase in the jet maximum from 400 mb up to 250 mb with a rapid wind increase of 75 kt in 3 hours could possibly be indicative of the strength and magnitude of upper-level frontogenesis that is occurring in IOP-5 during explosive cyclogenesis.

C. 1200 UTC 19 JANUARY 1989

The analyses at 1200 UTC 19 January 1989 all indicate that cyclogenesis has begun at all levels. The 1200 UTC satellite image (Fig. 10) indicates an increase in the clouds east and northeast of a 1004 mb surface low pressure center at 39.5° N 65° W. A band of shallow cloud trails to the southwest of the surface low indicating the development of a surface cold front. The cold frontal intensification is reflected in the 850 mb temperature and height analyses (Fig. 11) which show a much tighter baroclinic zone than 6 hours earlier (Fig. 4) in the trough to the southwest of the low center. Associated with this low-level amplification is an apparent increase in the geostrophic cold and warm air advection. The upper-level trough at 500 mb (Fig. 12) has moved 350 km further offshore and deepened considerably in the past 6 hours, with the NMC 500 mb vorticity maximum now in excess of $30 \times 10^{-5} s^{-1}$. Surprisingly, the upper-level trough amplification occurs with little or no height increase downstream of the trough (compare Figs. 5 and 12). The only height increase at this level occurs east of 55° W, which indicates that any thickness increases due to thermal advection in the 1000-500 mb layer to the east of the surface are being realized primarily as surface pressure falls. The 400 mb analysis (Fig. 13) indicates similar amplification of the trough/ridge as well as decreasing 400 mb heights over the cyclone area. The 400 mb isotherm analysis indicates the strongest thermal gradient in the base of the trough, which suggests that the jet maximum aloft is now positioned in the base of the trough.

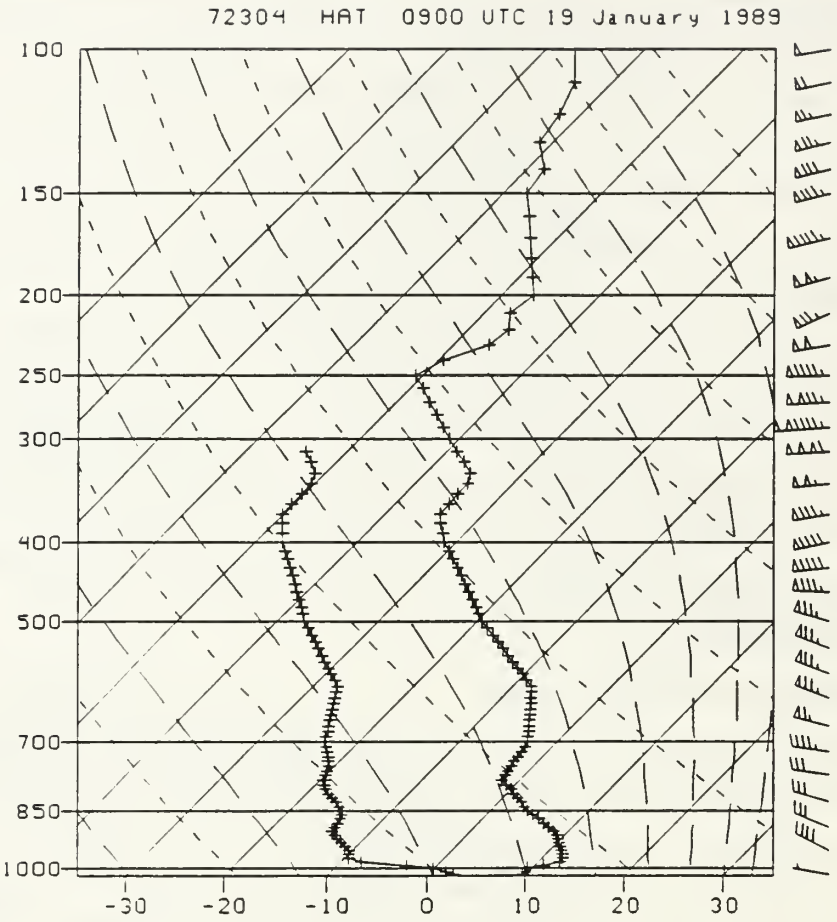

Fig. 9. Hatteras, NC Sounding: Skew T-logP profiles of temperature and dewpoint (°C) and wind speed (kt) at 0900 UTC 19 Jan 89.

The 400 mb dewpoint analysis (Fig. 14) is consistent with this jet position, which places the left exit region directly over the surface low. The multiple jet structure evident at 0600 UTC is still suggested by the dry air that extends across New York from the north and the dry air that extends out from the Mid-Atlantic states, which produces a wedge-shaped dewpoint structure off the Northeast coast. The extremely low dewpoints of -67.5 °C at BNL suggest strong subsidence and possible tropopause folding into the storm approximately 750 km to the west northwest of the surface low. The Bedford, Massacchuetts (BED) soundings (not shown) are typical of the subsidence and drying seen in the mid-troposphere along the coast between 1200 and 1800 UTC. The 400 mb inversion at 1200 UTC corresponding to the upper-level front just discussed in the 400 mb height/isotherm analyses drops to 500 mb at 1500 UTC and 700 mb by 1800 UTC.

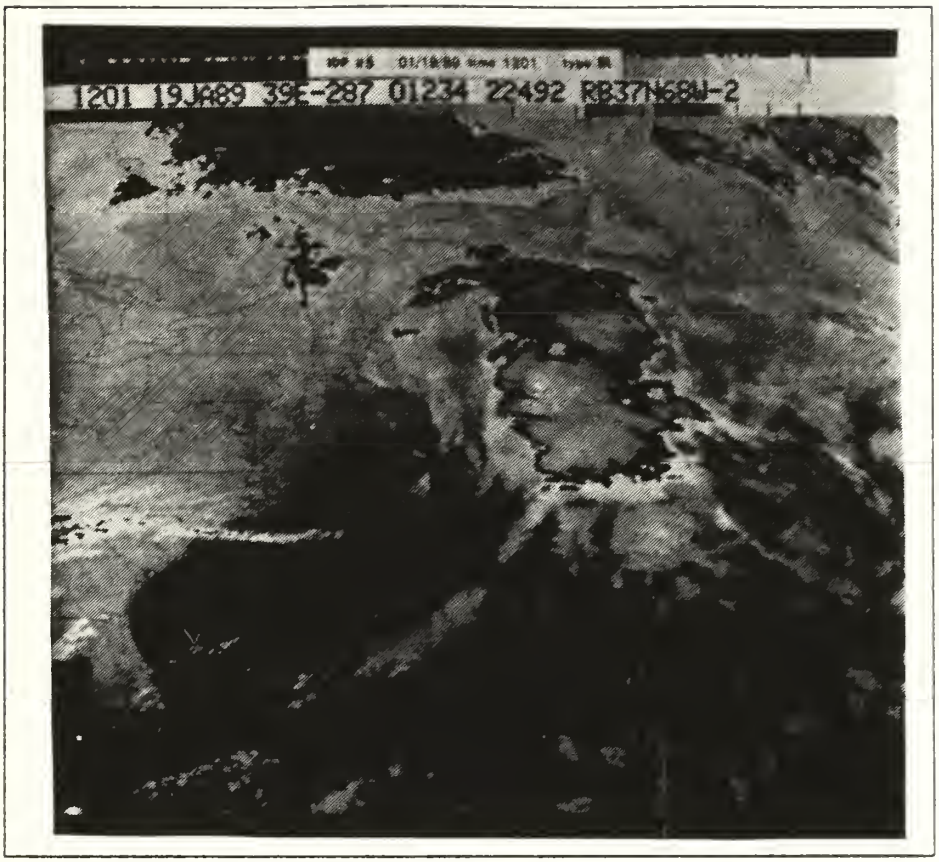

Fig. 10. GOES enhanced infrared imagery for 19/1201 UTC Jan 89.: U.S. East Coast sector

The tropopause folding and stratospheric extrusion occurs prior to and upstream of the surface cyclogenesis, consistent with results from Uccellini et al. (1985), Whitaker et al. (1988), and Reed and Albright (1986). They found that the stratospheric extrusion occurred 1500 km upstream and 12-24 hours prior to rapid cyclogenesis. Although complete analyses were not done, this seems to be the trend in this case also. As will be seen in the next section, IOP-5's most rapid deepening occurred between 1500 and 1800 UTC, just three hours after this exceptionally strong subsidence appeared on the New England coast.

The cross-section of potential temperature constructed along the East Coast (Fig. 15) shows a very sharp upper-level frontal zone between WAL and ORF, which supports the hypothesis that tropopause folding has occured prior to this time. The wind maximum of 140 kt is located between ORF and HAT at 300 mb above the strongest

potential temperature gradient along the coast. The 300° K isentrope has dropped from 550 mb down to 680 mb over ORF since 0600 UTC, which indicates the descent of high θ air in the frontal zone. This upper-level front has intensified since 0600 UTC and is a very good indication of just how strong the upper-level frontogenesis is over North Carolina/Virginia. The structure and intensity of the upper-level front at 1200 UTC are indicative of high potential vorticity values down as low as 600 mb. The strengthening of the upper-level trough and front due to subsidence in the rear of a cyclone was also found in an earlier study by Reed and Albright (1986).

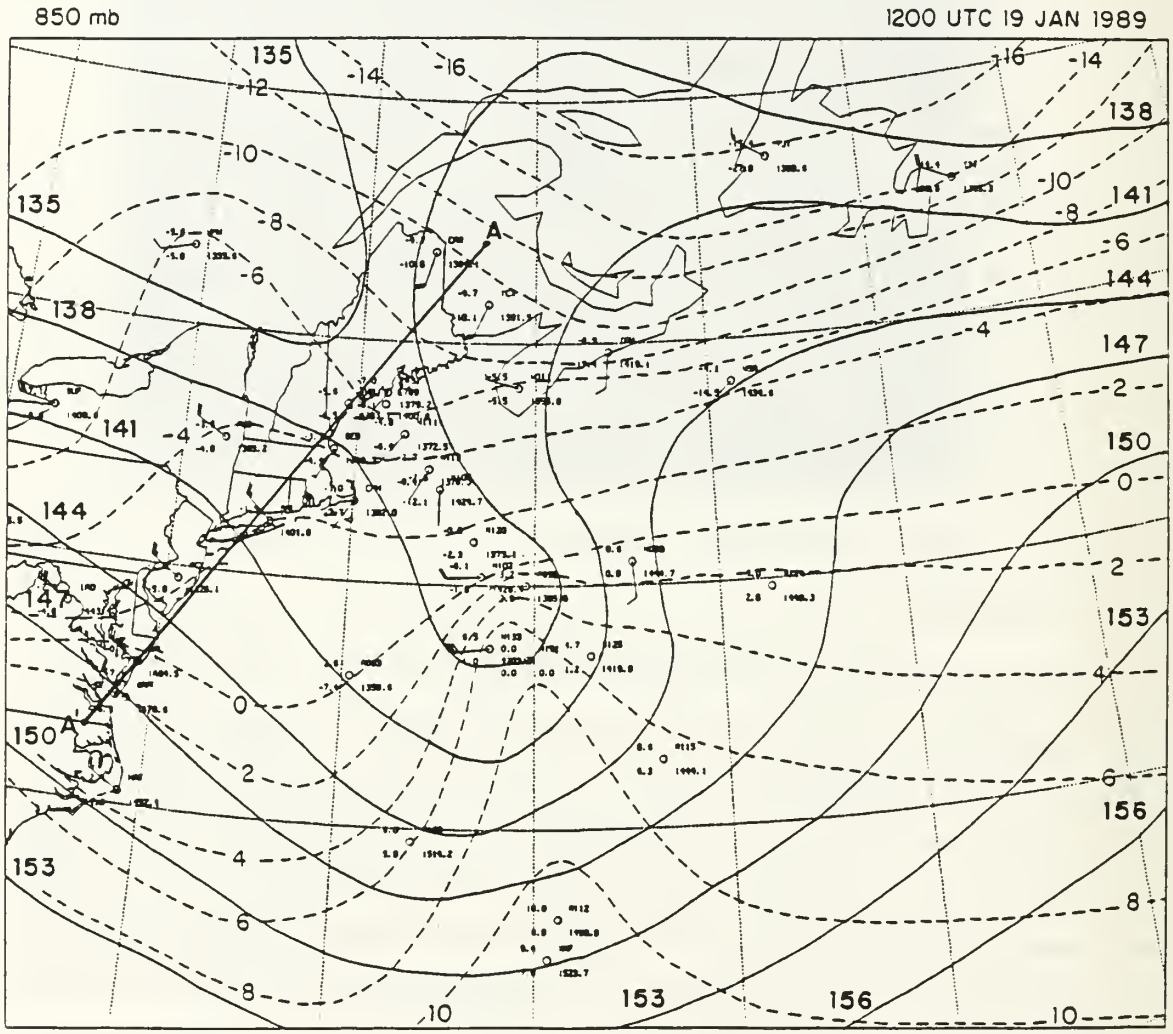

Fig. 11. 850 mb analysis at 19/1200 UTC Jan 89: Height and temperature contours as described in Fig. 4.

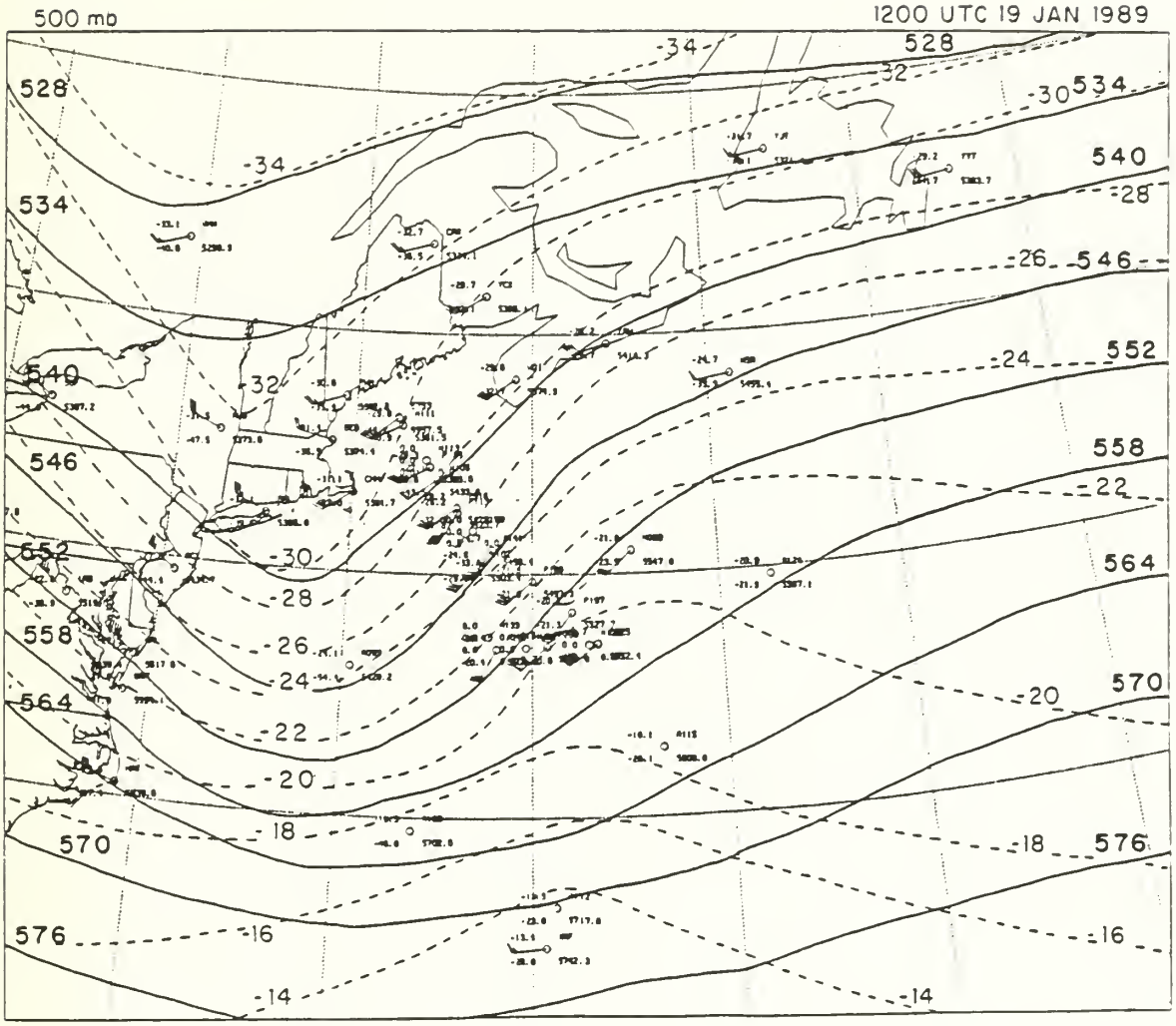

Fig. 12. 500 mb analysis at 19/1200 UTC Jan 89: Height and temperature contours as described in Fig. 5.

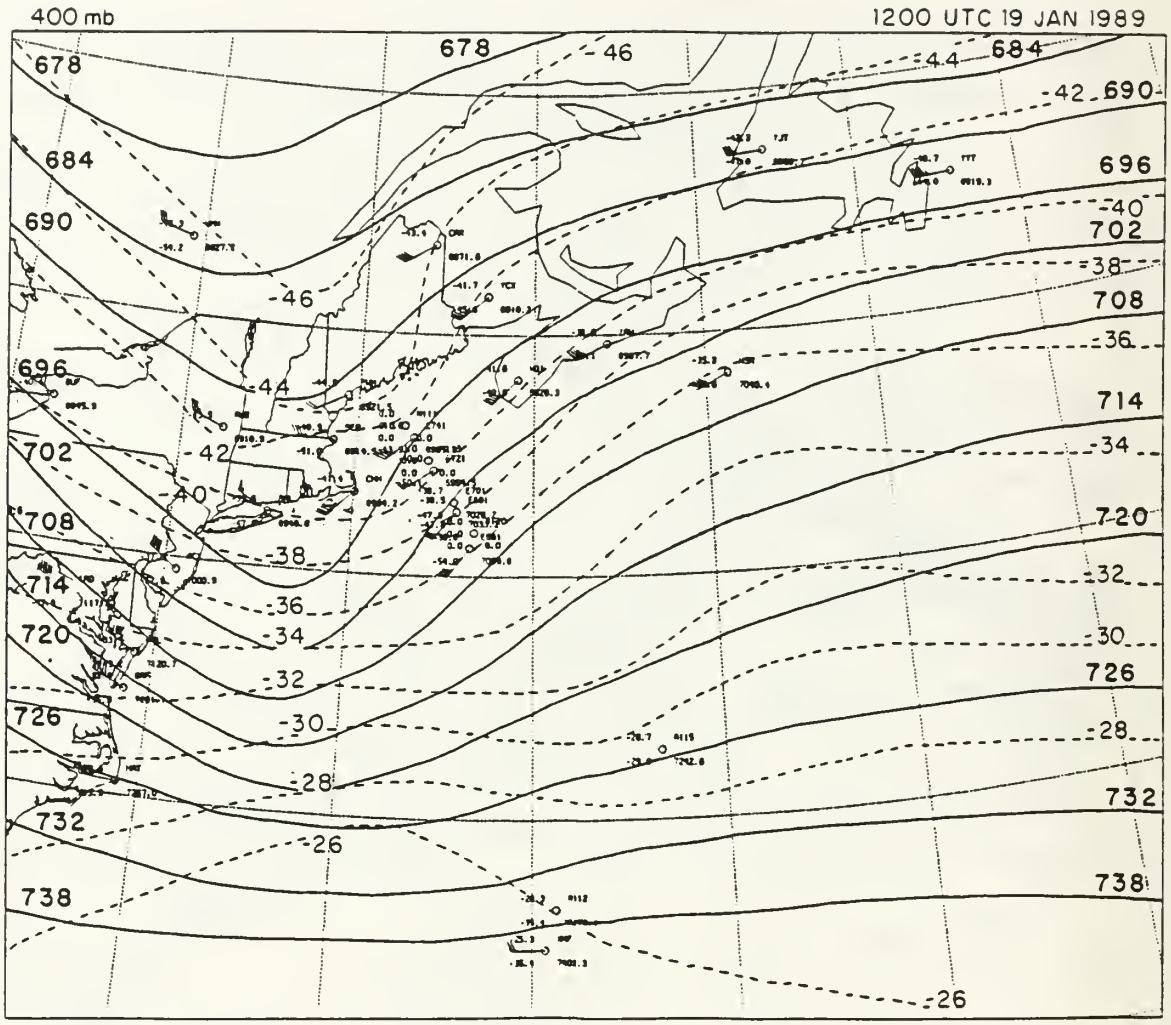

Fig. 13. 400 mb analysis at 19/1200 UTC Jan 89: Height and temperature contours as described in Fig. 5.

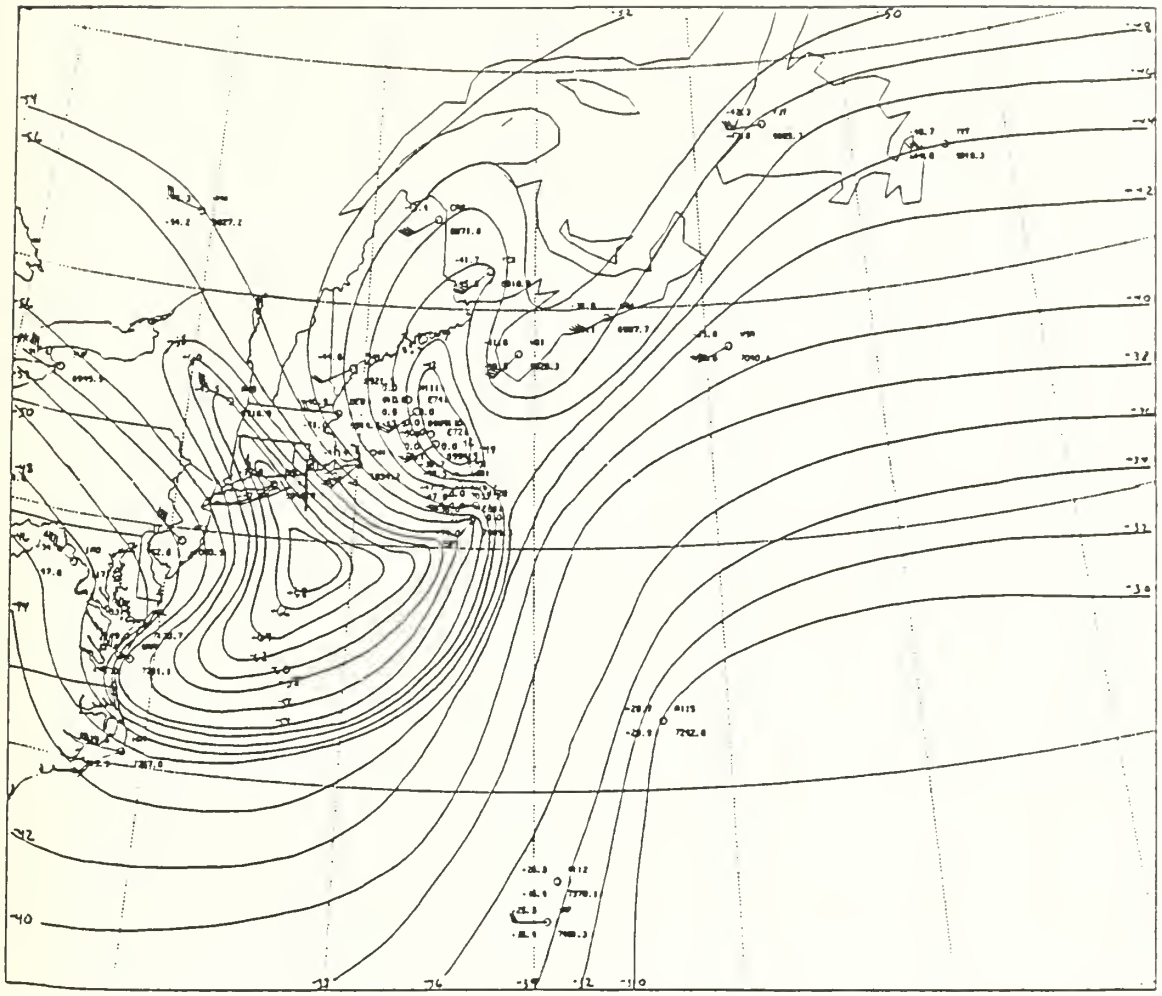

Fig. 14. **400 mb dewpoint analysis at 19/1200 UTC Jan 89:** Dewpoint contours every 2 °C.

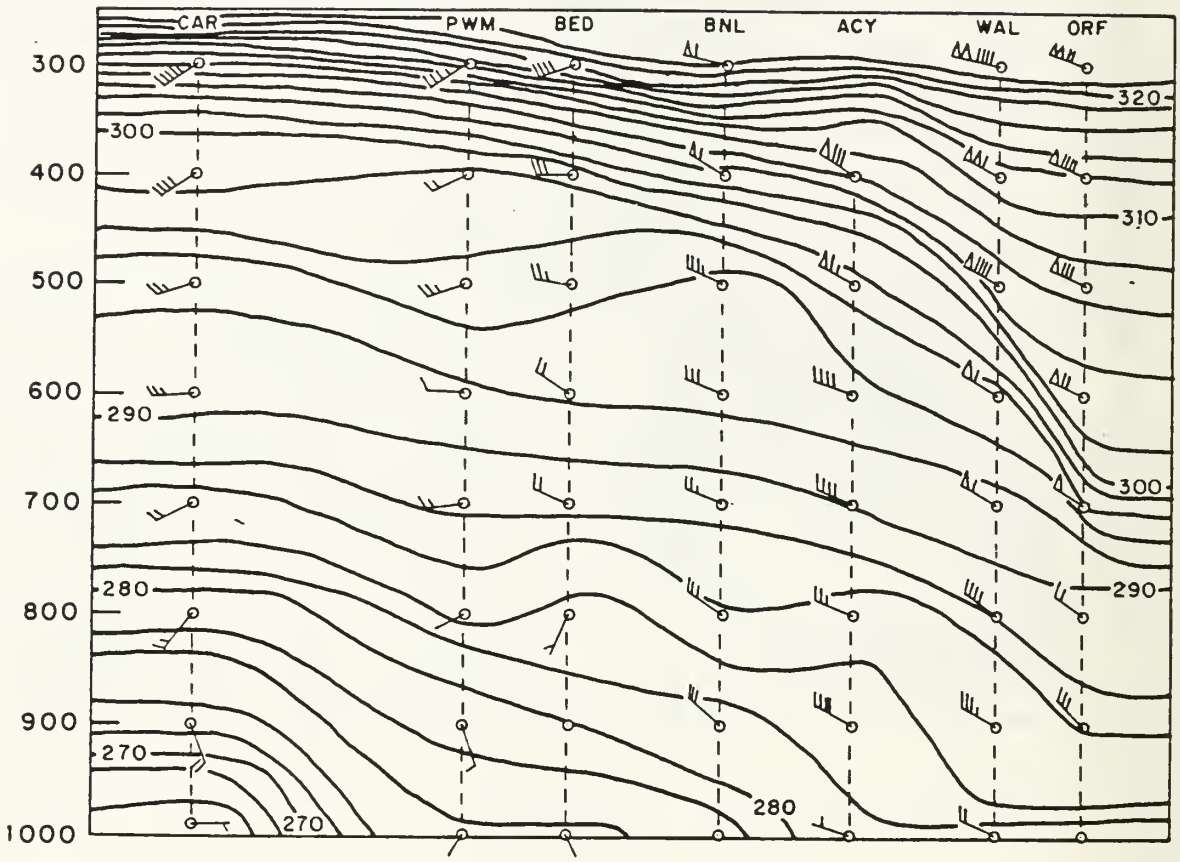

Fig. 15. **19/1200 UTC Jan 89 Coastal Cross-section:** Cross-section of potential temperature every 2 K along projection line AA′ shown in Fig. 11.

D. 1800 UTC 19 JANUARY 1989

Between 1200 and 1800 UTC, the storm deepened by 10 mb and traveled northeast at approximately 40 kt. The most significant drop in central pressure, from 1002 mb to 994 mb, occured in the 3-hour period from 1500-1800 UTC as determined from the Greer (1991) surface analyses. Rapid deepening of the storm since 1200 UTC is reflected in the upper-air analyses at 1800 UTC and the 1800 UTC satellite imagery (Fig. 16) that shows a well defined comma head and cold frontal band with embedded convection. The structure of the developing cyclone at 1800 UTC is characterized by closed circulation centers that stretch from the surface up to 700 mb and substantial increases in the low-level frontal intensity. Height falls of 100m occurred near the 850 mb low center to

produce the closed circulation seen in Fig. 17. The warm front has also contracted into a narrow baroclinic zone that stretches from west of the 850 mb low to the northeast, although the exact intensity of this gradient is uncertain due to the lack of data east of the low. The structure at 700 mb (Fig. 18) is similar to that at 850 mb as the cold air at mid-levels has moved south to a position west of the 700 mb low, as confirmed by flight-level aircraft observations at P907 and the N185 LeSonde to the north. This cold advection west of the 700 mb low results in a stronger temperature gradient west of the low between P181 and N185/P907 (almost 6° C) than in the warm frontal region between P181 and WSA (only 3° C over a longer distance). This suggests that the bent-back frontal structure described by Shapiro and Keyser (1990) occurs through most of the lower troposphere.

The structure aloft is characterized by the 500 mb analysis (Fig. 19), which shows a very short wavelength trough immediately west of the surface cyclone. As mentioned for 1200 UTC, the 500 mb heights have decreased over the entire domain of the surface low, which suggests that the 500 mb trough amplification is due principally to cold air advection. This is confirmed by the 850 mb, 700 mb, and 500 mb analyses (Figs. 17, 18, and 19 respectively), which all show strong cold air advection upstream and in the vicinity of the 500 mb trough axis. Strong cold air advection implies relatively strong descent is occurring, which is supported by the very dry air intruding into the rear of the storm as documented by coastal sounding stations and aircraft observations off the New England coast. BED experienced a 16° dewpoint depression, from -51° C to -67.6° C, between 1200 and 1800 UTC, which suggests strong descent has occured in the region. Aircraft observations approximately 500 km northwest of the surface low also indicate dewpoint temperatures as low as -62° C, which indicates the eastward extent to which the strong subsidence is probably occurring. This strong drying is possibly due to the upper-level front/tropopause fold associated with the very strong jet at 1200 UTC but could not be confirmed due to the lack of data at this time.

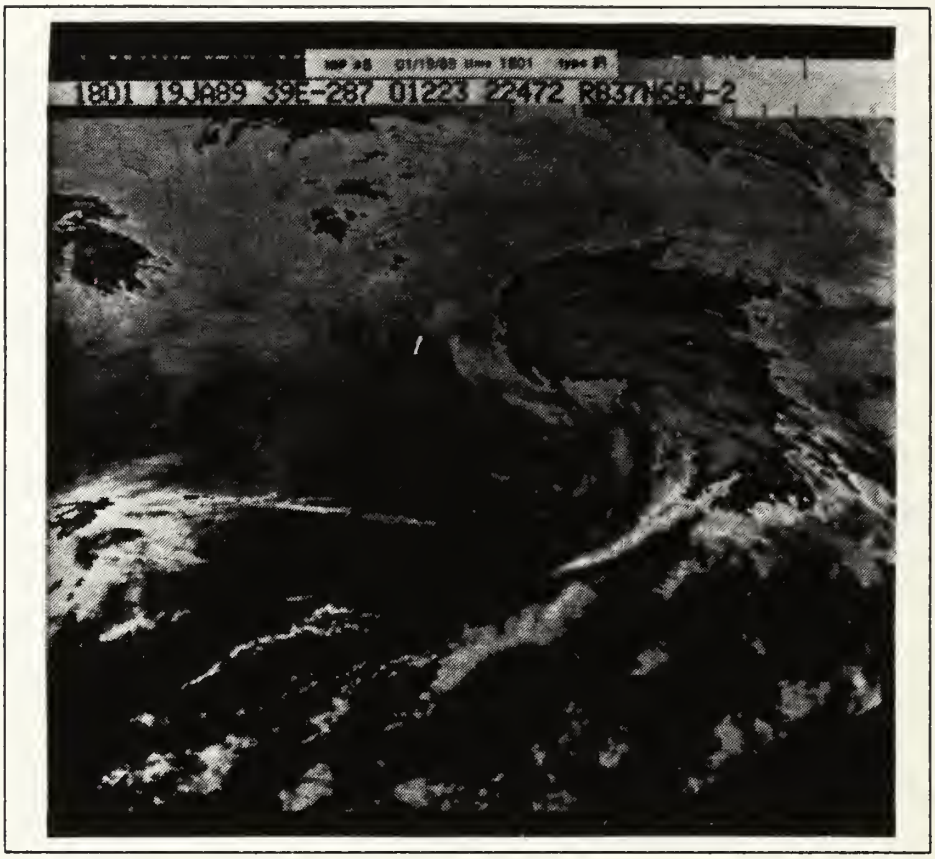

Fig. 16. GOES enhanced infrared imagery for 19/1801 UTC Jan 89.: U.S. East Coast sector

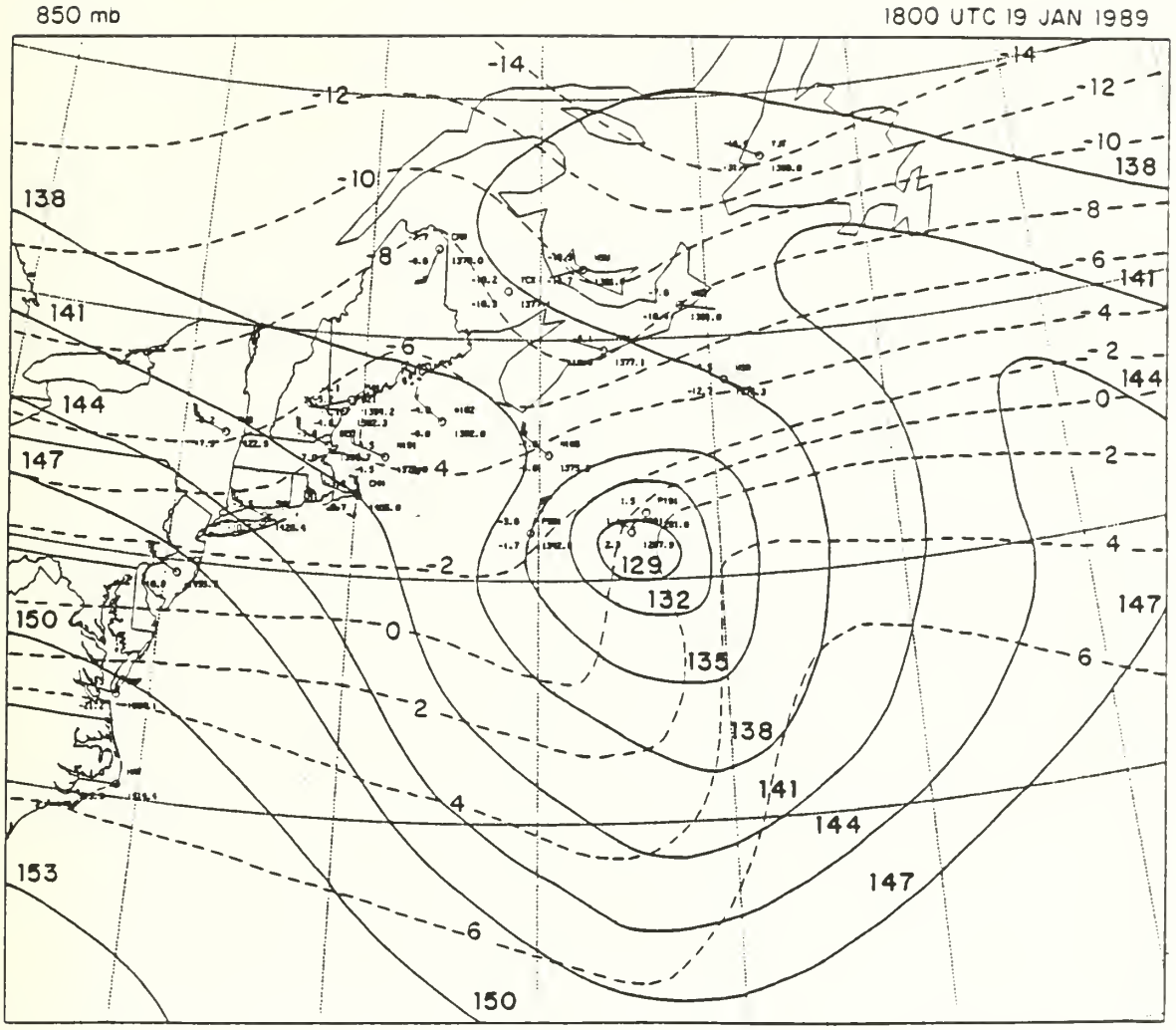

Fig. 17. 850 mb analysis at 19/1800 UTC Jan 89: Height and temperature contours as described in Fig. 4.

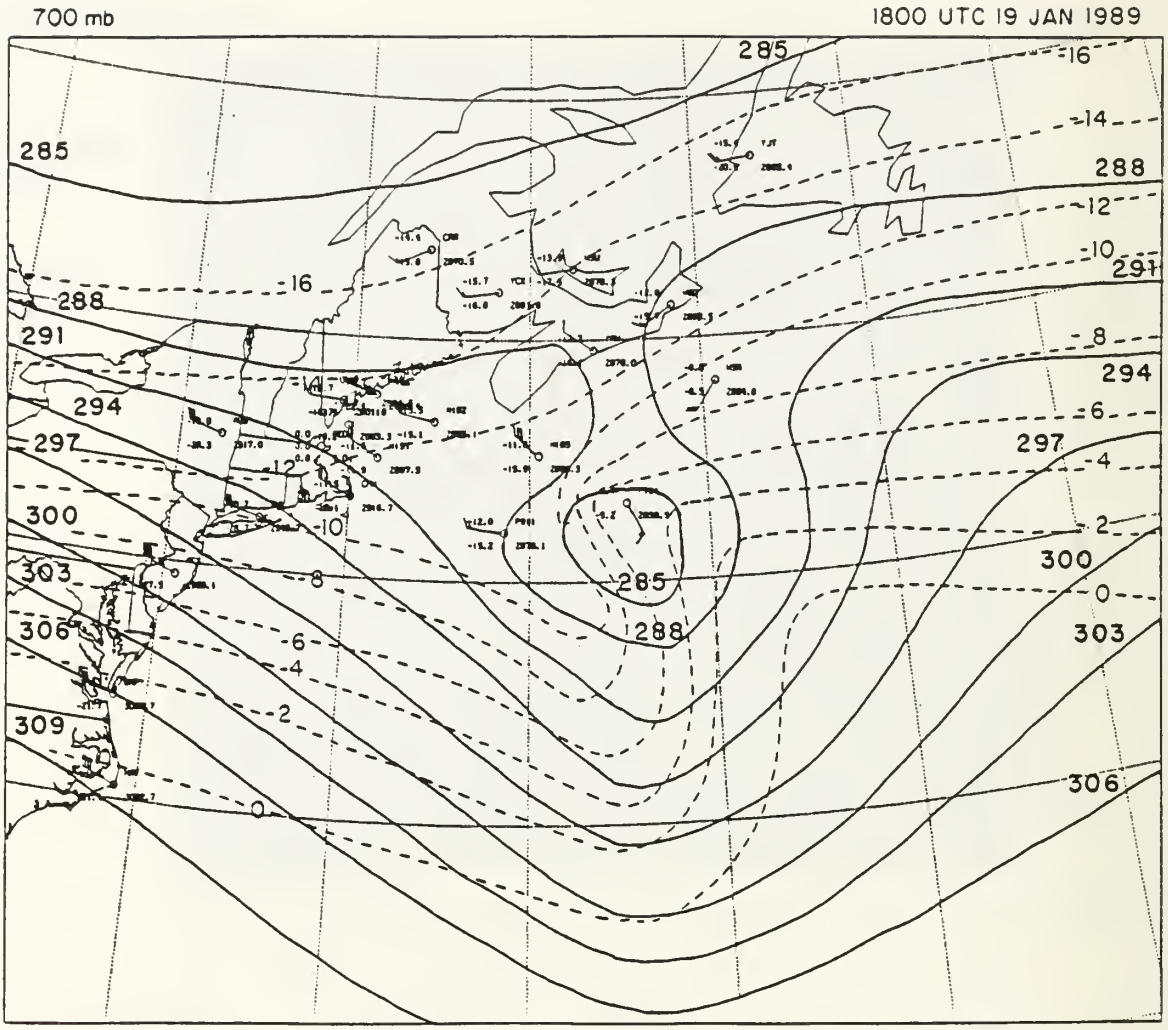

Fig. 18. 700 mb analysis at 19/1800 UTC Jan 89: Height and temperature contours as described in Fig. 4.

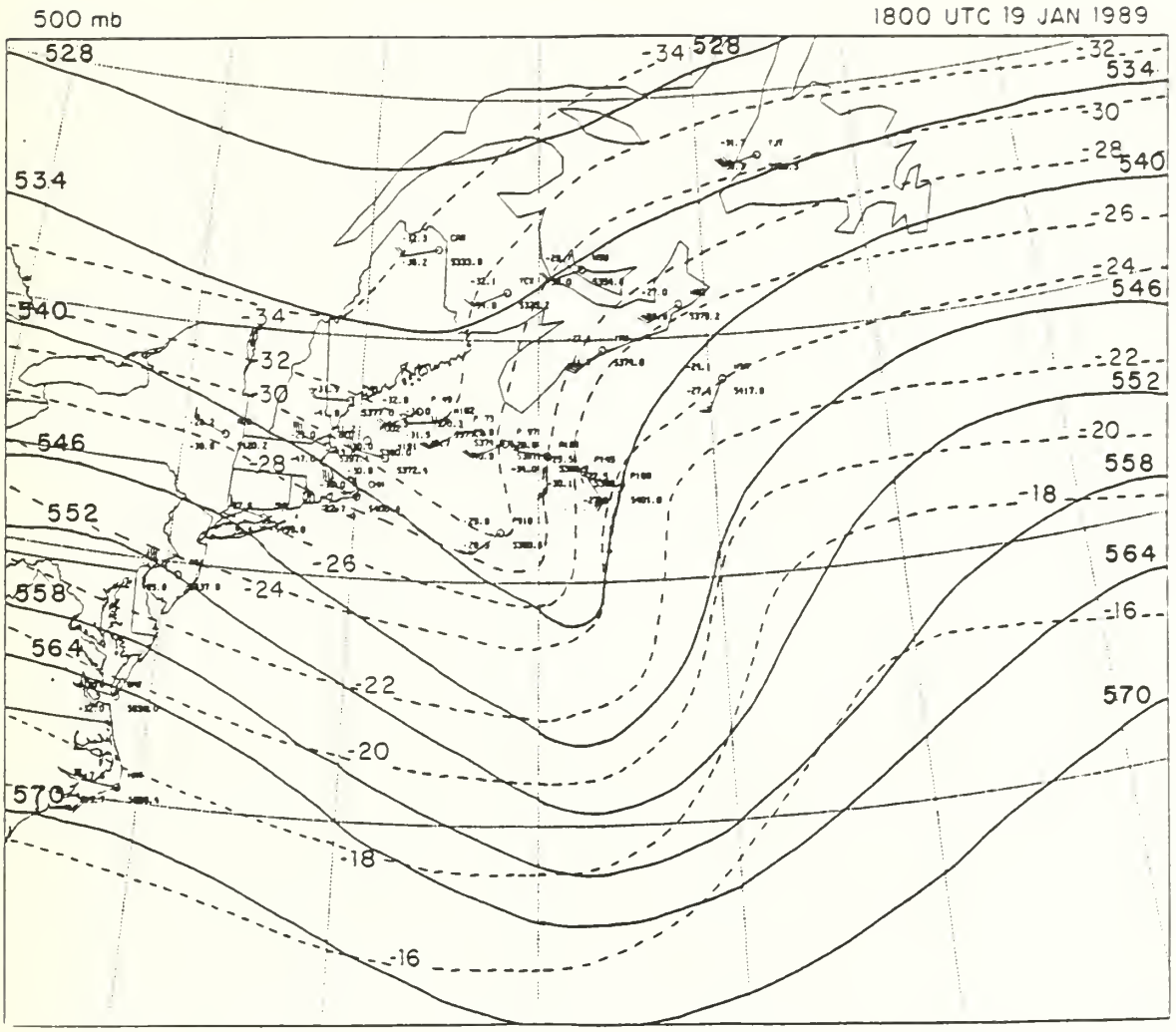

Fig. 19. **500 mb analysis at 19/1800 UTC Jan 89:** Height and temperature contours as described in Fig. 5.

E. 0000 UTC 20 JANUARY 1989

Between 1800 and 20 0000 UTC the storm dropped another 9 mb to a central low pressure of 985 mb. The 500 mb vorticity maximum (not shown) is almost over the surface, which places the strongest PVA to the east of the cyclone center allowing for continued height falls and eastward movement of the storm.

The analyses and the 20 0000 UTC enhanced infrared (EIR) satellite imagery (Fig. 20) indicate that the cyclone is beginning to occlude as the comma head cloud has wrapped around the low. The intensity of the storm is evident in the strong winds and tight temperature gradients observed in the 850 mb analysis (Fig. 21). The temperature

gradient across the 850 mb warm front is 10° C over 300 km, whereas the temperature gradient across the cold front is only 6° C over the same distance. As noted at 1800 UTC, a very strong thermal gradient is also found west of the 850 mb low, which is indicative of the occlusion process. There is very little tilt between the 500 mb low and the surface cyclone at this stage, although the surface low deepens by another 14 mb in the following 12 hours. The 500 mb analysis (Fig. 22) provides further indication that occlusion has began; a 500 mb closed low has formed. This analysis based on the aircraft observations shows that the system is closed off at 500 mb 12 hours earlier than the operational NMC final analysis. More detailed aircraft observations at 400 mb (Fig. 23) show that the circulation is almost closed off at 400 mb as well, with a definite circulation center and the 6960 m contour on the verge of closing off.

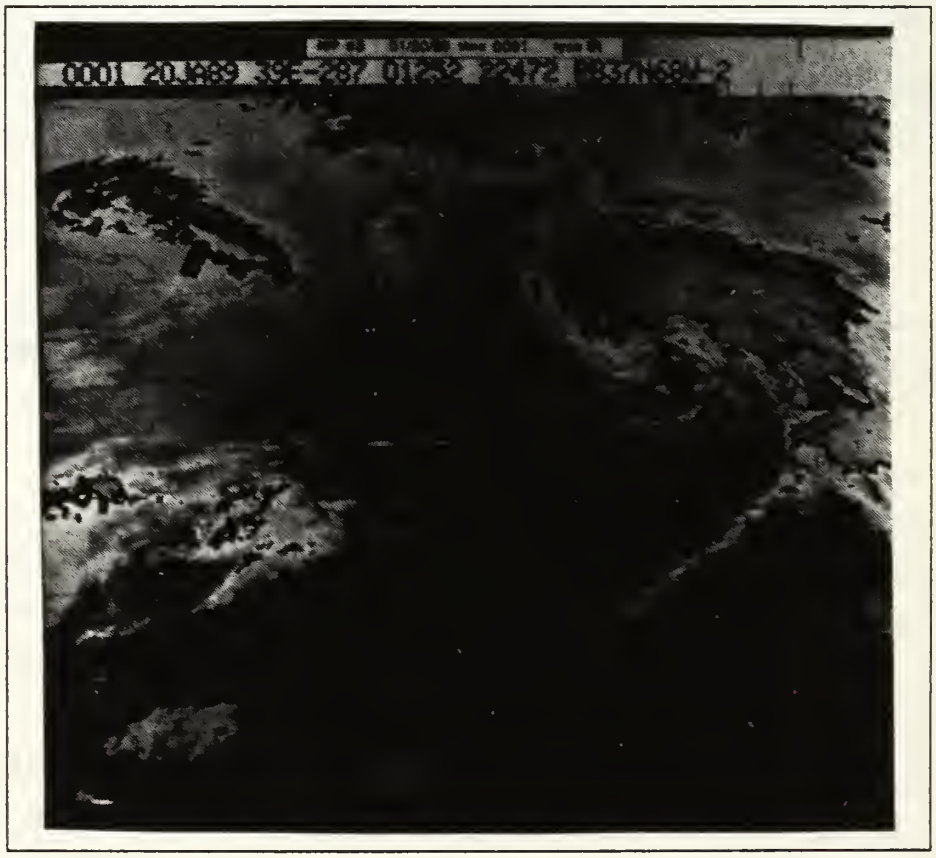

Fig. 20. GOES enhanced infrared imagery for 20/0001 UTC Jan 1989: U.S. east coast sector UTC Jan 89.

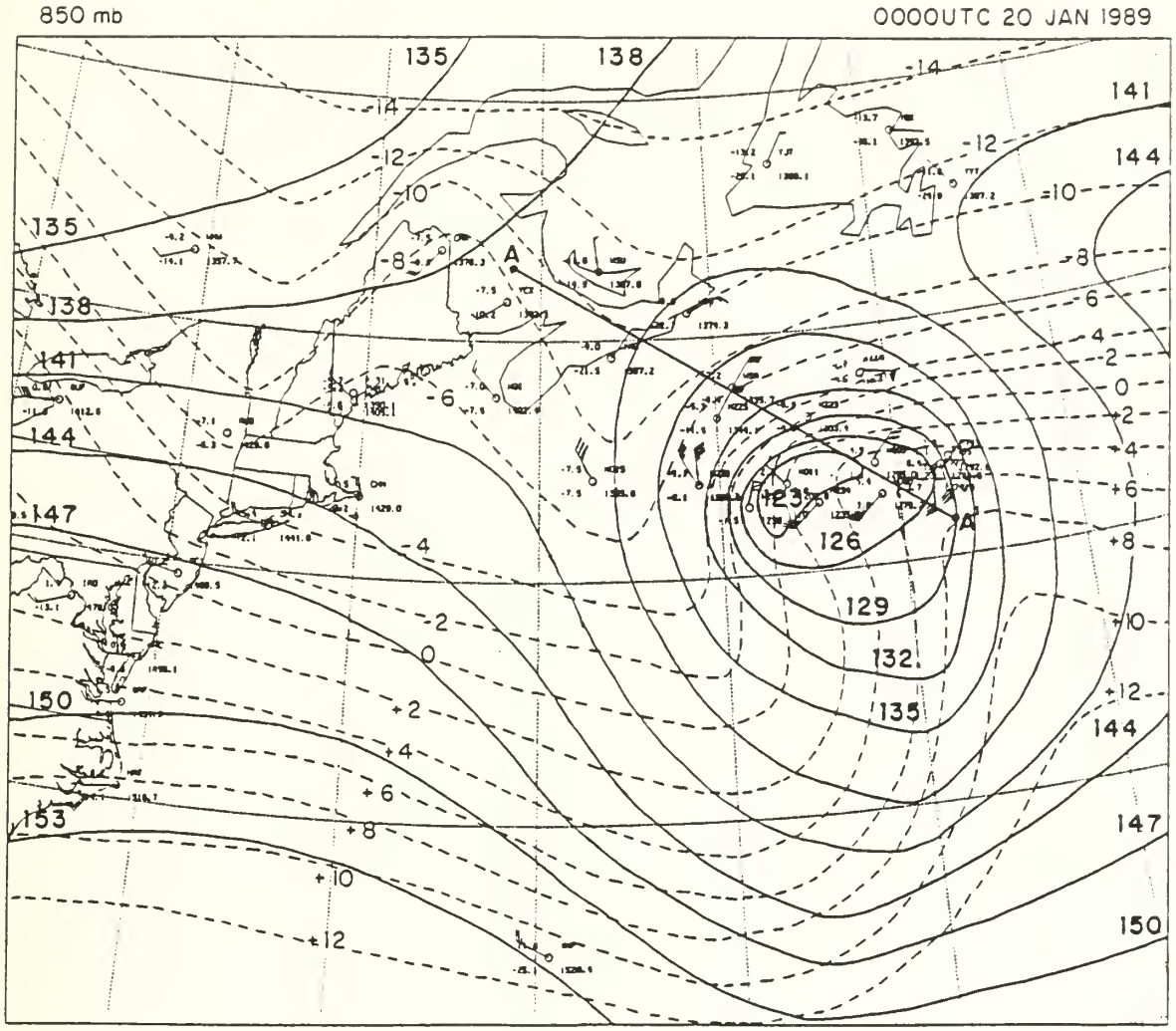

Fig. 21. 850 mb analysis at 20/0000 UTC Jan 89: Height and temperature contours as described in Fig. 4.

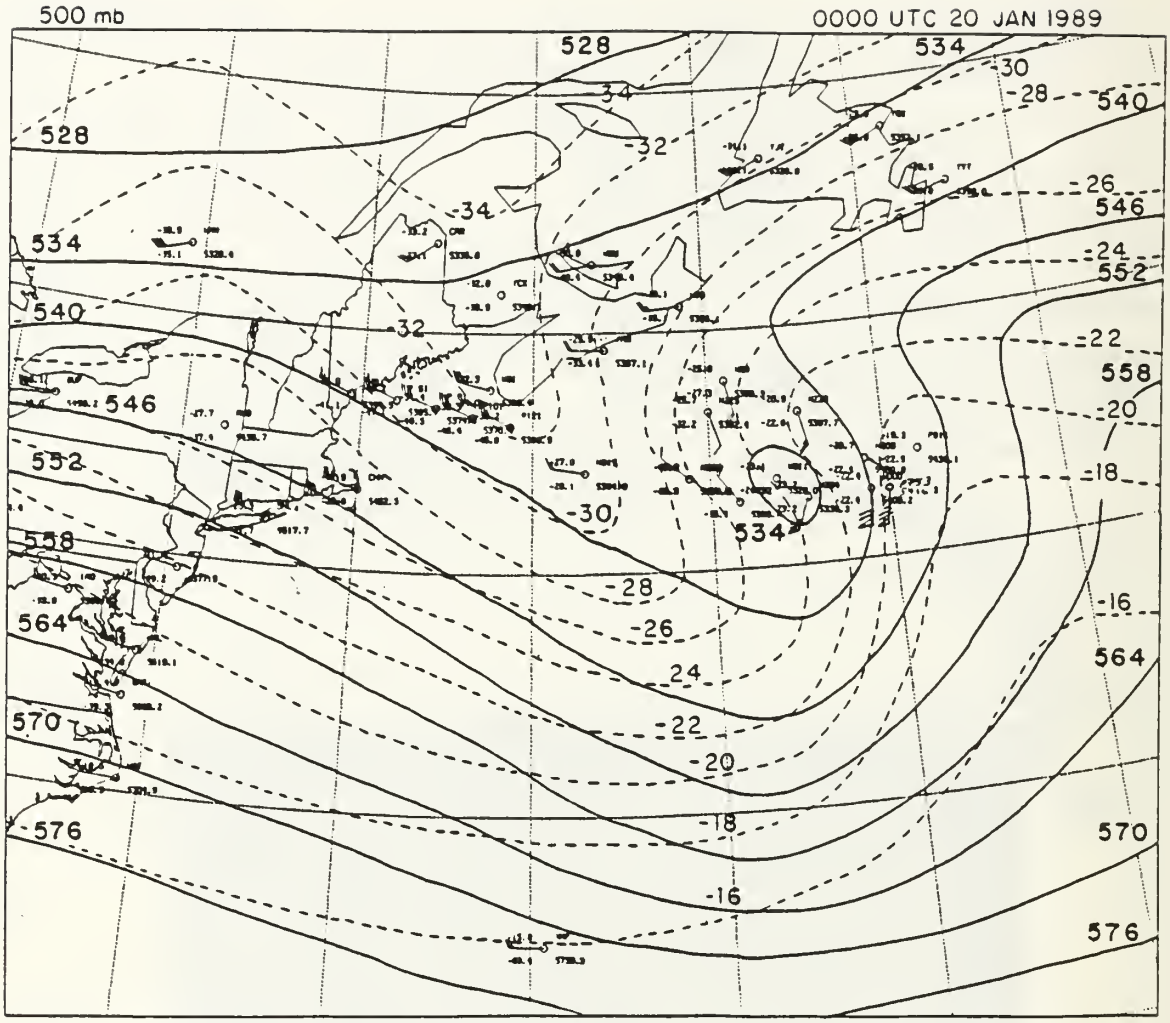

Fig. 22. **500 mb analysis at 20/0000 UTC Jan 89:** Height and temperature contours as described in Fig. 5.

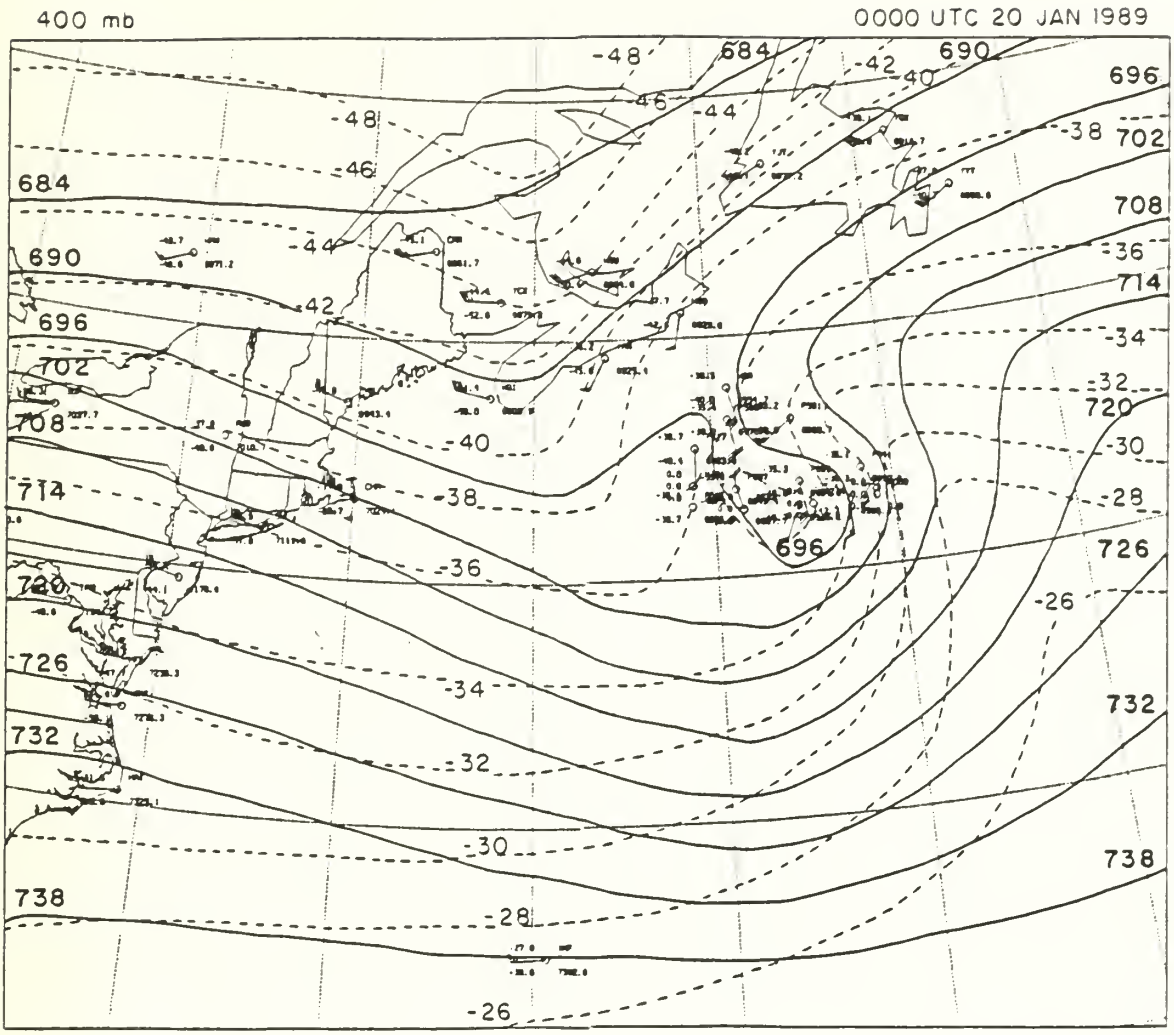

Fig. 23. 400 mb analysis at 20/0000 UTC Jan 89: Height and temperature contours as described in Fig. 5.

F. MESOSCALE ANALYSIS AT 0000 UTC 20 JANUARY 1989

To examine the mesoscale structure and dynamics occuring in the storm as it begins to occlude at 0000 UTC, detailed analysis using extensive aircraft and LeSonde and Omega dropsonde observations through the warm front, triple point, and occlusion were done. The most significant feature that appears at all levels of the analyses is the strength and intensity of the thermal gradients and winds as the storm occludes. The 850 mb mesoscale analysis (Fig. 24) shows that the thermal gradient is much tighter across the warm front than the cold front, as seen in the very high amplitude thermal

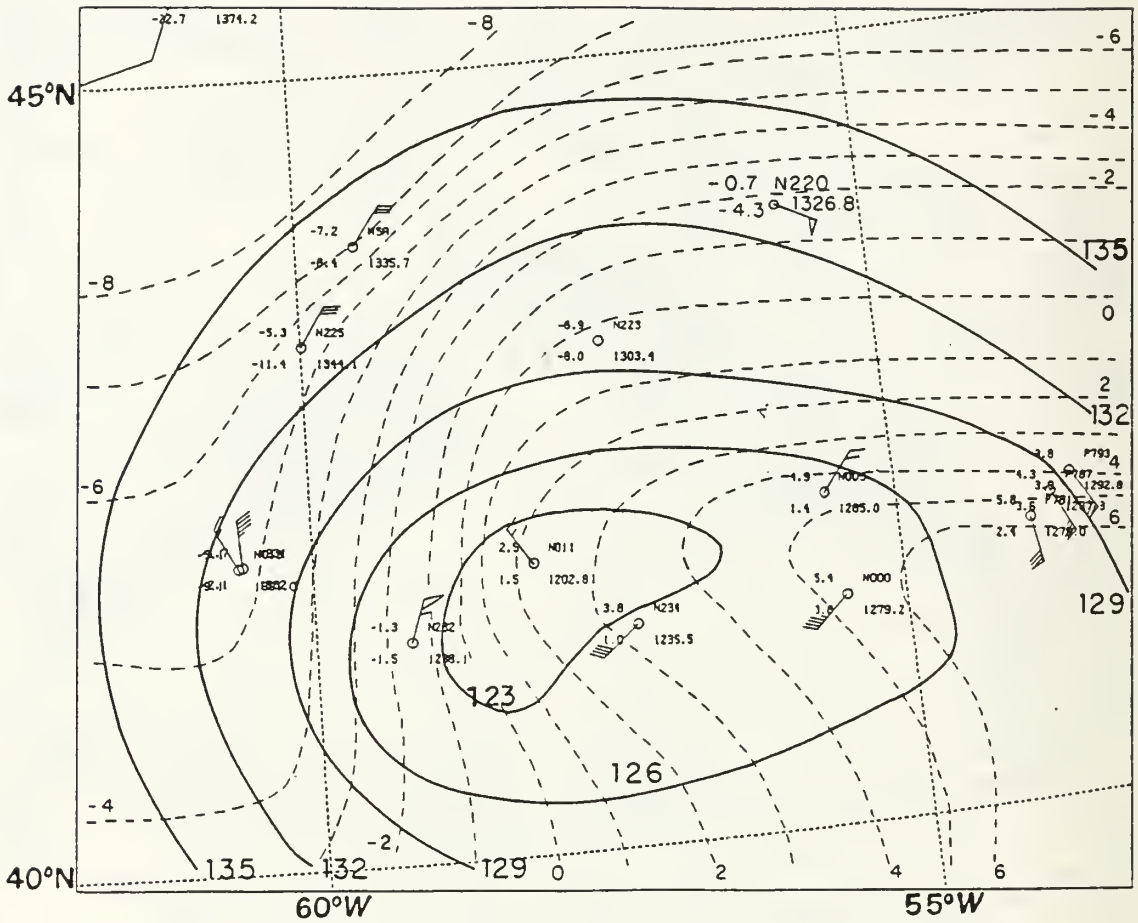

Fig. 24. 850 mb mesoscale analysis at 20/0000 UTC Jan 89: Heights contours (solid) every 30 m and temperature (dashed) every 1 °C.

ridge that extends back into the 850 mb low center. 70 kt winds across the tight thermal gradient in the warm sector are documented by aircraft flight-level wind observations.

Northwest of the low in the occlusion, the winds near the surface approach 80 kt. Sounding N232 (not shown) has an 80 kt wind maximum in the boundary layer near 920 mb and 65 kt winds near the surface at 970 mb. The vertical shear due to the decrease in wind speed down from the top of the boundary layer can be attributed to frictional effects near the sea surface. The strongest vertical shear ($\approx$ 25 kt/190 m) takes place above the boundary layer between 860 and 830 mb. This agrees with Shapiro and Keyser's (1990) ERICA IOP-4 description of the T-Bone and bent-back warm frontal stage of development discussed earlier. Their study shows that the strongest winds in the bent-back warm front are north to northeasterly winds with speeds approaching 80 kt within the marine boundary layer beneath the front at 920 mb. They found mesoscale

magnitudes of horizontal temperature gradient ($\approx$ 10° C/100 km) and vertical wind shear ($\approx$ 80 kt/100mb). Comparable results at 850 mb were found in this study with a horizontal temperature gradient of 5° C/100 km and a vertical wind shear of 25 kt/30 mb in the bent-back warm front above the boundary layer. Convergence along the warm front and triple point at 850 mb is documented by LeSonde wind observations approximately 100 km on either side of the triple point. Northeasterly winds at N005 converge with stronger southerly winds at N000 near the 850 mb triple point near 55° W 41.5° N. The 850 mb temperature at N000 is warmer than the temperatures north of the occluded front at N005. Warmer air is starting to wrap around the cyclone forming a warm pocket of air southeast of the 850 mb low. This reversal in the temperature pattern, with warmer temperatures behind the cold front, could be an indication that the cyclone is starting to form a warm core seclusion as proposed by Shapiro and Keyser (1990).

The boundary layer stability at this stage in the occlusion process is also very different across the warm and cold fronts. The warm sector of the storm underwent 10° C cooling in 12 hours which resulted in a change from a moist adiabatic temperature profile to a boundary layer profile indicating large static stability. Neiman et al. (1990) also found large static stability ($-\partial\theta/\partial p \approx$ 26 K/100 mb) in the modified warm sector of the pre-ERICA field test cyclone of 25-27 January 1988. The stability change due to the heating/cooling pattern found by Neiman et al. is also evident in the boundary layer stability across the occluded front in IOP-5. Sounding N005 (Fig. 25a) shows relatively large static stability in the boundary layer ($\partial\theta/\partial p \approx$ 20 K/100 mb) north of the triple point in the cooler air, while N000 (Fig. 25b), south of the triple point, is almost 7° C warmer at the surface and is saturated throughout most of lower troposphere.

To examine the vertical structure of the warm and occluded fronts, cross-sections of θ (Fig. 26a) and θ_e (Fig. 26b) were constructed in a northwest-southeast orientation across the bent-back occlusion, through the occluded front, and into the warm sector of the cyclone. The cross-section of θ shows a well mixed boundary layer below 920 mb north of the occlusion. At 1200 UTC, the cross-section through the trough (not shown) indicated that the well mixed boundary layer was significantly lower north of the low (approximately 980 mb). This suggests that the boundary layer has undergone a good deal of mixing over the past 12 hours. The occluded front tilting westward with height from N000 is characterized by near neutral conditions in the frontal zone up to approximately 850 mb. The cross-section of θ_e shows that the warm front and triple point regions are convectively unstable, with the θ_e contours tilting eastward with height.

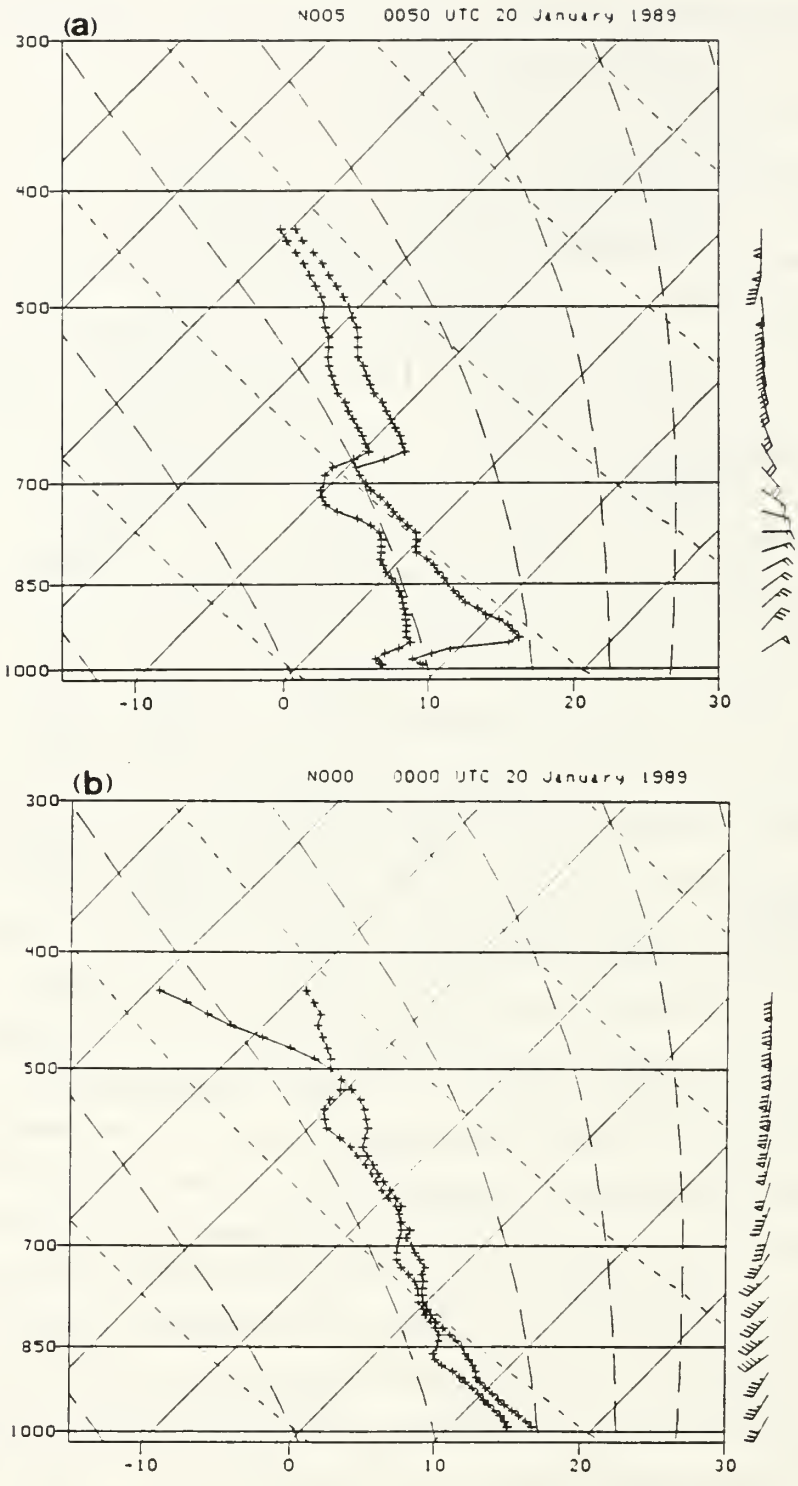

Fig. 25. Aircraft LeSondes: Skew T-logP profiles of temperature and dewpoint (°C) and wind speed (kt) at (a) N005 and (b) N000. See Fig. 24 for LeSonde locations.

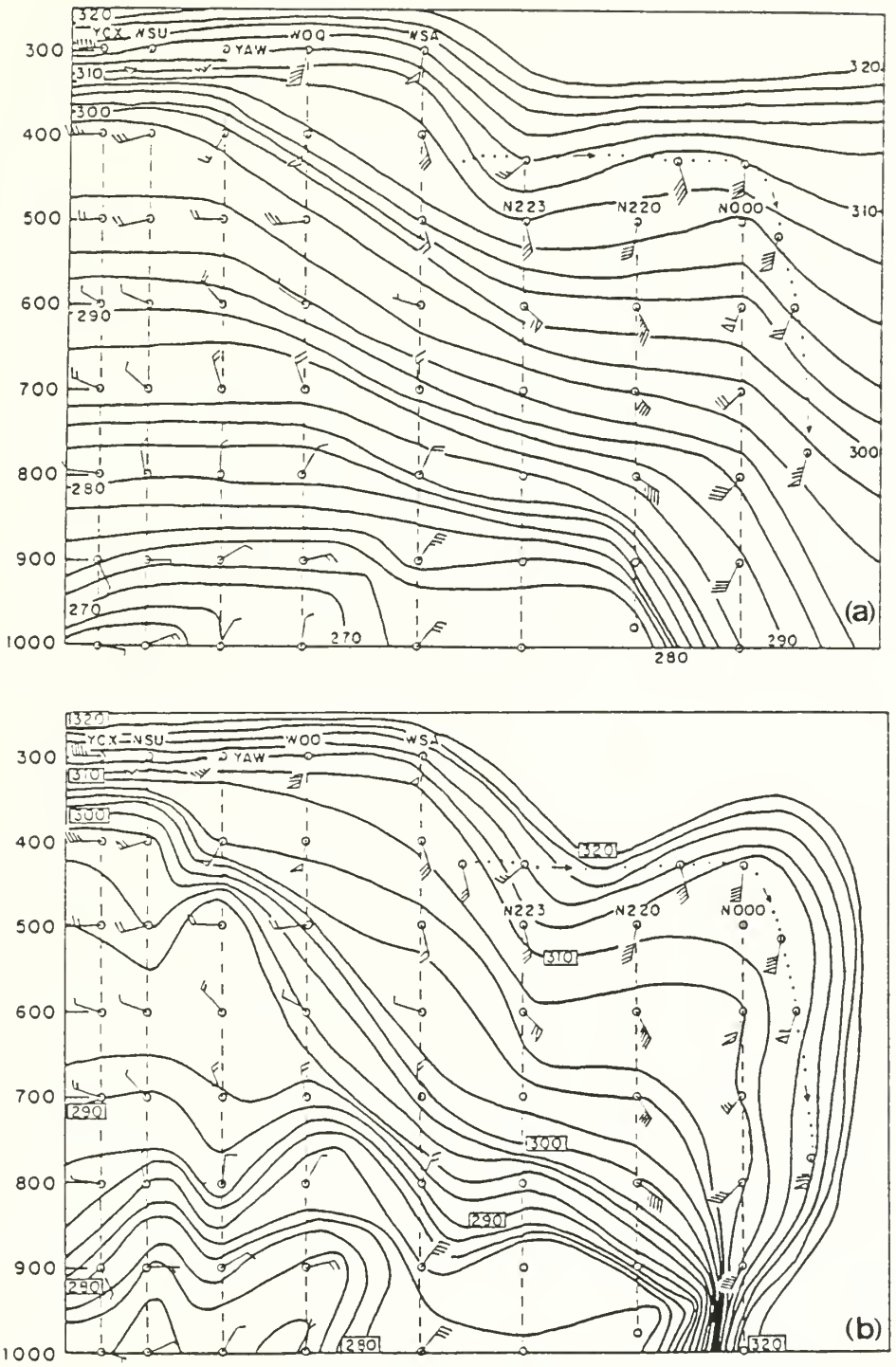

Fig. 26. 20/0000 UTC Jan 89 Cross-sections: (a) Cross-section of potential temperature and (b) equivalent potential temperature every 2 K along projection line AA′ shown in Fig. 21. Flight track (dotted line) between 0020 and 0100 UTC.

The 0000 UTC satellite imagery (Fig. 20) confirms the convective activity occuring at this time with cells of convection along the cold front wrapping around the surface low center.

A strong jet maximum in the boundary layer associated with the cold conveyer belt (Carlson 1980) is evident in most of the soundings north and northwest of the occlusion. The winds exceed 75 kt below 950 mb, with the maximum winds just below the top of the boundary layer decreasing rapidly to 20-30 kt by 850 mb. The strongest winds in the cold conveyer belt are found west of the occlusion at sounding N232, reporting wind speeds of 80 kt at 950 mb. The strong winds in this area of the bent-back warm front are confined to the lower troposphere; by 700 mb (-- Fig. id '700meso' unknown --) there has been a relaxation in the temperature gradient and winds aloft. The 80 kt winds observed near the surface show a rapid decrease up to 700 mb, where they are only 20 kt. By 500 mb (-- Fig. id '500meso' unknown --), the temperature gradient is tight again, with cold air entering the cyclone center from the southwest and the warm tongue spiraling into the rear of the storm from the northeast. The extensive upper-level aircraft observations at 400 mb (-- Fig. id '400meso' unknown --) confirms this structure. A warm pocket of air completely surrounds the 400 mb circulation center with a strong surge of cold air approaching about 100 km to the east. The cold air is right over the warm tongue at 850 mb (Fig. 24), which corresponds well with the very unstable vertical profile seen in the θ_e cross-section (Fig. 26) and the convection noted in the 0000 UTC satellite imagery. The upper-level jet stream is further south than is seen in the mesoscale analyses but the left-front quadrant of the jet streak is evident at 400 mb as the jet exits the base of the trough. The winds decrease from 85 to 70 kt in less than 100 km between N000 and N005. This still puts some upper-level divergence northeast of the surface cyclone over an area of strong warm air advection as seen at 850 mb. The cross-front horizontal wind shear is approximately 35 kt/100 km at 400 mb still supporting the indirect circulation in this jet exit region. This allows for further development and movement of the surface cyclone as it continues to occlude.

The 400 mb mesoscale analysis of dewpoint (-- Fig. id 'mesotd' unknown --) shows the complex moisture pattern in the upper-levels as the storm occludes. There is a warm, dry slot over the almost vertically stacked low and a moisture band circling the low from the northeast. This structure is well represented in the satellite imagery at 0000 UTC (Fig. 20). The two convective cells seen in the satellite imagery on either side of the low center south of the main comma head cloud line up with the -38° C dewpoint temperature band with the dry slot in the center of the upper-level low. The satellite imagery

shows the dry tongue entering into the storm from the southwest and is seen in the analysis south of the moisture band.

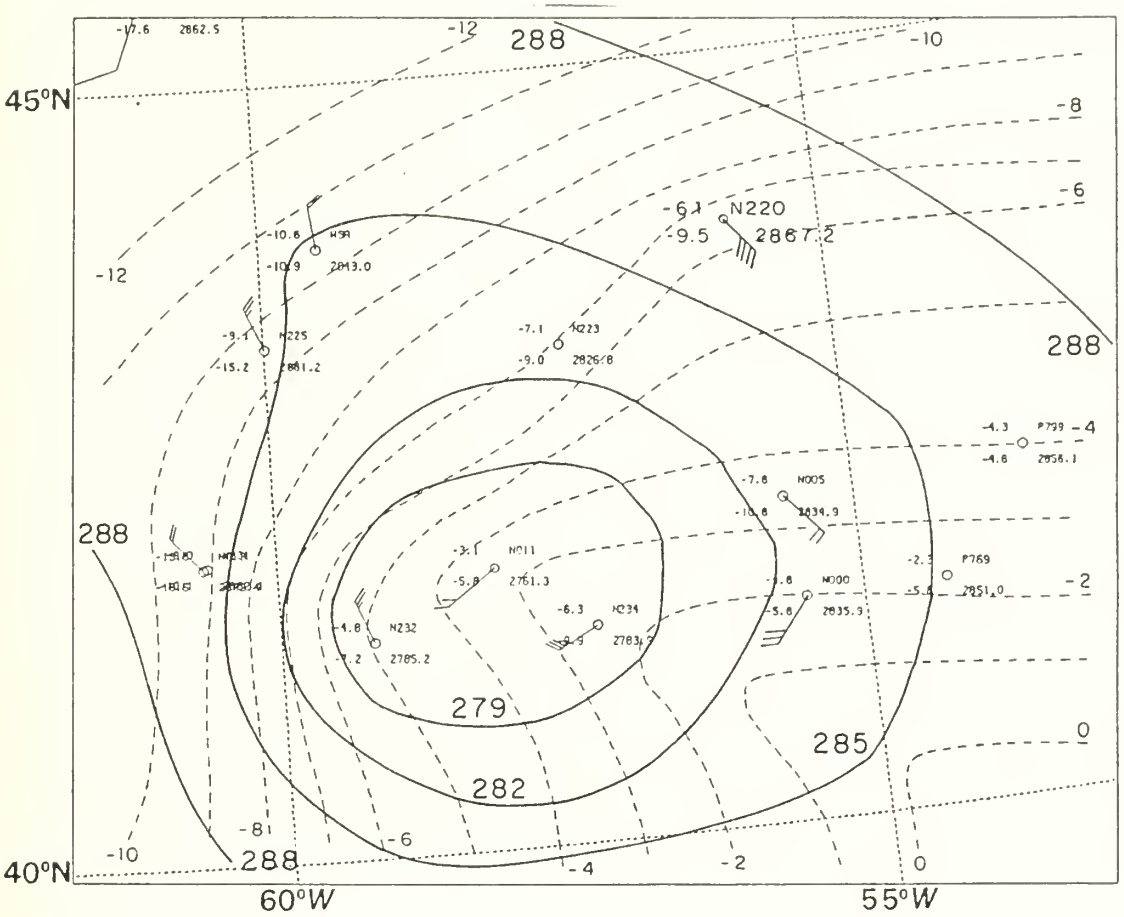

Fig. 27. 700 mb mesoscale analysis at 20/0000 UTC Jan 89: Height and temperature contours as described in Fig. 24.

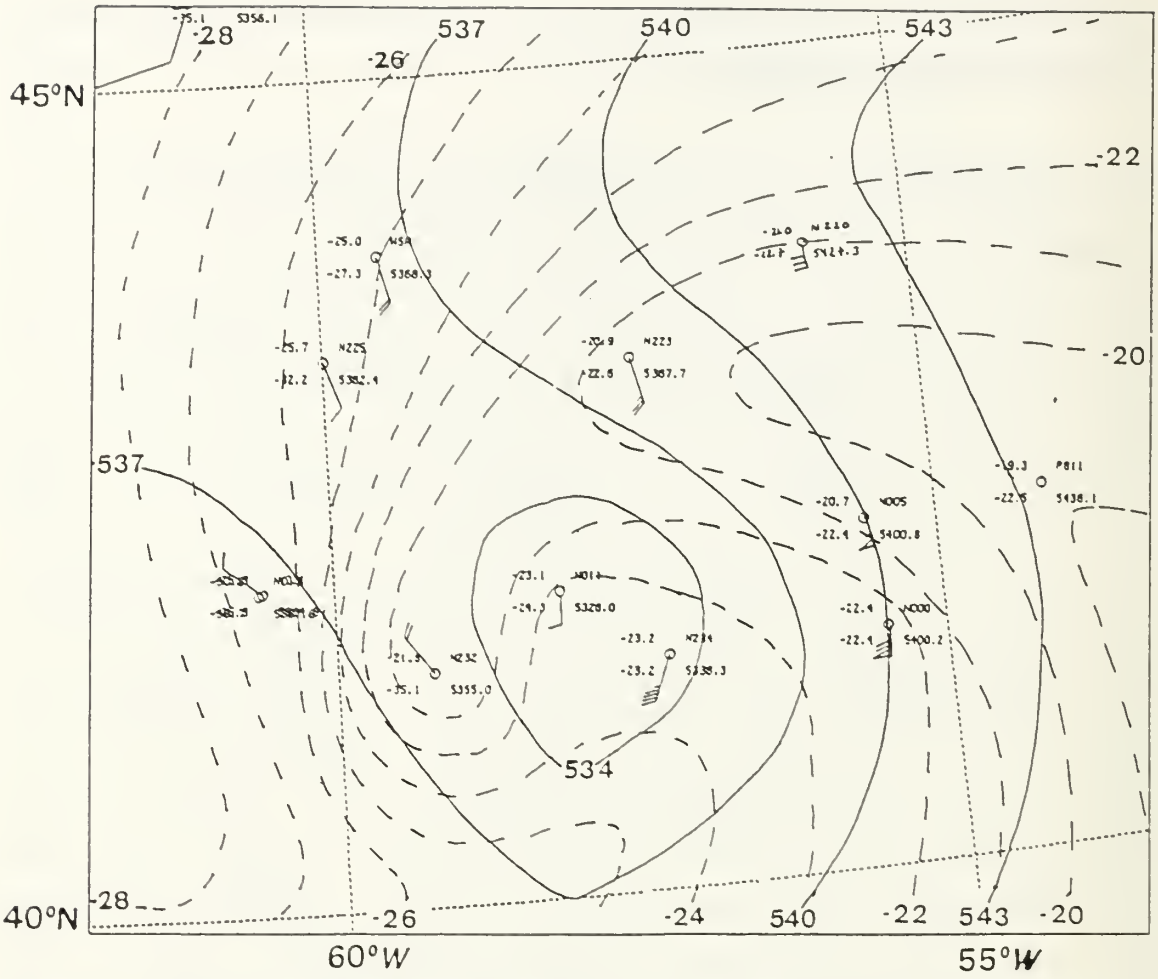

Fig. 28. 500 mb mesoscale analysis at 20/0000 UTC Jan 89: Height and temperature contours as described in Fig. 24.

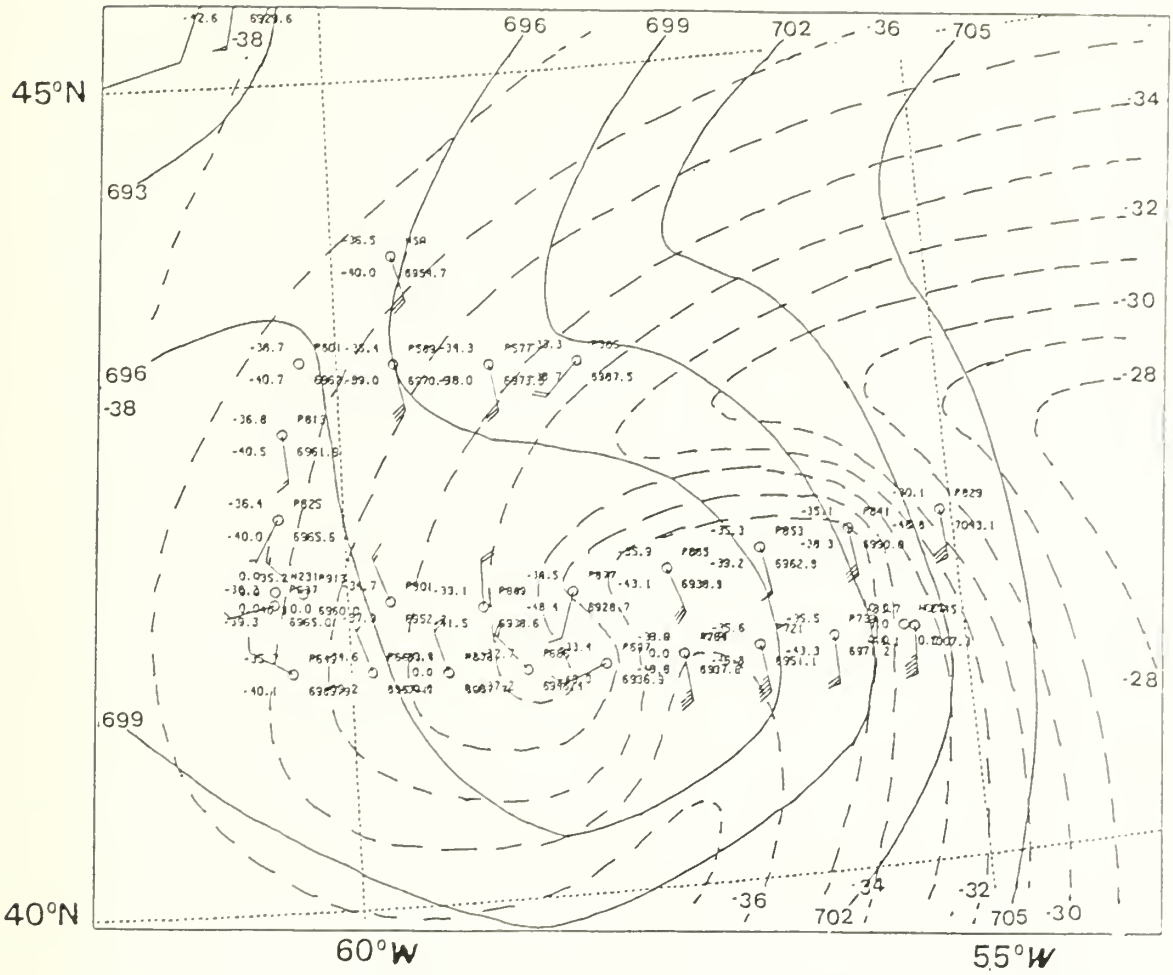

Fig. 29. 400 mb mesoscale analysis at 20/0000 UTC Jan 89: Height and temperature contours as described in Fig. 24.

The moisture in the upper-levels is enhanced by the arrival of high θ_e air in the warm conveyer belt (Carlson 1980). This low-level jet is located approximately 450 km east of the 850 mb low (Fig. 24). The vertical extent of the warm conveyer belt is shown in the 0000 UTC θ_e cross-section (Fig. 26) discussed earlier. The flight-level aircraft wind observations about 150 km east of the cold front show that the wind maximum at 850 mb ascends up and over the warm front into the upper-level westerly jet stream. The low-level jet acts to increase the moisture transport towards the region of heavy precipitation discussed earlier. The low-level jet is bringing warm, high θ_e air into the convective region east of the low center and possibly enhances the vertical motion in the region due to coupling of the upper and lower jets. The enhanced vertical motion then acts to in-

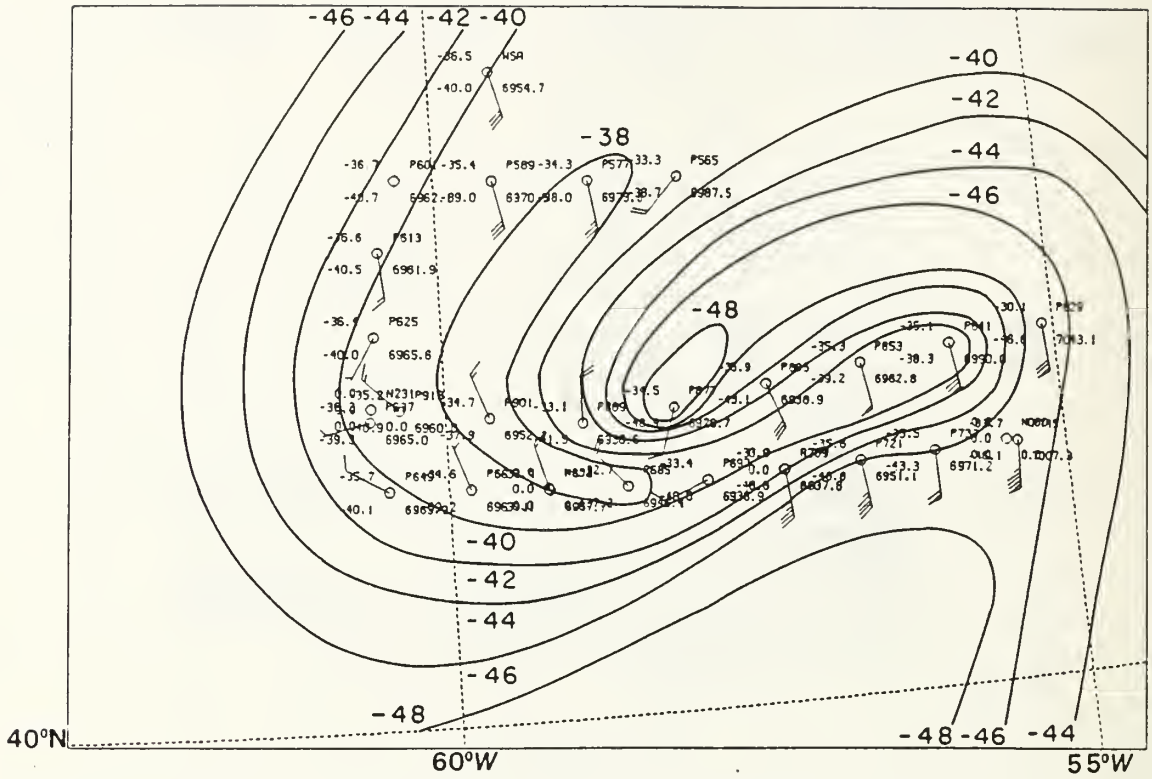

Fig. 30. 400 mb mesoscale dewpoint analysis at 20/0000 UTC Jan 89: Dewpoint temperature every 2 °C.

crease latent heat release due to precipitation, which contributes to further development of the surface low.

G. 1200 UTC 20 JANUARY 1989

The storm rapidly moved out of the ERICA observing region after 0000 UTC were not accomplished due to a lack of aircraft observations precluding further detailed analyses of the storm during the final occlusion stage. The upper-level dynamics at 20 0000 UTC are still favorable for continued development, and the cyclone deepened another 14 mb, to a central low pressure of 971 mb, in the 12 hour period between 0000 UTC and 1200 UTC 20 January 1989.

V. DISCUSSION

From the foregoing analyses, the importance of increased temporal resolution of the upper-air data is evident in the early stages of development of the IOP-5 cyclone. The intensity of the jet streak over HAT would not have been known if 3-hourly upper-air soundings had not been taken at most of the ERICA sounding stations. The true speed and time that the jet streak moved offshore is still not clear due to the 3 hour gap in data but it is an improvement over the 12 hour soundings used operationally. The narrow confines of the jet and the asynoptic sounding reports showing at least 155 kt winds aloft were not picked up in the initial upper-air analyses of the Nested-Grid Model (NGM), the GSM, or the NMC final analysis. The 1200 UTC 19 January 1989 analyses had relatively broad jet streaks with wind speeds 25 to 45 kt weaker than what was reported at 0900 UTC. This is certainly an issue that requires attention in future attempts to model the evolution of IOP-5. A call for upper-air data with 2-3 hour temporal resolution to resolve processes responsible for cyclogenesis was recognized as early as 1951 by Palmen (1951). Uccellini (1990) thought hourly upper-air soundings would be needed for some cases of rapid development and summed up the need for enhanced data sets best by stating, "This call is often repeated, seldom heeded, and is still relevant to today's research requirements." This case study, once again, exemplifies the need for accurate and timely upper-air observations in order to study and understand the evolution of the upper atmosphere during explosive cyclogenesis.

The thermal patterns seen at 1800 UTC at 850 mb and 700 mb are consistent with Shapiro and Keyser's proposed conceptual model of the evolution and structure of extratropical cyclones in which the largest frontal baroclinicity during the cyclone's life cycle occurs within the bent-back warm front to the rear (west) of the cyclone center. Their 4-phase conceptual model consists of an incipient frontal cyclone, a frontal fracture, a T-Bone and bent-back warm front, and a final warm-core seclusion stage. The incipient cyclone is characterized by a broad, zonally continuous frontal zone. As the cyclone evolves, the front "fractures" near the center with discontinuous temperature gradients at the cold and warm fronts contracting to a frontal-zone width of approximately 100 km. This frontal fracture was not evident in the 6-hourly analyses of IOP-5 although it probably occured between analysis times. The mid-point of cyclogenesis is then characterized by the frontal T-Bone and bent-back warm front shapes seen in the

temperature gradients. Frontogenesis stops as the cold polar air encircles the low center forming a warm-core seclusion in the fully developed cyclone. Prior to 1987, some of these frontal structures had been simulated by numerical models but not seen in the "real" atmosphere. The conceptual model evolution described above incorporated both model simulations and documented studies using observational data from the Alaskan Storm Program (ASP) in 1987 and ERICA IOP-4 on 4-5 January 1989. This study of IOP-5 also shows evidence of this pattern of storm evolution and not the early conceptual models of the Norweigan frontal-cyclone. Although Shapiro and Keyser noted these patterns near the surface, the IOP-5 storm exhibits these characteristics up into the middle and upper troposphere. The contraction of the frontal gradients was evident in the 1200 UTC height/temperature analyses at 850 mb and 700 mb when the storm started to rapidly deepen. By 1800 UTC, the bent-back warm front stage was evident up to 700 mb as the storm continued to rapidly deepen. The mesoscale view as the storm began to occlude at 20/0000 UTC revealed the same bent-back warm front pattern in the lower-levels. The 850 mb analysis also revealed the evidence of a warm-core seclusion starting to take place in the lower-levels south of the triple point near N000 (see Fig. 25 for location). The same bent-back pattern exists in the temperature and dewpoint analyses at 500 mb and 400 mb although the cyclone evolution proposed by Shapiro and Keyser (1990) does not explain the processes that would produce this structure aloft. The effects of latent heat release in the convection seen in this early stage of occlusion may have contributed to the formation of this complex mesoscale temperature and dewpoint structure.

The low-level jets, frontal structures and upper-level features described at 20/0000 UTC may have started or developed earlier, but the lack of sufficient upper-level data at 1800 UTC precluded an indepth, mesoscale view of the storm as it evolved in the 6-hour period between 1800 and 0000 UTC. The most significant features evident in the 20 0000 UTC analyses of height and temperature are the strong low-level jets evident at 850 mb associated with the warm and cold conveyer belts. Uccellini (1990) found low-level jets to be an important feature in cases of explosive cyclogenesis over the ocean. The formation of a low-level jet in the warm sector enhanced warm air advection and possibly the moisture fluxes, which acted to increase the moisture transport towards a region of heavy precipitation. The low-level jet that appears in the warm sector of IOP-5 is just under the southern edge of the convective cell east of the surface low at 20 0000 UTC and the same process of increasing the moisture transport into the storm is probably occuring here also. The increased moisture transport along with coupling

of the upper- and lower-jets would act to increase the upward vertical motion in the region, increase the latent heat release due to precipitation, and further enhance the development of the surface low.

The extensive aircraft observations at 20.0000 UTC made it possible to construct a cross-section of θ_e through an extensive area of convection, which was found to be potentially unstable. Although the role of symmetric instability in IOP-5 was not analyzed in this study, Greer (1991) found that moist symmetric neutrality existed in the early stages of IOP-5. The low-level jet is feeding warm, moist air into this region and transporting it up to the cold upper-levels as seen at 500 mb and 400 mb. The satellite imagery reveals the convective nature of the clouds near N000 which is very close to the triple point. This instability is seen throughout the evolution of IOP-5 and is well documented by aircraft and soundings in and around the warm frontal region. This gives some observational evidence that convection, and in particular, convective instability, plays a role in rapid cyclogenesis as hypothesized by Bosart (1981) and Gyakum (1983b).

Kuo et al. (1991) did a numerical simulation of a rapidly intensifying oceanic cyclone to study the effects of adiabatic and diabatic processes on storm development. They found that the heavy precipitation, vorticity generation, and pressure decreases occurred near the warm front during rapid cyclogenesis. They determined that rapid cyclogenesis must be viewed in the context of moist baroclinic instability with strong nonlinear interaction between adiabatic and diabatic processes. The explicit moisture scheme used in their simulation does not deal with convectively unstable regimes though. The moisture effects were based on the premise that the precipitation was stable. The fact that moist potential instability and convective instability exists throughout IOP-5 suggests that the question of stable versus unstable regions in modeling explosive cyclogenesis needs to be explored further.

VI. CONCLUSIONS AND RECOMMENDATIONS

This study has shown that significant upper-level forcing enhanced the development of IOP-5. The cyclone's central pressure dropped 32 mb in 24 hours between 19/1200 UTC and 20/1200 UTC January 1989. The initial development occurred several hundred kilometers off the coast of North Carolina under strong upper-level confluence. A pre-existing jet streak across the Gulf Coast merged with an upper-level short wave from the northwest about 19/0600 UTC January 1989. This put the left-front quadrant of both jet streaks in the cyclogenetic region, allowing for increased vertical motion and divergence aloft due to the indirect ageostrophic circulation in the left-front jet exit region. Strong upper-level frontogenesis took place on the coast of North Carolina between 0600 and 1200 UTC, with a 75 kt increase in jet speed and an increase in the height of the jet maximum in response to the rapid development starting near the surface. Unusually strong subsidence was also noted on the northeastern seaboard approximately 650 km west of the low at 1200 UTC, providing indirect evidence that stratospheric extrusion was taking place prior to rapid deepening.

The entire period of rapid development was characterized by moist potential instability in the warm sector. The 20/0000 UTC mesoscale analyses showed very high θ_e air being forced aloft in the warm conveyer belt into a cold pocket of air aloft. This resulted in a highly unstable region of convection near the triple point with pronounced convergence occurring near the triple point at 850 mb.

The temperature and dewpoint structure during the early occlusion stage bears a striking resemblance to the T-bone and warm-core seclusion structures proposed by Shapiro and Keyser (1990). Although their frontal structures were based near the surface, the IOP-5 cyclone exhibits these frontal characteristics into the upper levels. This suggests that both upper- and lower-level processes are acting together in such a way as to produce this thermal pattern throughout the depth of the atmosphere.

This study has addressed some of the upper-level dynamics and processes involved in explosive cyclogenesis and has brought up several areas of future research.

1. The transverse ageostrophic circulations of the two initial jet streaks needs to be simulated and verified by numerical models to get an idea of the vertical motions and divergence of these two jet streaks and how they interact and influence the initial development.

2. A more thorough study needs to be done to determine the initial location and subsequent distribution of stratospheric air into the IOP-5 cyclone.
3. The moist potential instability found throughout IOP-5 needs to be studied in detail as well as the role of unstable convection in explosive cyclogenesis.
4. Numerical modeling experiments need to be conducted in order to duplicate the mesoscale analyses presented in this study.
5. The vertical resolution in the models needs to be good enough to duplicate the vertical wind shear in the boundary layer as well as the upper-level temperature and dewpoint structures in the occluded stage.
6. The boundary layer study of IOP-5 by Greer (1991) needs to be incorporated with this upper-level study to determine the interactions between the upper- and lower-level processes that contributed to explosive cyclogenesis.

APPENDIX HAND ANALYSES

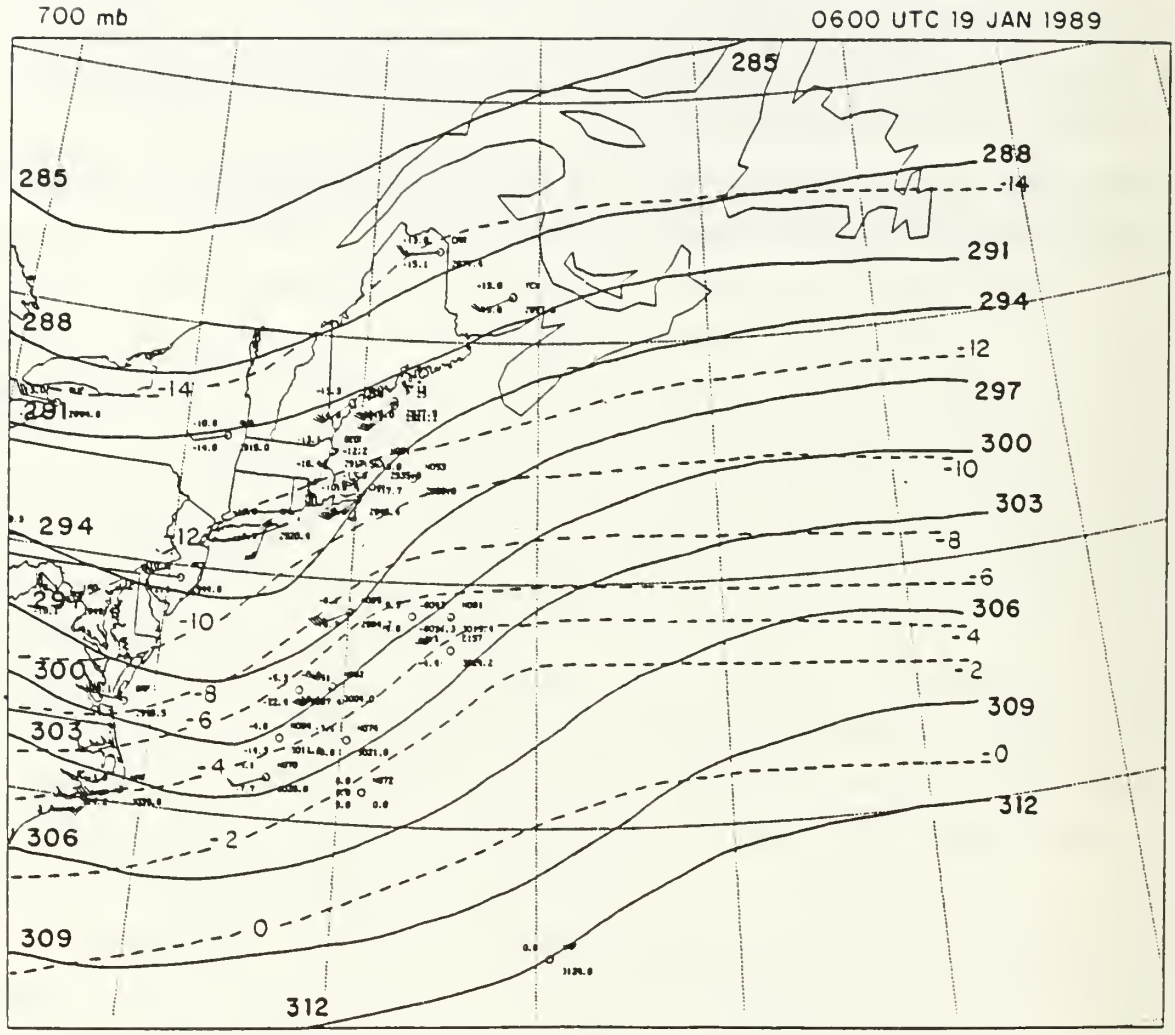

Fig. 31. 700 mb analysis at 19/0600 UTC Jan 89: Height (solid) every 30 m and temperature (dashed) every 2° C.

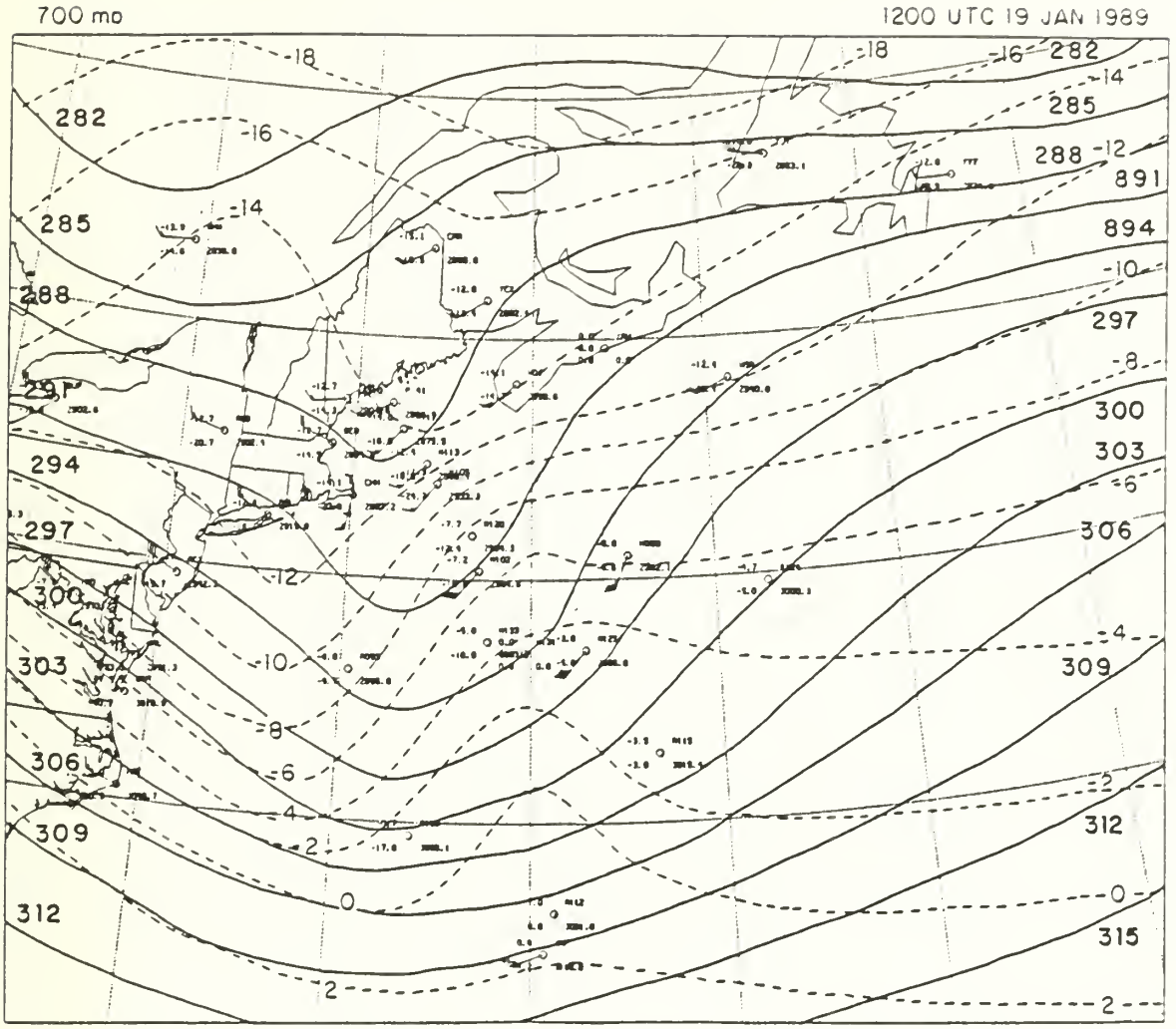

Fig. 32. 700 mb analysis at 19/1200 UTC Jan 89: Height (solid) every 30 m and temperature (dashed) every 2° C.

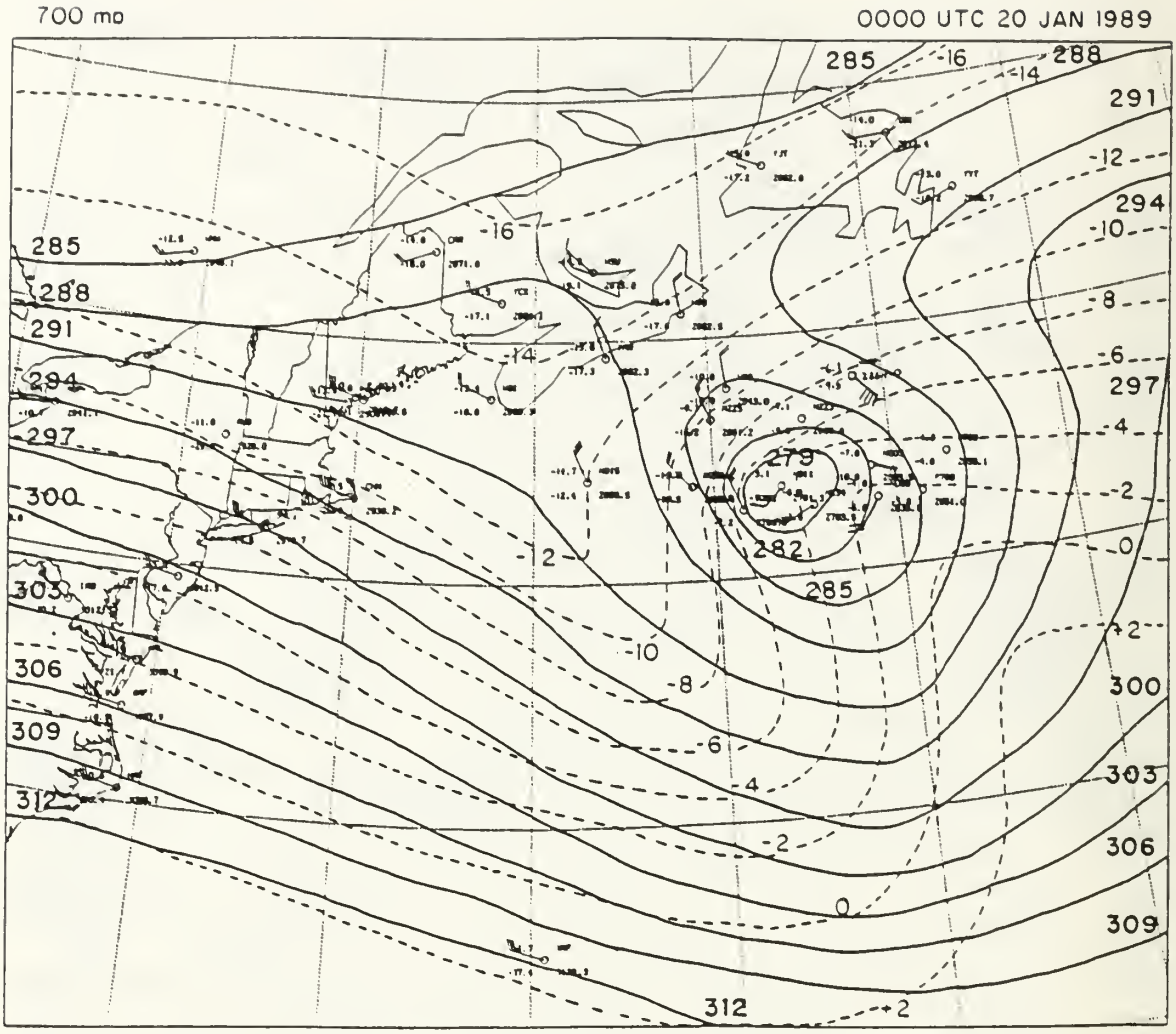

Fig. 33. 700 mb analysis at 20/0000 UTC Jan 89: Height (solid) every 30 m and temperature (dashed) every 2° C.

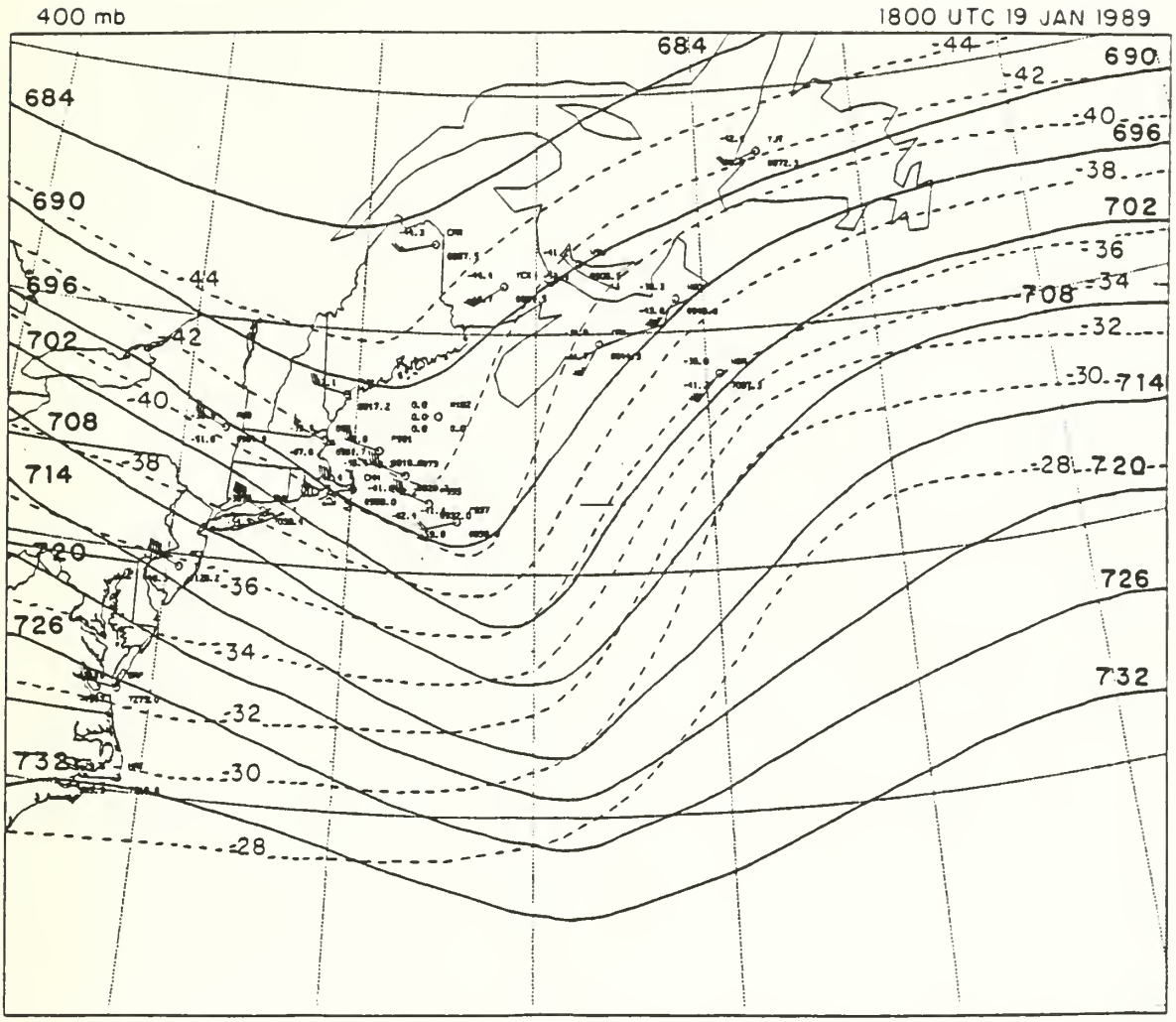

Fig. 34. 400 mb analysis at 19/1800 UTC Jan 89: Height (solid) every 60 m and temperature (dashed) every 2° C.

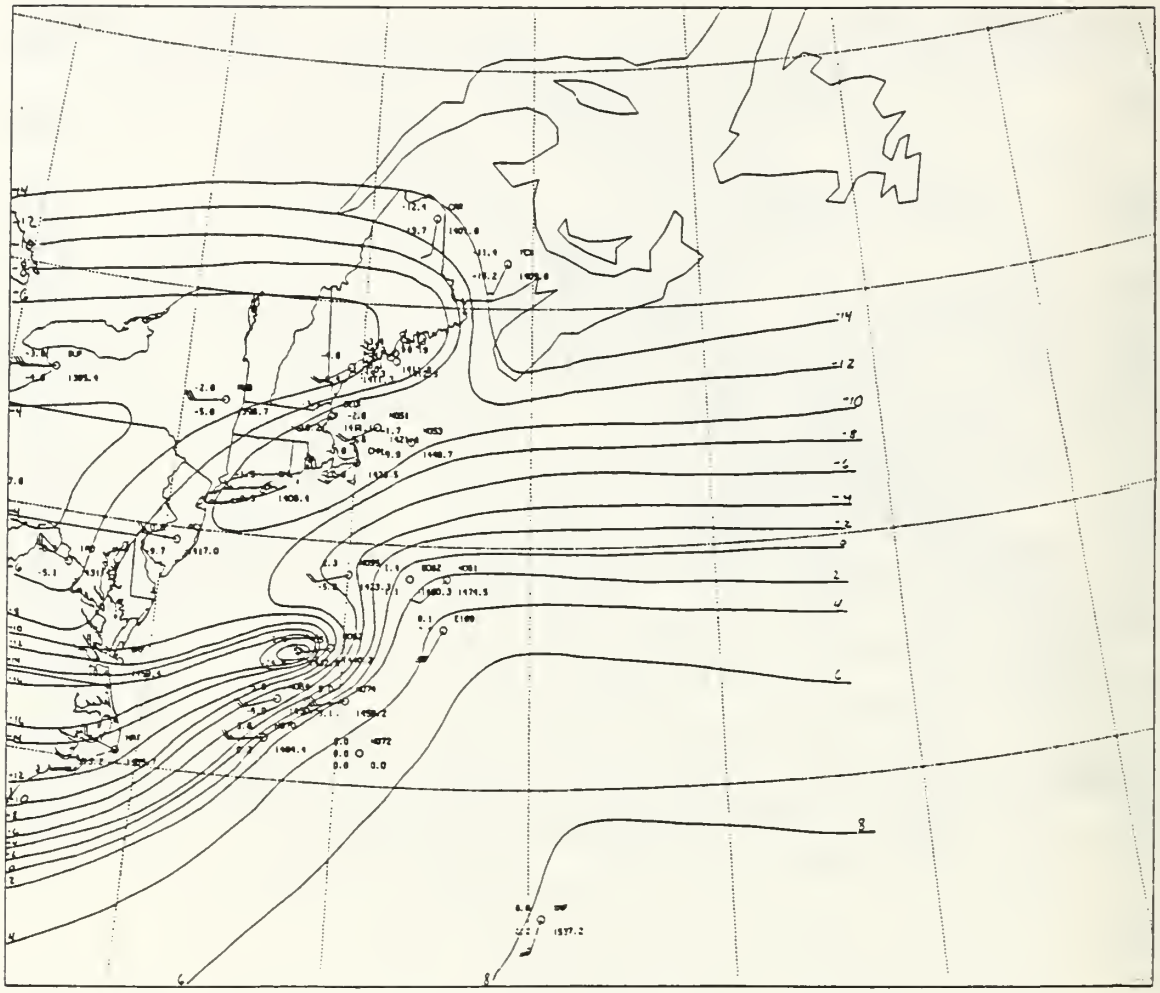

Fig. 35. 850 mb dewpoint analysis at 19/0600 UTC Jan 89: Dewpoint contours every 2 °C.

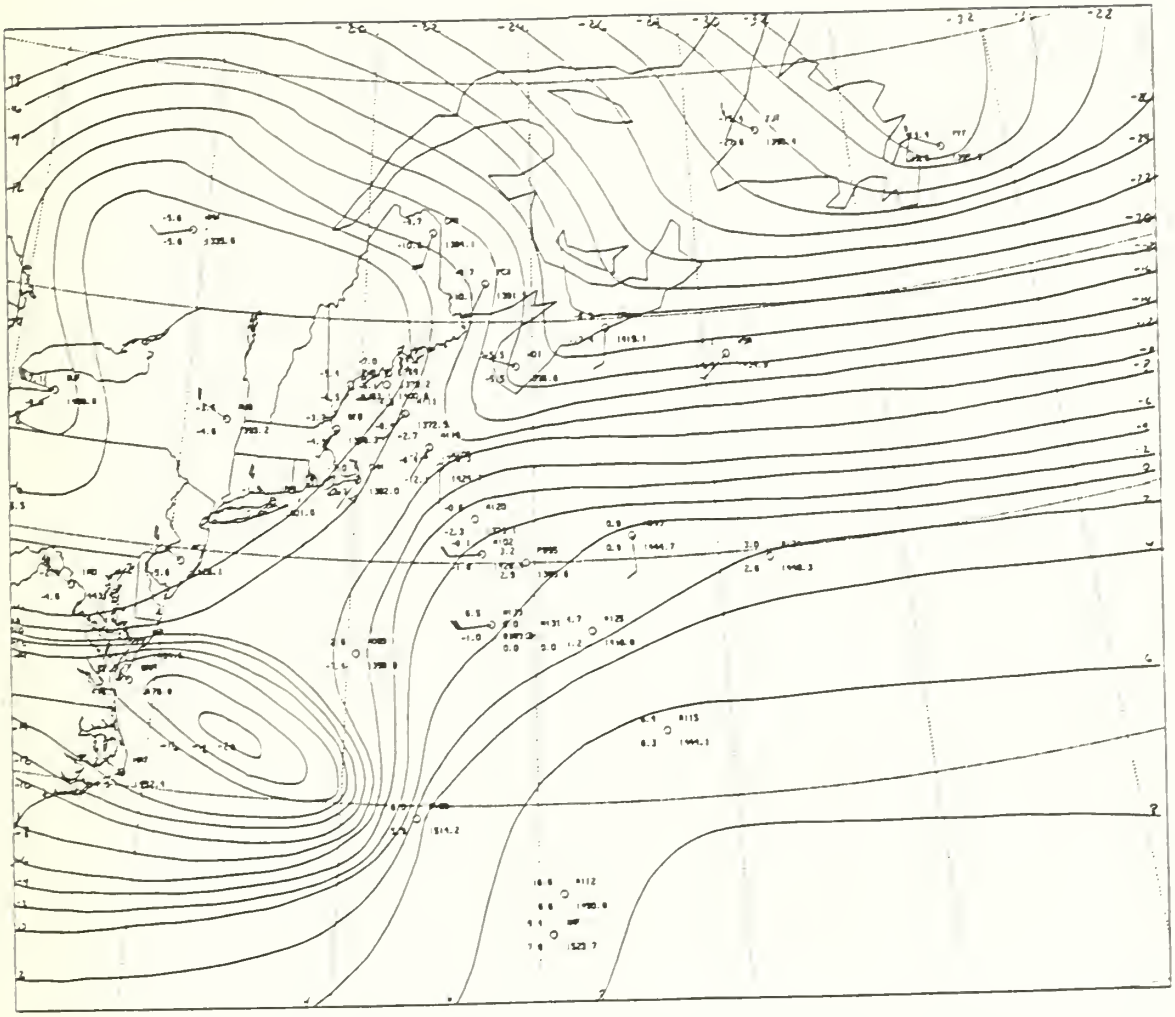

Fig. 36. 850 mb dewpoint analysis at 19/1200 UTC Jan 89: Dewpoint contours every 2 °C.

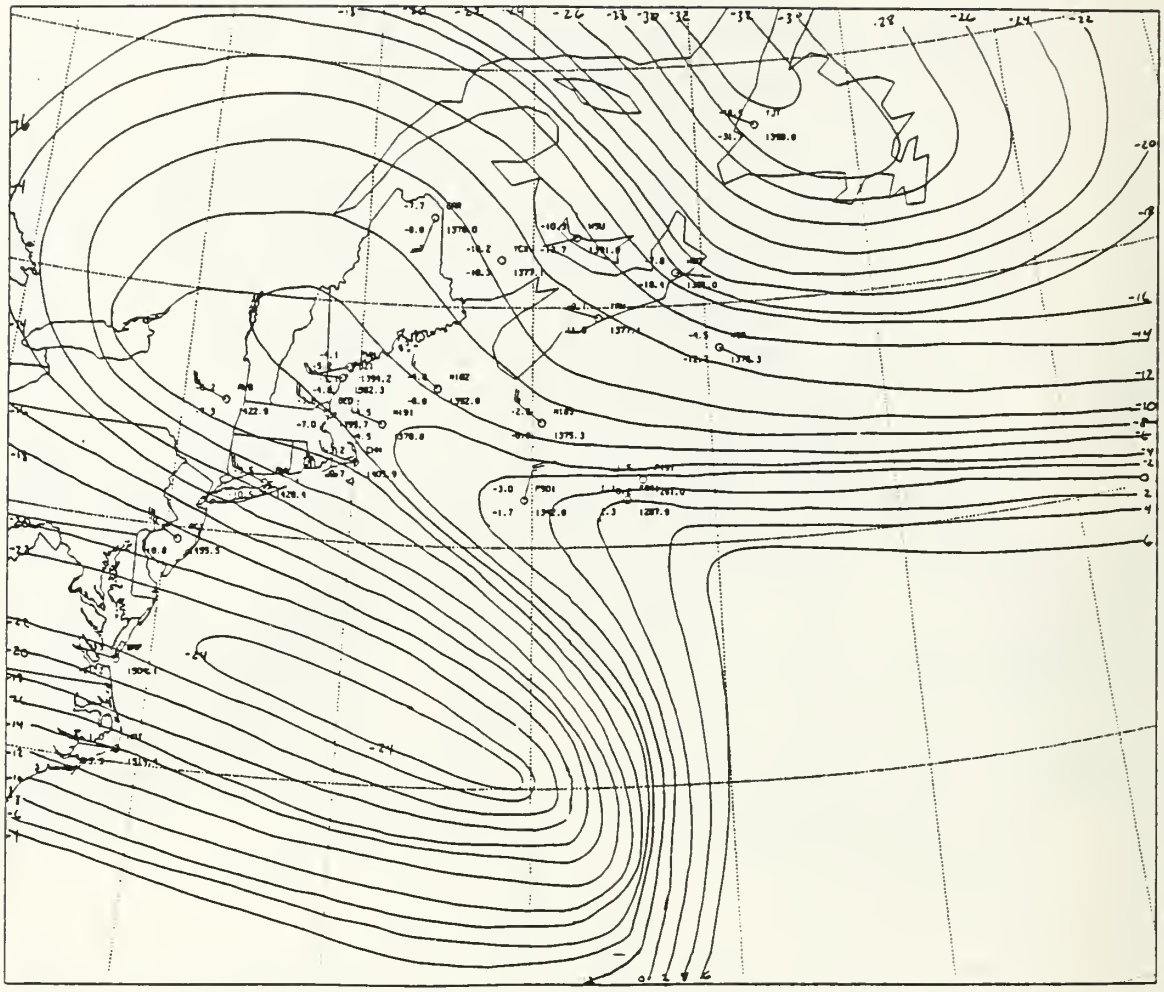

Fig. 37. 850 mb dewpoint analysis at 19/1800 UTC Jan 89: Dewpoint contours every 2 °C.

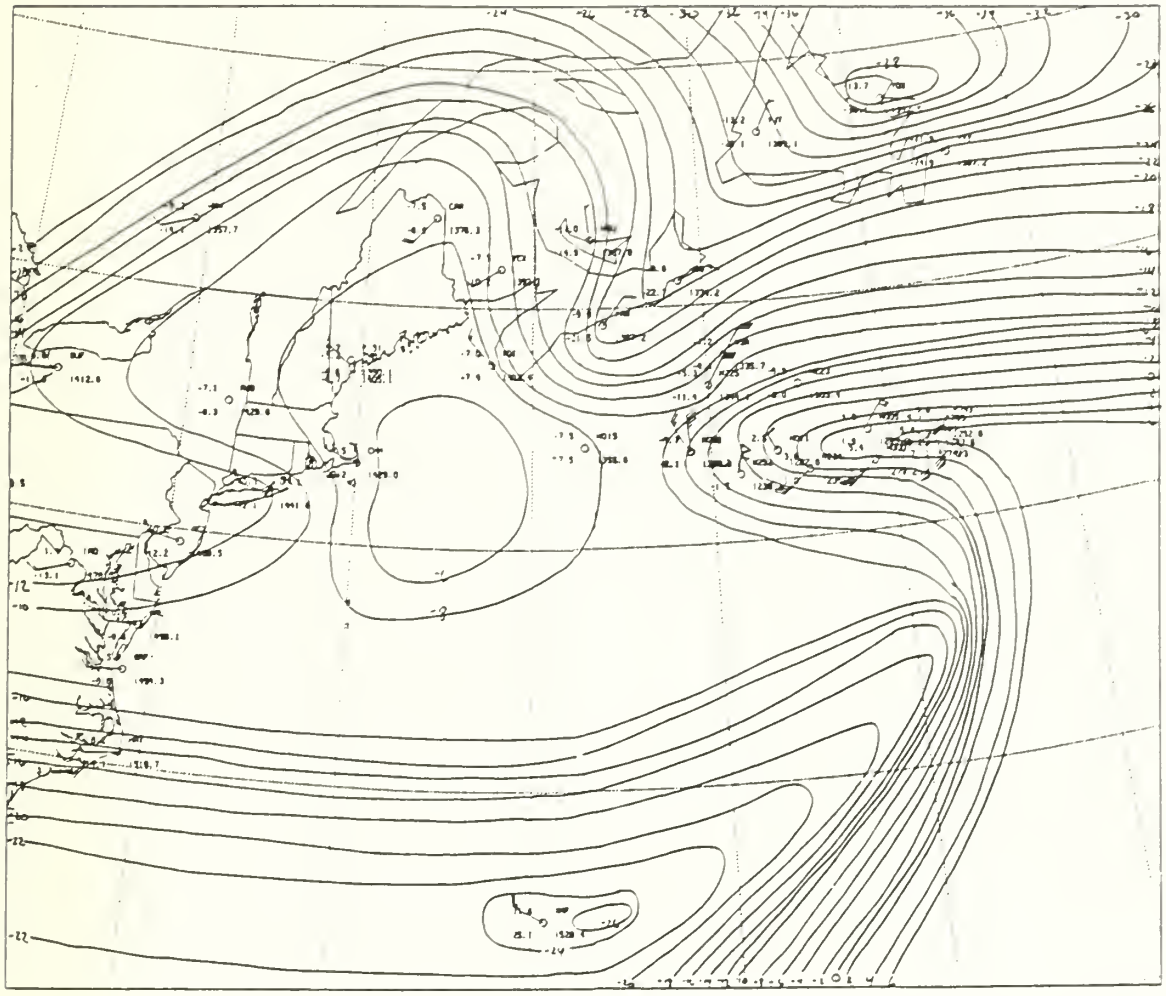

Fig. 38. 850 mb dewpoint analysis at 20/0000 UTC Jan 89: Dewpoint contours every 2 °C.

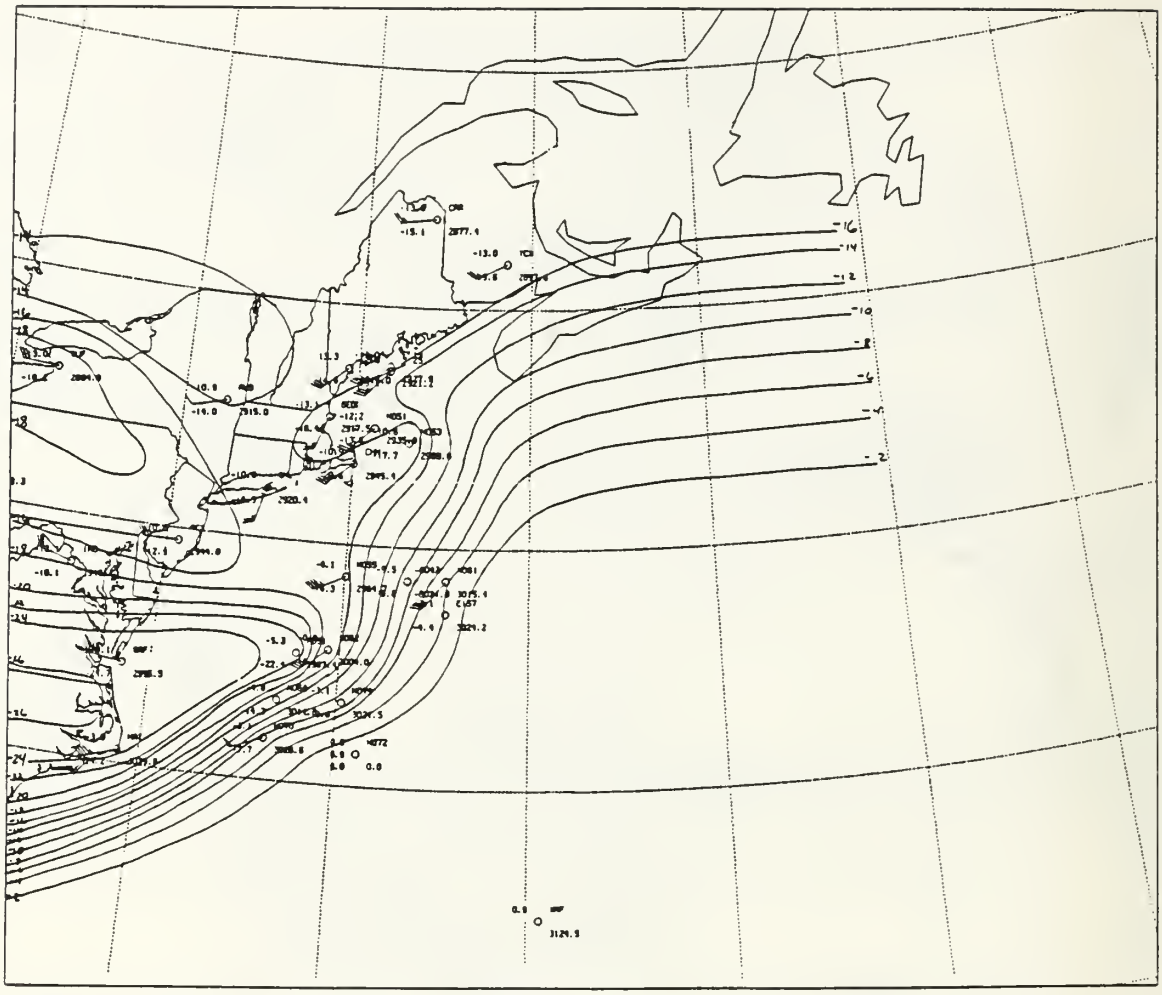

Fig. 39. 700 mb dewpoint analysis at 19/0600 UTC Jan 89: Dewpoint contours every 2 °C.

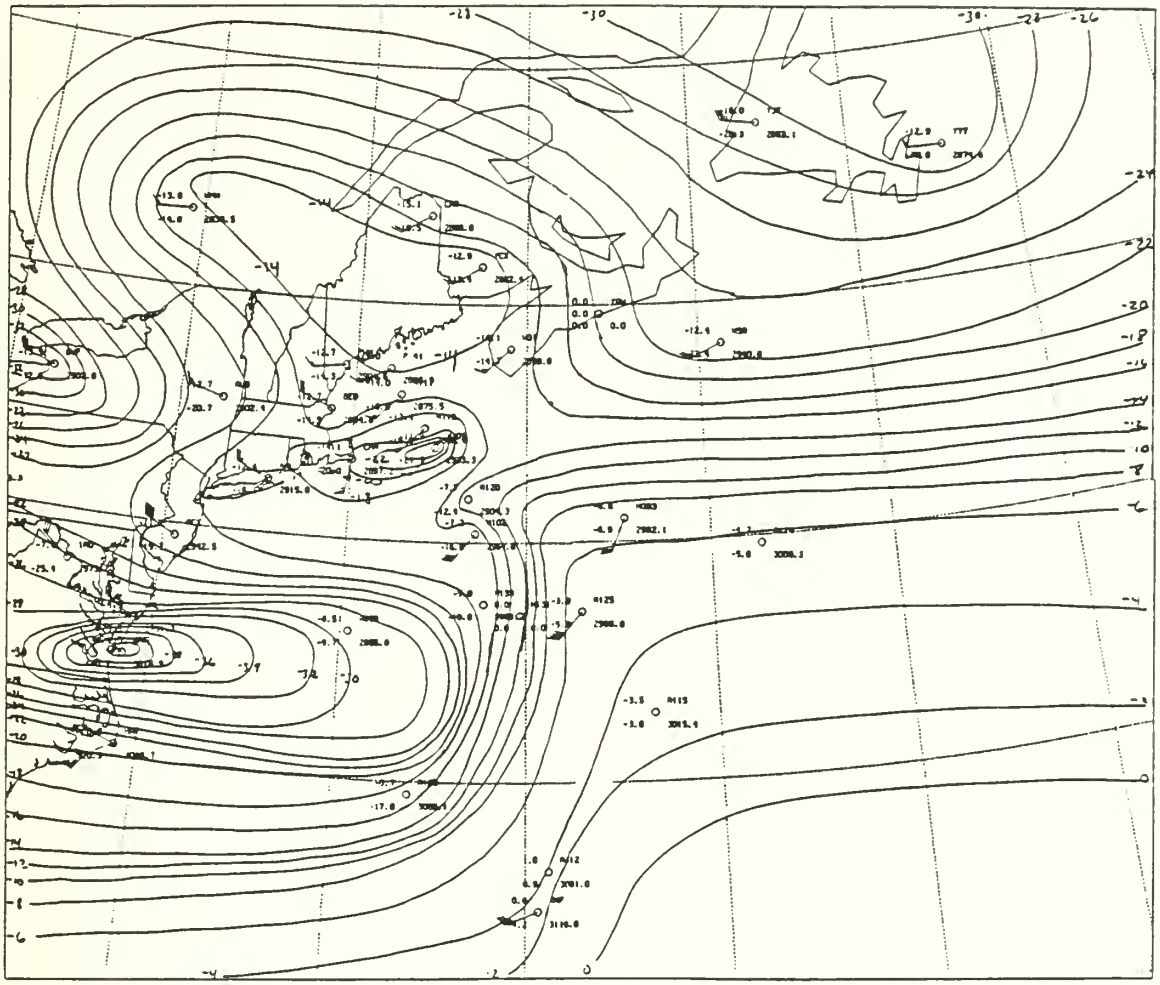

Fig. 40. 700 mb dewpoint analysis at 19/1200 UTC Jan 89: Dewpoint contours every 2 °C.

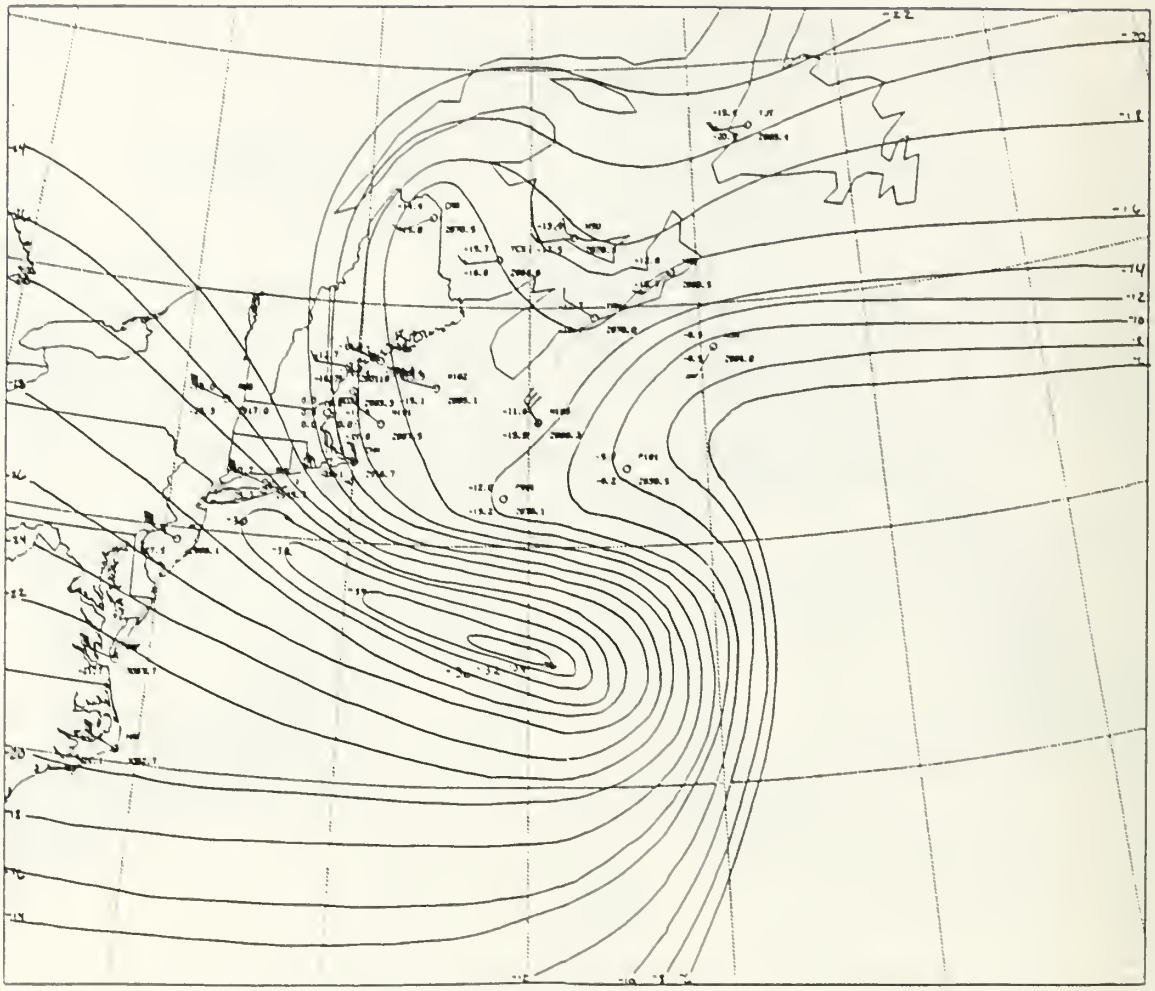

Fig. 41. 700 mb dewpoint analysis at 19/1800 UTC Jan 89: Dewpoint contours every 2 °C.

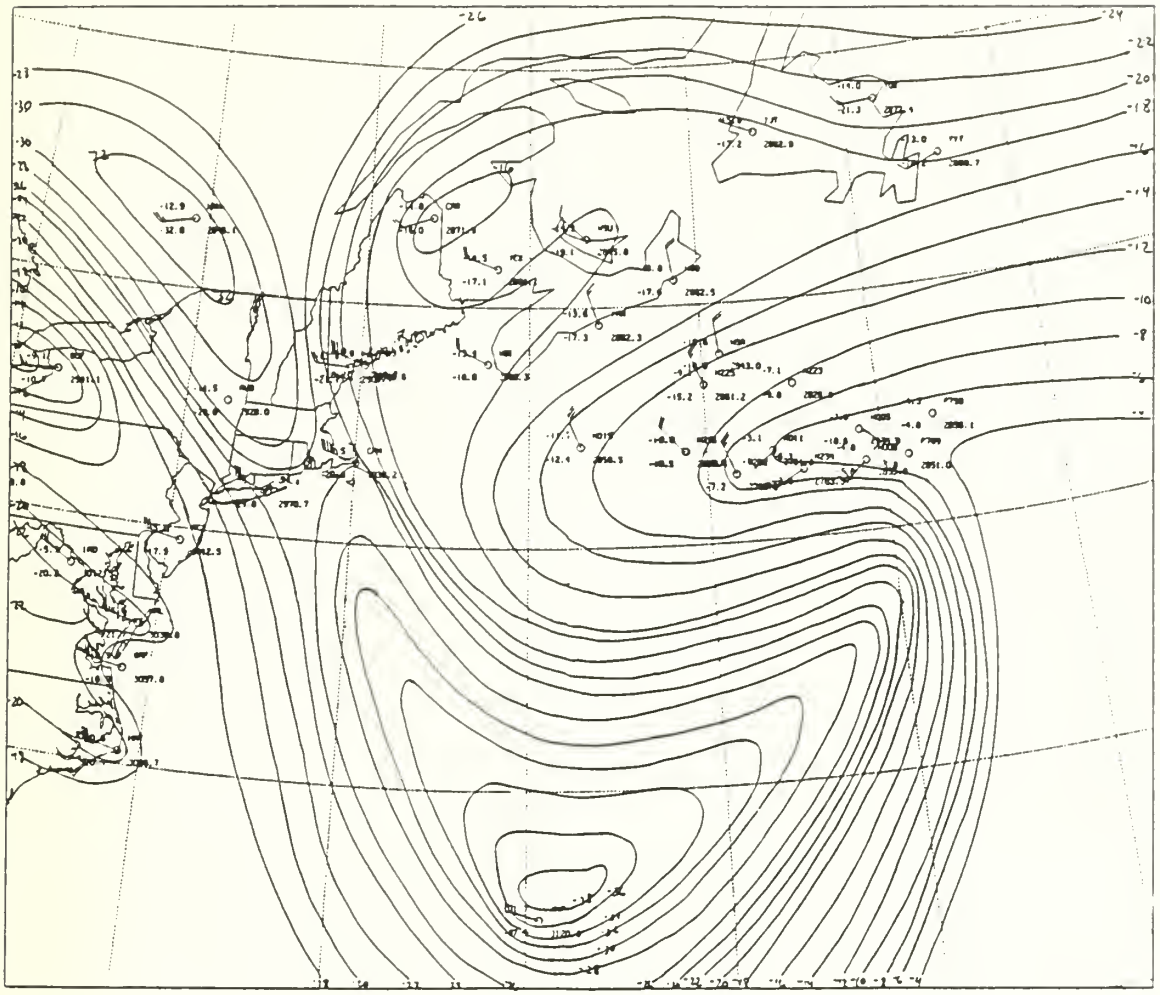

Fig. 42. 700 mb dewpoint analysis at 20/0000 UTC Jan 89: Dewpoint contours every 2 °C.

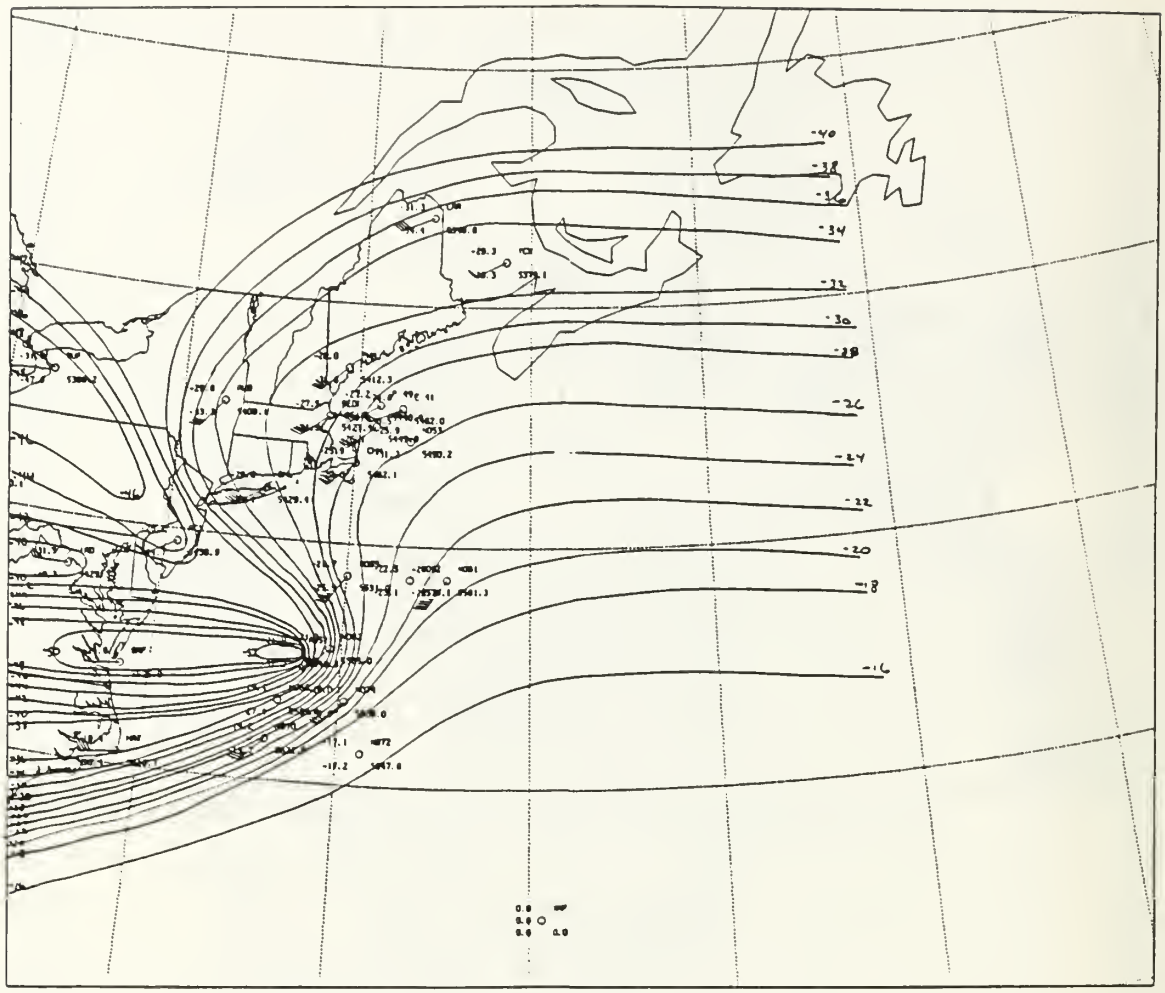

Fig. 43. **500 mb dewpoint analysis at 19/0600 UTC Jan 89:** Dewpoint contours every 2 °C.

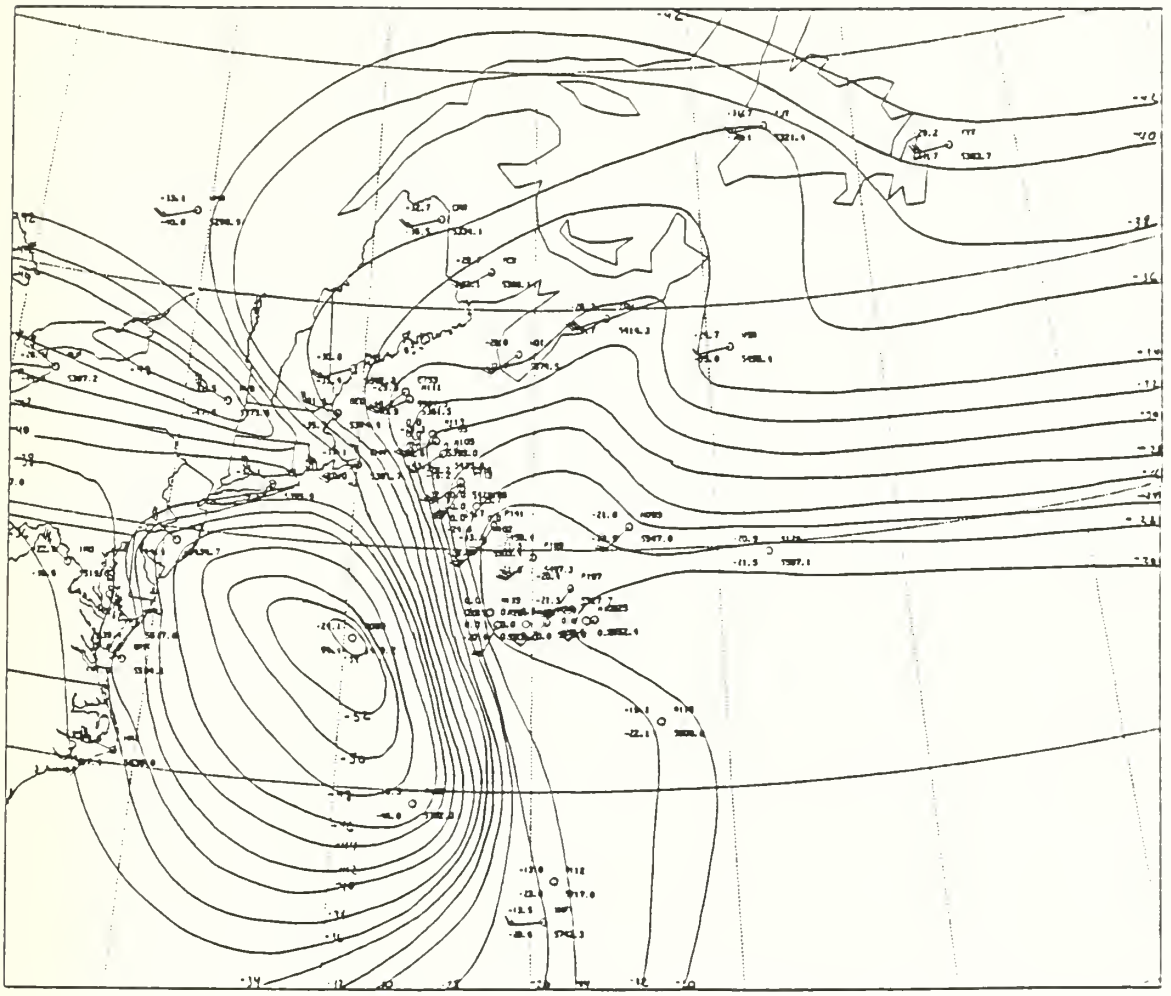

Fig. 44. 500 mb dewpoint analysis at 19/1200 UTC Jan 89: Dewpoint contours every 2 °C.

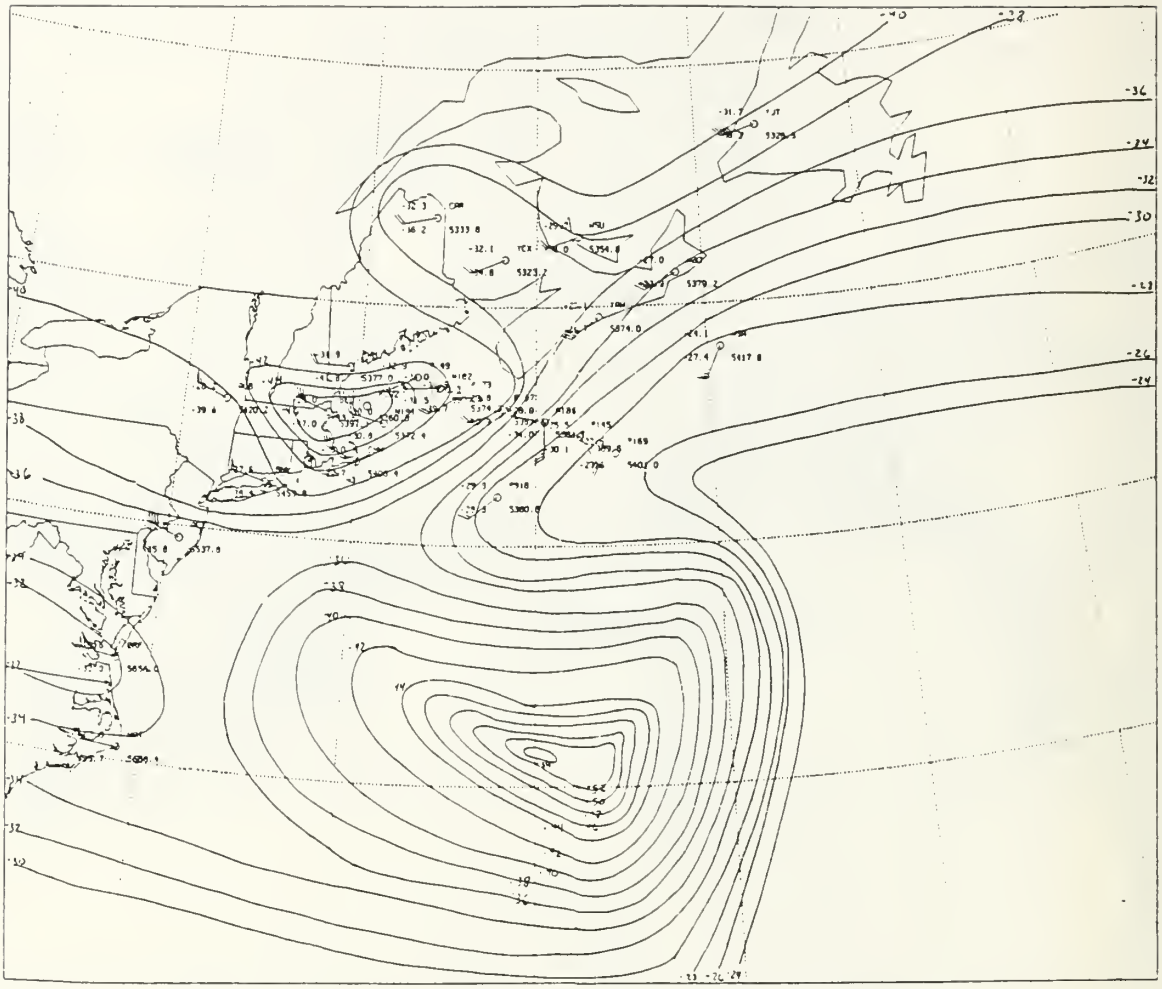

Fig. 45. 500 mb dewpoint analysis at 19/1800 UTC Jan 89: Dewpoint contours every 2 °C.

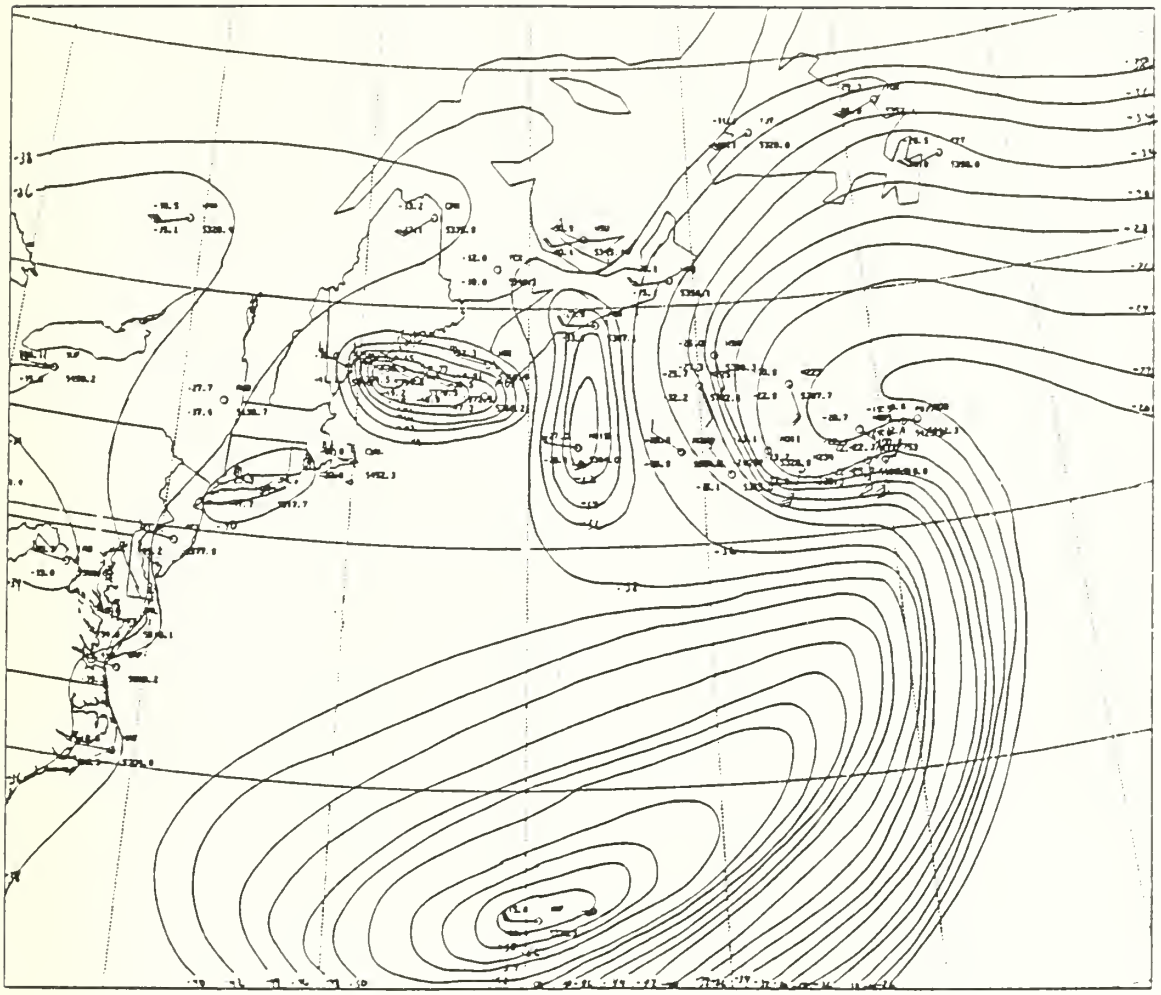

Fig. 46. 500 mb dewpoint analysis at 20/0000 UTC Jan 89: Dewpoint contours every 2 °C.

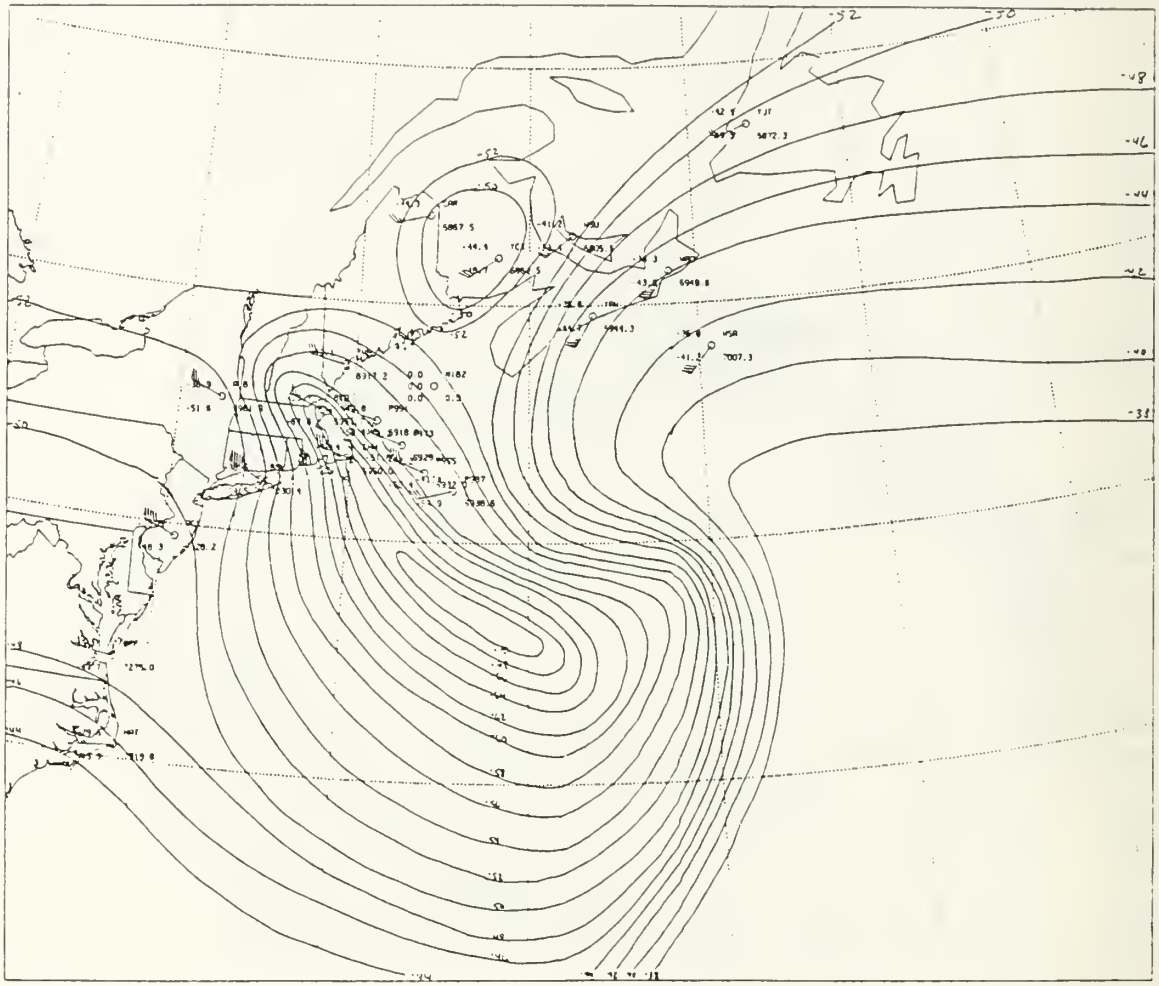

Fig. 47. 400 mb dewpoint analysis at 19/1800 UTC Jan 89: Dewpoint contours every 2 °C.

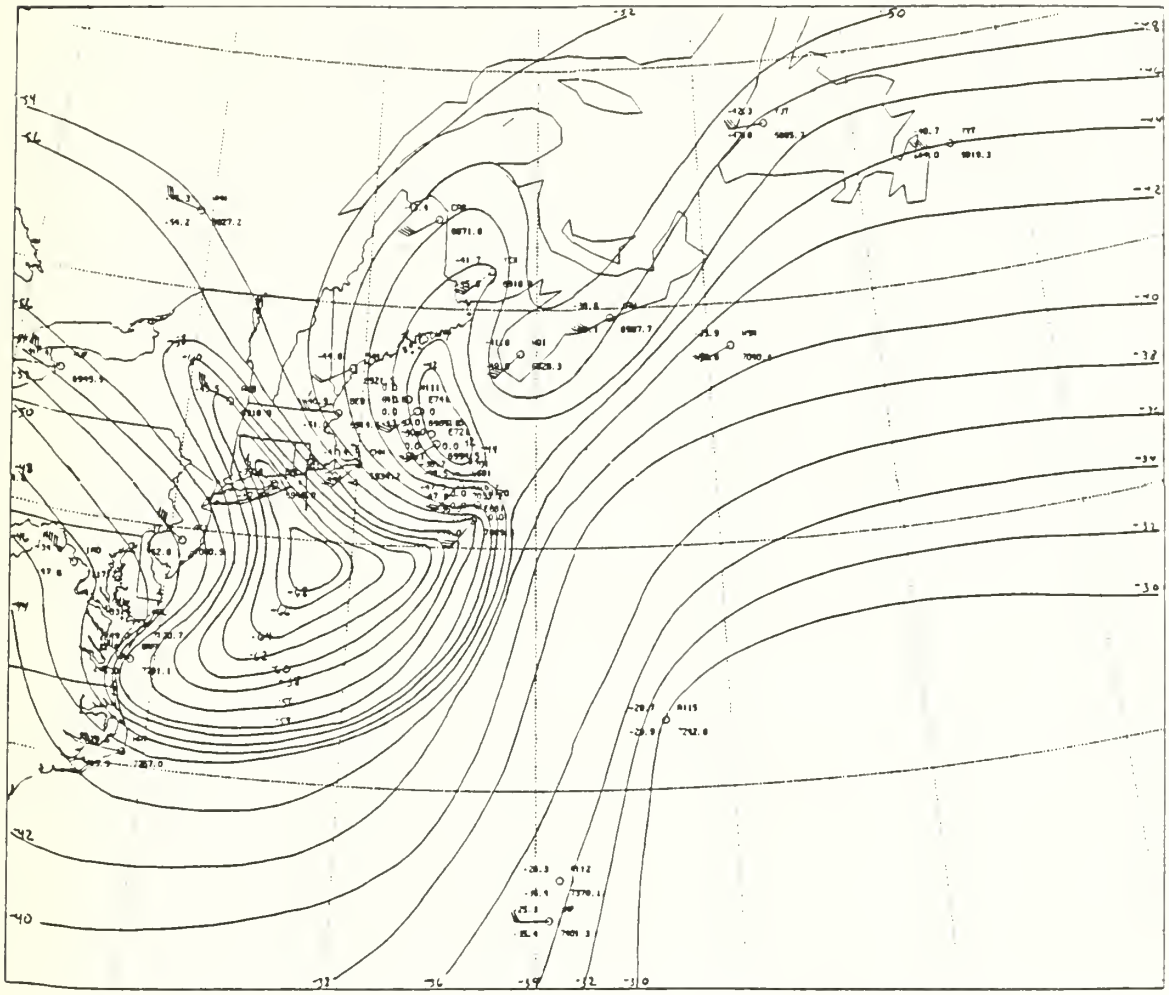

Fig. 48. 400 mb dewpoint analysis at 20/0000 UTC Jan 89: Dewpoint contours every 2 °C.

LIST OF REFERENCES

Bosart, L. F., and S. C. Lin, 1984: A diagnostic analysis of the Presidents' Day storm of February 1979. *Mon. Wea. Rev.*, **112**, 2148-2177.

Carlson, T. N., 1980: Airflow through midlatitude cyclones and the comma cloud pattern. *Mon. Wea. Rev.*, **108**, 1498-1509.

Danielsen, E. F., 1968: Stratospheric-tropospheric exchange based upon radioactivity, ozone and potential vorticity. *J. Atmos. Sci.*, **25**, 502-518.

Elsberry, R. L., and P. J. Kirchoffer, 1988: Upper-level forcing of explosive cyclogenesis over the ocean based on operationally analyzed fields. *Wea. Forecasting*, **3**, 205-216.

Emanuel, K. A., 1985: Frontal circulations in the presence of small moist symmetric instability. *J. Atmos. Sci.*, **42**, 1002-1071.

_____, 1988: Observational evidence of slantwise convective adjustment. *Mon. Wea. Rev.*, **116**, 1805-1816.

Gyakum,1983: On the evolution of the QE II storm. II: Dynamic and thermodynamic structure. *Mon. Wea. Rev.*, **111**, 1156-1173.

_____, and E. S. Barker, 1988: A case study of explosive subsynoptic-scale cyclogenesis. *Mon. Wea. Rev.*, **116**, 2225-2253.

Greer, S. N., 1991: Mesoscale surface analysis of the ERICA IOP-2 cyclone. Master's thesis, Naval Postgraduate School, Monterey, CA, 65p.

Hadlock, R., and C. W. Kreitzberg, 1988: The Experiment on Rapidly Intensifying Cyclones over the Atlantic (ERICA) field study: Objectives and plans. *Bull. Amer. Meteor. Soc.*, **69**, 1309-1320.

Holton, J. R., 1979: *An Introduction to Dynamic Meteorology.* Academic Press, Inc., New York, 391 pp.

Keyser, D., and M. A. Shapiro, 1986: A review of the structure and dynamics of upper-level frontal zones. *Mon. Wea. Rev.*, **114**, 452-499.

Kocin, P. J., and L. W. Uccellini, 1990: Snowstorms along the Northeastern coast of the United States: 1955 to 1985, AMS, Boston, MA., 280 pp.

_____, _____, J. W. Zack and M. L. Kaplan, 1985: A mesoscale numerical forecast of an intense convective snowburst along the East Coast. *Bull. Amer. Meteor. Soc.*, 66, 1412-1424.

Kuo, Y. H., M. A. Shapiro and E. G. Donall, 1991: The interaction between baroclinic and diabatic process in a numerical simulation of a rapidly intensifying extratropical marine cyclone. *Mon. Wea. Rev.*, **119**, 368-384.

Lyne, W. H., R. Swinback and N. T. Birch, 1982: A data assimilation experiment and the global circulation during the FGGE special observing periods. *Quart. J. R. Met. Soc.*, **108**, 575-594.

Neiman, P. J., M. A. Shapiro, E. G. Donall and C. W. Kreitzberg, 1990: Diabatic modification of an extratropical marine cyclone warm sector by cold underlying water. *Mon. Wea. Rev.*, **118**, 1576-1590.

Newton, C. W., 1954:Frontogenesis and frontolysis as a three-dimensional process. *J. Meteor.*, **11**, 449-461.

Palmén, E., 1951: The aerology of extratropical disturbances. *Compendium of Meteorolgy*, T. F. Malone, Ed.,Amer. Meteor. Soc., 599-620.

Reed, R. J., and M. D. Albright, 1986: A case study of explosive cyclogenesis in the eastern Atlantic. *Mon. Wea. Rev.*, **114**, 2297-2319.

Roebber, P. J., 1984: Statistical analysis and updated climatology of explosive cyclones. *Mon. Wea. Rev.*, **112**, 1577-1589.

Sanders, F., 1986: Explosive cyclogenesis in the west-central North Atlantic Ocean 1981-84. Part I: Composite structure and mean behavior. *Mon. Wea. Rev.*, **104**, 1781-1794.

_____, 1987: Skill of NMC operational dynamical models in predicting explosive cyclogenesis. *Wea. and Forecasting*, **2**, 322-336.

_____, 1989: Surface temperature and pressure analysis for Rapidly Intensifying Cyclones over the Atlantic (ERICA) Intensive Observation Periods (IOPs). [Available from ERICA Data Center, Department of Physics and Atmospheric Science,Drexel University, Philadelphia, PA 19104].

_____, 1990: Surface analysis over the oceans-searching for sea truth. *Wea. and Forecasting*, **5**, 596-612.

_____, and J. R. Gyakum, 1980: Synoptic-dynamic climatology of the "bomb". *Mon. Wea. Rev.*, **108**, 1589-1606.

Shapiro, M. A., and D. Keyser, 1990: Fronts, jet streams and the tropopause. *Extratropical Cyclones (The Erik Palmén Memorial Volume)*, C. W. Newton and E. O. Holopainen, Eds., American Meteorological Society, 167-191.

Smith, D. H., 1986: Diagnostic investigation of explosive martime cyclogensis during FGGE. Master's thesis, Naval Postgraduate School, Monterey, CA, 55p.

Uccellini, L. W., 1984: Comments on "Comparative diagnostic case study of East Coast secondary cyclogenesis under weak versus strong synoptic-scale forcing. *Mon. Wea. Rev.*, **112**, 2540-2541.

_____, 1990: Processes contributing to the rapid development of extratropical cyclones. *Extratropical Cyclones (The Erick Palmén Memorial Volume)*, C. W. Newton, and E. O. Holopainen, Eds., Amer. Meteor. Soc., 81-105.

_____, D. Keyser, K. F. Brill and C. H. Wash,1985: The Presidents' Day cyclone of 18-19 February 1979: Influence of upstream trough amplification and associated tropopause folding on rapid cyclogenesis. *Mon. Wea. Rev.*, **113**, 962-988.

_____, R. A. Petersen, K. F. Brill, P. J. Kocin and J. J. Tuccillo, 1987: Synergistic interactions between an upper-level jet and diabatic processes that influence the development of a low-level jet and a secondary coastal cyclone. *Mon. Wea. Rev.*, **115**, 2227-2261.

Wash, C. H., J. E. Peak, W. E. Calland and W. A. Cook, 1988: Diagnostic study of explosive cyclogenesis during FGGE. *Mon. Wea. Rev.*, **116**, 431-451.

Whitaker, J. S., L. W. Uccellini and K. F. Brill, 1988: A model-based diagnostic study of the rapid development phase of the Presidents' Day cyclone. *Mon. Wea. Rev.*, **116**, 2337-2365.

INITIAL DISTRIBUTION LIST

		No. Copies
1.	Defense Technical Information Center Cameron Station Alexandria, VA 22304-6145	2
2.	Library, Code 52 Naval Postgraduate School Monterey, CA 93943-5002	2
3.	Chairman (Code MR/Hy) Department of Meteorology Naval Postgraduate School Monterey, CA 93943-5000	1
4.	Professor Wendall A. Nuss (Code MR/Nu) Department of Meteorology Naval Postgraduate School Monterey, CA 93943-5000	3
5.	Professor Patricia M. Pauley(Code MR/Pa) Department of Meteorology Naval Postgraduate School Monterey, CA 93943-5000	1
6.	Capt Elizabeth B. Gardner, USAF Det. 1, 1st Weather Wing Box 20 FPO SF 96630	2
7.	Commanding Officer AFIT/CIR Wright-Patterson Air Force Base, OH 45433-6583	1
8.	Commander Air Weather Service Scott Air Force Base, IL 62225	1
9.	Commanding Officer Air Force Global Weather Central Offutt Air Force Base, NE 68113-5000	1

10. USAF ETAC/LD
Air Weather Service Technical Library
Scott Air Force Base, IL 62225 1

Thesis
G1854 Gardner
c.1 Mesoscale vertical
structure of an explosive
oceanic cyclone.

Thesis
G1854 Gardner
c.1 Mesoscale vertical
structure of an explosive
oceanic cyclone.

DUDLEY KNOX LIBRARY
3 2768 00014484 4